

DANISH METEOROLOGICAL INSTITUTE

SCIENTIFIC REPORT

00-18

**In-situ analysis of aerosols and gases in the polar stratosphere
A contribution to THESEO**

**Environment and Climate Research Programme
Contract n° ENV4-CT97-0523
Final Report**

N. Larsen, I.S. Mikkelsen, B.M. Knudsen
Danish Meteorological Institute

K. Mauersberger, J. Schreiner, C. Voigt, A. Kohlmann
Max-Planck- Institut für Kernphysik

J. Ovarlez, H. Ovarlez, J. Crespin, B. Gaubicher
Laboratoire de Météorologie Dynamique

A. Adriani, F. Cairo, F. Cardillo, G. Di Donfrancesco,
R. Morbidini, L. Pulvirenti, M. Viterbini
Consiglio Nazionale delle Ricerche, Istituto di Fisica dell' Atmosfera

C. David, S. Bekki, G. Mégie
Service d'Aéronomie du CNRS

C. Flesia, A. Starkov
Group de Physique Appliquée, Université de Geneve

T. Deshler, C. Kröger, J. Rosen, N. Kjome
University of Wyoming



COPENHAGEN 2000

In-situ analysis of aerosols and gases in the polar stratosphere
A contribution to THESEO

Environment and climate research programme
Contract n?: ENV4-CT97-0523
Final report

N. Larsen et al.

Danish Meteorological Institute, Division of Middle Atmosphere Research,
Lyngbyvej 100, DK-2100 Copenhagen Ø, Denmark

ISBN 87-7478-429-3
ISSN 0905-3263
ISSN 1399-1949 (ONLINE)

In-situ analysis of aerosols and gases in the polar stratosphere A contribution to THESEO

ENVIRONMENT AND CLIMATE RESEARCH PROGRAMME

Contract n°: ENV4-CT97-0523

Final report



N. Larsen, I.S. Mikkelsen, B.M. Knudsen
Danish Meteorological Institute

K. Mauersberger, J. Schreiner, C. Voigt, A. Kohlmann
Max-Planck- Institut für Kernphysik

J. Ovarlez, H. Ovarlez, J. Cressin, B. Gaubicher
Laboratoire de Météorologie Dynamique

A. Adriani, F. Cairo, F. Cardillo, G. Di Donfrancesco,
R. Morbidini, L. Pulvirenti, M. Viterbini
Consiglio Nazionale delle Ricerche, Istituto di Fisica dell' Atmosfera

C. David, S. Bekki, G. Mégie
Service d'Aéronomie du CNRS

C. Flesia, A. Starkov
Group de Physique Appliquée, Université de Geneve

T. Deshler, C. Kröger, J. Rosen, N. Kjome
University of Wyoming

ENVIRONMENT AND CLIMATE RESEARCH PROGRAMME**RESEARCH AREA: 1.2.1.1****STRATOSPHERIC CHEMISTRY AND DEPLETION OF THE OZONE LAYER****FINAL REPORT**

Contract n°: ENV4-CT97-0523

Title: In-situ analysis of aerosols and gases in the polar stratosphere:
A contribution to the THESEO campaign.

Acronym: PSC-analysis

Scientific coordinator: Danish Meteorological Institute, Research and Development Department,
Middle Atmosphere Research Division (DMI)

Contractor(s):

C1: Max-Planck-Gesellschaft zur Förderung der Wissenschaften e.V.,
Institut für Kernphysik (MPI)

C2: Centre National de la Recherche Scientifique, UPR 1211,
Laboratoire de Météorologie Dynamique (CNRS-LMD)

C3: Consiglio Nazionale delle Ricerche, Istituto di Fisica dell' Atmosfera (CNR-IFA)

C4: Centre National de la Recherche Scientifique, UPR 3501,
Service d'Aéronomie (CNRS-SA)

C5: Université de Genève, Groupe de Physique Appliquée Energie,
Section de Physique, Optics Division (UG)

Collaboration: University of Wyoming, Dept. of Atmospheric Science (UW-AS)
University of Wyoming, Dept. of Physics and Astronomy (UW-PA)

Key words (max. 5): PSC, composition, size-distributions, microphysics, THESEO

Reporting period: 1 February 1998 – 31 July 2000.

PART A: SUMMARY REPORT OF THE PROJECT.

I. EXECUTIVE SUMMARY

In-situ balloonborne experiments have provided the first combined measurements of the chemical composition and optical properties of polar stratospheric cloud (PSC) particles, formed in leewaves over the Scandinavian mountains.

The project has aimed at a complete characterisation of PSC particles in terms of their chemical composition, physical phase, size distributions, and optical properties together with observations of the ambient atmospheric environment in which the particles form. These aims have been accomplished by performing balloonborne multi-instrument measurements using an aerodynamic focusing lens and a mass spectrometer for condensed phase chemical analysis, optical and CCN counters for measurements of PSC particles size distributions, (laser) backscatter sondes for observations of optical properties and physical phase (backscatter ratios and depolarisation), and a hygrometer for measurements of gas phase concentrations of water vapour. The balloonborne measurements have been supported by airborne lidar observations of the PSC evolution. The measurements have been analysed applying meteorological mesoscale, microphysical, and optical modelling.

A preliminary test flight was performed on 25 January 1998 from Esrange, Sweden, carrying only the aerosol composition mass spectrometer and a backscatter sonde. *These first measurements have shown consistency with liquid supercooled ternary solution (STS) compositions of the observed PSC particles* [Schreiner et al., 1999; Voigt et al., 2000a; Larsen et al., 2000].

The first fully equipped PSC-analysis gondola was launched from Esrange 19 Jan 2000 at 20.43 UTC. On ascent a PSC layer was observed between 35 and 45 hPa. Another thinner PSC layer was observed between 25 and 30 hPa. Temperatures in the lower layer were around 194 K and between 190 and 195 K in the upper layer. The balloon operation team from Centre National d'Étude Spatiales (CNES) was able to adjust the altitude of the balloon with the valve/ballast system, based on on-line reporting of the PSC backscatter ratios. The upper layer was penetrated 4 times in two ascent/descent manoeuvres. All instruments provided data without problems during ascent and in the upper-layer penetrations.

The second fully equipped PSC-analysis gondola was flown very successfully 25 January 2000, launched 19.46 UTC from Esrange. The balloon was manoeuvred in 3 up/down movements through a PSC layer between 38 and 24 hPa. Temperatures were between 185-197 K. In this altitude range the balloon stayed inside PSC for nearly the whole flight and all instruments worked without problems.

More comprehensive investigations in two later flights identified for the first time PSC particles composed of nitric acid trihydrate (NAT) at temperatures up to or even slightly above the NAT existence temperatures (T_{NAT}), surrounded by layers of STS particles at much lower temperatures close to ice frost point (T_{ice}) [Voigt et al., 2000b]. *These flights showed a clear correspondence between chemical composition, size distributions, and optical properties of the particles.*

Both PSC-analysis flights were performed as part of the European/US THESEO-2000/SOLVE campaigns in winter 1999/2000 from Esrange near Kiruna in Sweden. It had been foreseen in the workplan that the PSC-analysis gondolas were flown in winter 1998/1999. However, unusual high stratospheric temperatures prevented the formation of PSCs over Kiruna in January/February 1999 and the experiments were postponed for one year. The project was extended for 6 months, terminating by 31 July 2000.

II. GENERAL OBJECTIVES

The objective of the project has been to obtain a complete and simultaneous characterisation of polar stratospheric cloud particles in terms of their chemical composition and physical phase, particle size distributions, optical properties, and the ambient atmospheric conditions in which the particles form. The objectives have been met by two balloonborne flights with multi-instrument payloads, supplemented by simultaneous airborne lidar measurements during the THESEO-2000 campaign in January 2000. By the complete particle characterisation the goal has been to improve the detailed microphysical modelling and thereby understanding of PSC formation.

III. SPECIFIC OBJECTIVES

During the preparation stage:

The main specific objectives have been to prepare the instruments and the modelling framework for the THESEO-2000 campaign. The specific objectives have been:

1. Conduct test flight with the MPI mass-spectrometer from Kiruna and analyse the data.
2. Make detailed specifications and plans for integration of different instruments onboard the common gondolas, including specifications for telemetry. Preparations of the individual instruments. Preparation of the airborne lidar to an operational stage.
3. Detailed planning of flights during the campaign.
4. Non-hydrostatic mesoscale meteorological and microphysical model developments.

During the campaign stage:

The main objectives have been to obtain PSC observations during the THESEO-2000 campaign. The specific objectives have been:

1. Perform two balloonborne flights with multi-instrument payloads from Kiruna during the THESEO-2000 campaign, supplemented by simultaneous airborne lidar measurements.

During the data interpretation stage:

The main objectives have been to perform data analysis of the observations. The specific objectives have been:

1. Data retrieval and analysis. Submission of data to the common European data base.
2. Model based analysis of observations.
3. Presentation and discussions of scientific results at European workshops and international conferences.

IV. SCIENTIFIC DESCRIPTION OF THE PROJECT:

PSC particles are assumed to form by co-condensation of nitric acid (HNO_3) and water (H_2O) vapour in the stratosphere at temperatures below 195 K (-78°C). In addition, halogen reservoir species (HCl and HBr) are assumed to condense on the particles. PSCs play an important role in stratospheric ozone depletion in two ways: heterogeneous chemical reactions in the bulk and on the surface of the particles convert halogen reservoir species into potentially ozone destroying radicals. Secondly, by gravitational sedimentation of PSC particles reactive nitrogen compounds could be depleted (denitrification) which prolong the ozone destroying reactions. Both processes depend on the chemical composition, physical phase, and sizes of the PSC particles¹.

Different instrumentation onboard common balloon borne gondolas have been used to obtain in-situ measurements of the PSC characteristics. The measurement of PSC particle composition requires a separation of the condensed phase from atmospheric gases without a change in particle properties. To accomplish this, a newly developed differentially pumped aerodynamic lens has been used, producing a beam of particles, which enter a mass spectrometer for composition analysis (MPI). A cryogenic frostpoint-hygrometer has provided measurements of gas phase H_2O concentrations (CNRS-LMD). Optical particle counters have been used for measurements of the particle size distributions (UW-AS), and combined optical measurements by backscatter sondes (CNR-IFA, UW-PA, DMI) have been used for physical phase determination, and used to derive refractive indices and other optical properties of the particles.

An airborne lidar (CNRS-SA) has been used for measurements of the spatial and temporal development of the PSCs, providing a three dimensional (horizontal and vertical) vision of the extent of the PSCs. The airborne lidar has been operated simultaneously with the balloonborne experiments, following the general trajectory of the balloon.

The observed PSCs can be assumed to be formed in large-scale lee waves. A non-hydrostatic model has been used to simulate the meteorological conditions in connection with the balloon- and airborne experiments (DMI).

¹ Godin, S., L. Poole, S. Bekki, T. Deshler, N. Larsen, and T. Peter, Global distributions and changes in stratospheric particles, cp. 3 in World Meteorological Organization (WMO), Scientific assessment of ozone depletion: 1998, Rep. 44, Global Ozone Res. and Monit. Proj., Geneva, 1999.

A microphysical model, describing type 1a, 1b, and type 2 PSCs, has been used in the project to simulate the evolution of PSC size distributions, their chemical compositions and physical phase, and the atmospheric conditions in which the particles form (DMI). The observational data will be used to constrain the microphysical model, and results from the field may lead to radical adjustments of the model in order to explain the observations.

V. MAIN RESULTS:

Test flight.

The first successful test flight with the MPI instrument under PSC conditions was performed on 25 January 1998 from Kiruna. A backscatter sonde from University of Wyoming-PA/DMI was also onboard the gondola. The payload passed PSC layers several times during climbing/diving balloon manoeuvres in a nearly 4 hours flight. The observations have been analysed within the PSC-analysis project. The compositions measurements showed PSC cloud particles, composed of highly diluted solutions of nitric acid and water with $\text{H}_2\text{O}:\text{HNO}_3$ molar ratios above 10 in good agreement with predictions from liquid supercooled ternary solution models, and the meteorological mesoscale/microphysical model indicated the particles to be in the liquid state. This was the first time that the chemical composition of PSC particles was measured [Schreiner *et al.*, 1999; Larsen *et al.*, 2000; Voigt *et al.*, 2000a]. Figure 1 shows the main results from the test flight.

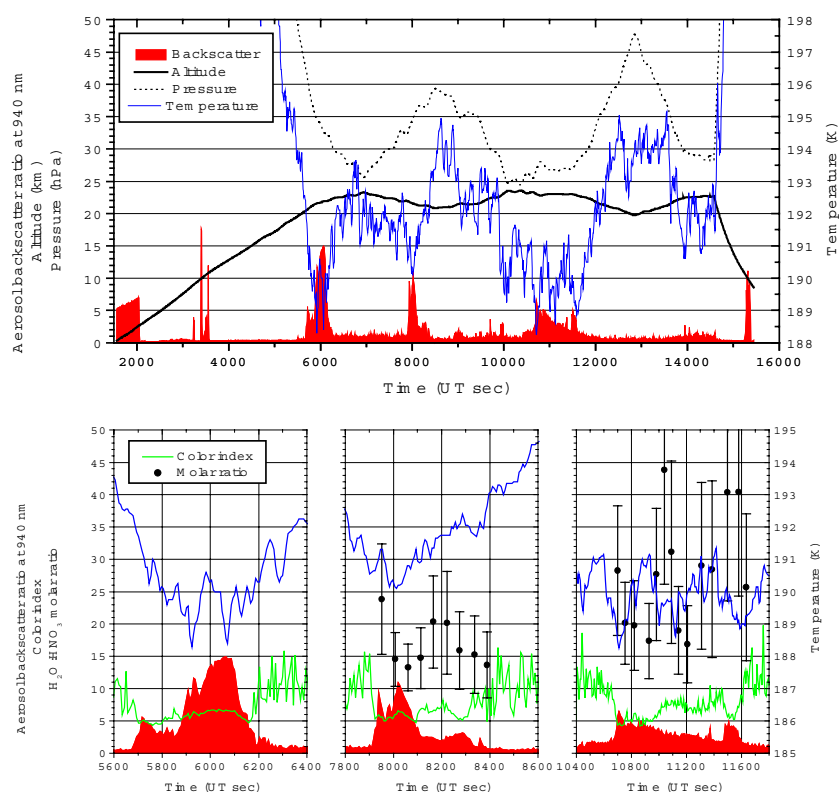
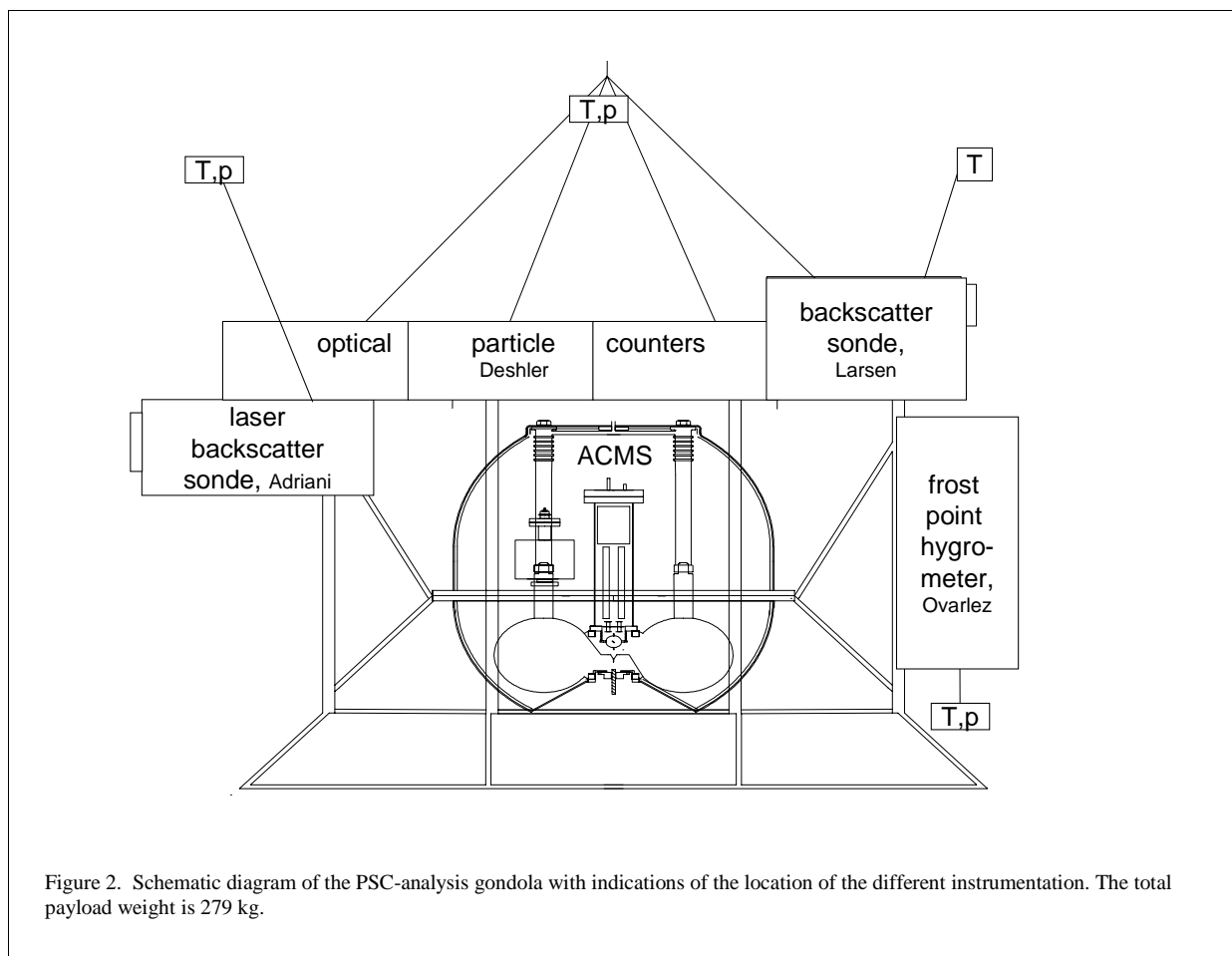


Figure 1 Composite plot of chemical and optical measurements as a function of time (UT seconds) during the balloon-borne flight from Kiruna on January 25, 1998. The upper panel shows the aerosol backscatter ratio (β_{940} , red area), air temperature (blue solid), geopotential altitude (thick black), and air pressure (dotted) throughout the whole flight. PSC layers were encountered around 6000, 8000, and 11,000 s as seen from the elevated values of the backscatter ratios. The lower panels show in more detail, during these PSC encounters, the aerosol backscatter ratio, color index (β_{940}/β_{480} , green curve), temperature, and the $\text{H}_2\text{O}:\text{HNO}_3$ molar ratios (symbols with error bars), measured during the last two PSC encounters. Temperatures are read off the right-hand axes, the other quantities off the left-hand axes.

PSC-analysis instrument specification and preparations.

A number of project meetings have been held, mainly focussed on specifications for the integration of the individual instruments onboard the two common PSC-analysis gondolas together with plans for bringing the airborne lidar to the operational stage. The layout of the PSC-analysis gondola appears in Figure 2. Two identical and completely independent gondolas were built and flown.



At the centre of the gondola is located the aerosol composition mass spectrometer (ACMS) from the MPI. Above this main instrument are located the laser backscatter sonde (LABS) from CNR-IFA, the backscatter sonde from UW-PA/DMI, the optical particle counters from UW-AS, and the frost point hygrometer from CNRS-LMD. The individual instruments are described in more detail in Part B of this report. It was experienced by the test flight from Kiruna January 1998 that temperature measurements could be influenced by heating from the payload, and that temperature should be measured at a horizontal distance away from or above/below the gondola during flight. Several temperature and pressure sensors were therefore placed on booms or on the load line for the THESEO-2000 flights. A photograph of the payload on the launch trolley is shown in Figure 3.

The gondolas were constructed at the MPI and the individual instruments were shipped to the MPI in fall 1999 for integration and telemetry (TM) tests. A common TM system, provided by the MPI, was used for all instruments. Gondolas and all instruments were transported by the MPI from Heidelberg to Kiruna in November 1999 where the final integration and tests took place in December 1999.

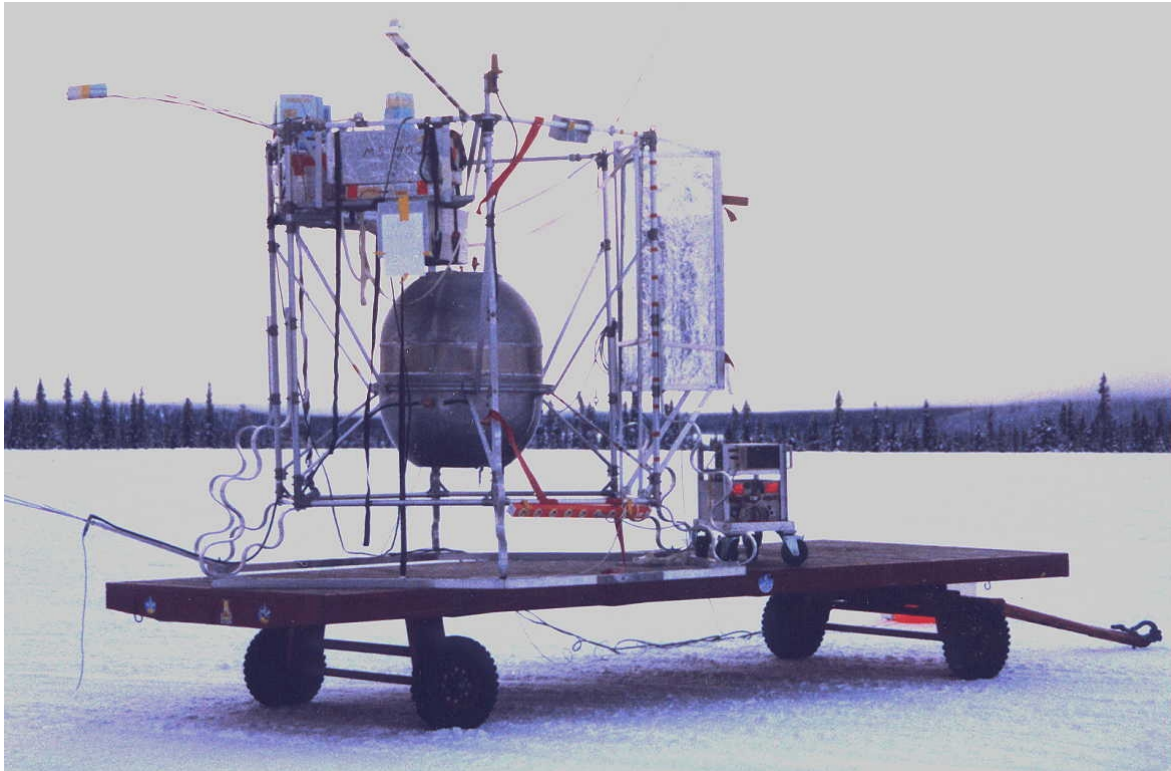


Figure 3 Photograph showing the PSC-analysis gondola on the launch trolley at Esrange, Kiruna.

Flight planning.

Daily 10-days forecasts of stratospheric temperatures and the location of the polar vortex were produced and distributed by DMI. For the flight planning, daily operational meetings were held at Esrange during the THESEO-2000 campaign in collaboration with the Coordinating Unit, based upon available meteorological information, PSC lidar observations, ground conditions, balloon forecast trajectories, and in coordination with other experiments. The PSC analysis project was granted a high flight priority at PSC conditions. After a preliminary flight decision was taken at the first daily operational meeting, U. Wyoming/DMI launched one or two backscatter sondes. Information from these flights was used to gauge the PSC occurrence and altitudes and was used together with other updated information in later operational meetings before a flight was finally scheduled. Two ARAT flights were performed in connection with the latter balloon flight on 25 January 2000, one flight before launch upwind, and a second flight tracking the balloon after launch. The flights tracked the stratospheric air parcel trajectories as close as possible up and downwind of the mountains.

PSC-analysis balloonborne flights.

Composite graphs of the results from the two balloonborne PSC-analysis flights are shown in Figures 4 and 5 below. The graphs shows various simultaneous measurements as function of UT time (seconds and decimal hours) during the flights. Details and analysis of the different measurements are given in part B of this report and only a brief overview is presented here in this part A. The measurements are still in the process of being analysed and the following description is of a preliminary character.

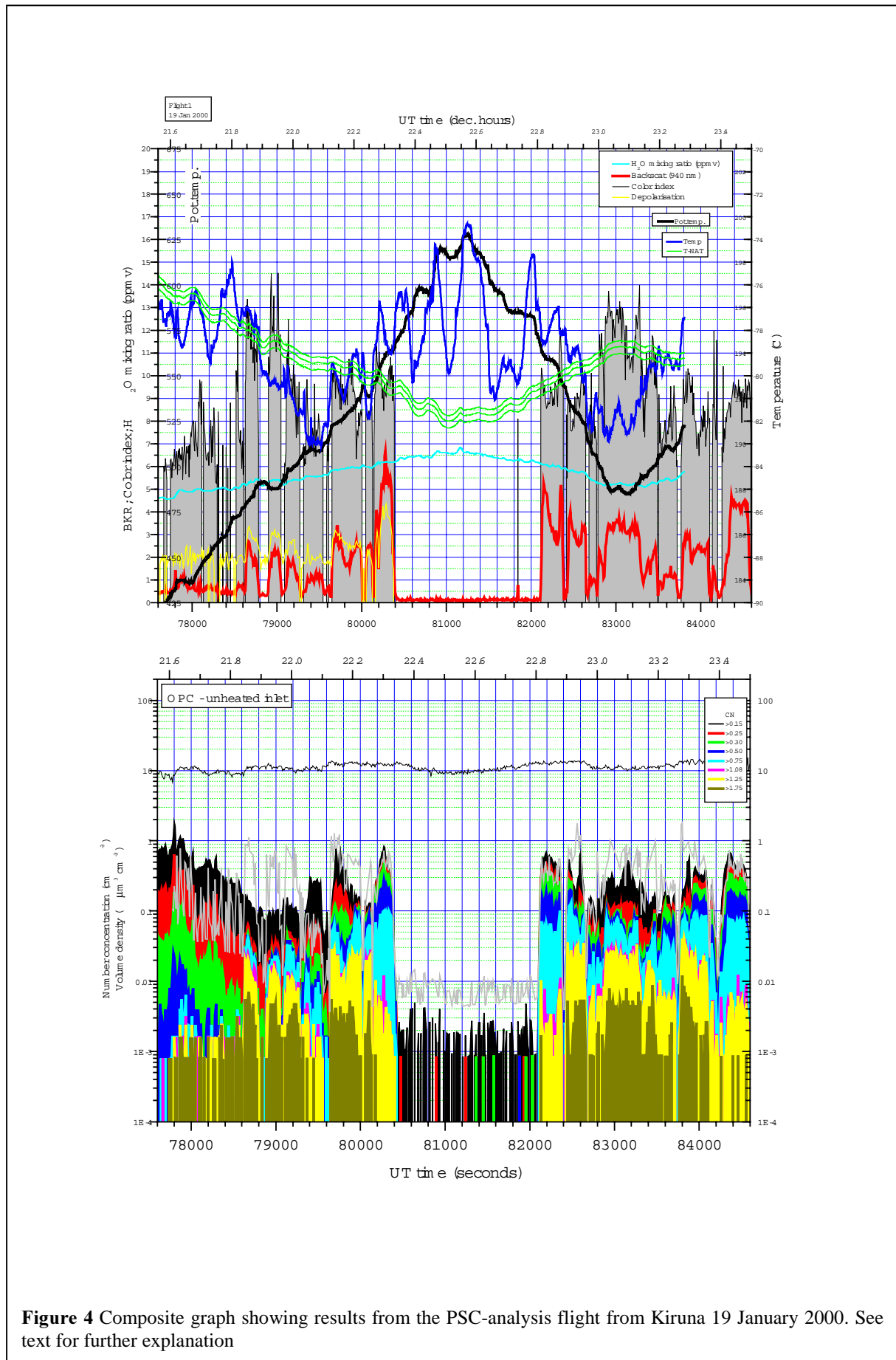


Figure 4 Composite graph showing results from the PSC-analysis flight from Kiruna 19 January 2000. See text for further explanation

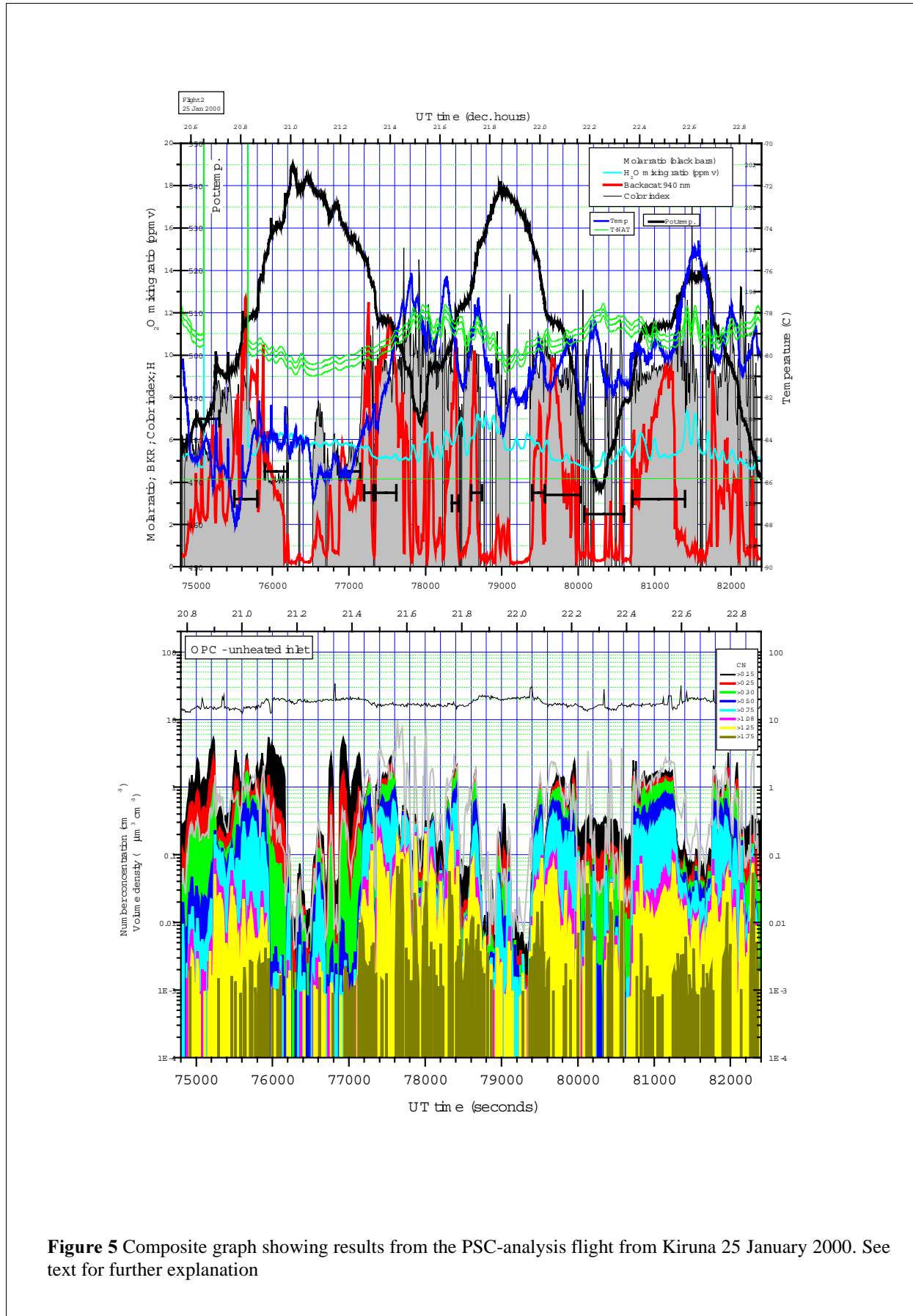


Figure 5 Composite graph showing results from the PSC-analysis flight from Kiruna 25 January 2000. See text for further explanation

Flight # 1, 19 January 2000.

The thick black curves in the upper panels (read off on the inner left ordinate) show the altitude of the gondolas in terms of potential temperature. In the first flight (Figure 4, upper panel) a PSC layer was penetrated between 425 and 575 K as shown by the backscatter ratio (940 nm; red curve, outer left ordinate) and the colour index (gray curve, outer left ordinate). The water vapour mixing ratio increased with altitude between 4.5 and 6.9 ppmv (cyan curve, outer left ordinate). The temperature (blue curve, right ordinate) stayed below the NAT condensation temperature T_{NAT} (green curves, right ordinate) in most of the lower part of the cloud and a few degrees above T_{NAT} in the upper layers. The three T_{NAT} -curves have been calculated from the measured water vapour concentrations, assuming 8, 10, and 12 ppbv nitric acid, respectively. The yellow curve in the upper panel (outer left ordinate) shows the total volume depolarisation ratio, measured at 532 nm by the LABS. The lower panel in Figure 4 shows the measured integral size distributions, obtained by the optical particle counters. The upper black curve shows the total particle concentration (cm^{-3}) and the lower curves the number concentrations of particles with radii larger than 0.15, 0.25, 0.30, 0.50, 0.75, 1.08, 1.24, and 1.75 μm . The grey curve gives the particle volume density ($\mu\text{m}^3 \text{cm}^{-3}$). The lower part of the cloud (between 77700 and 78600 sec) is characterised by low backscatter ratio, low colour index, low volume depolarisation, and relatively small particles. This indicates that the cloud was dominated by liquid particles at relatively high temperatures, slightly below T_{NAT} . At the higher altitudes, large colour indices and volume depolarisation, and the higher concentrations of large particles, are characteristic of solid type PSCs. Preliminary analysis of the chemical measurements indicate that these particles have $\text{H}_2\text{O}:\text{HNO}_3$ molar ratios larger than 3, but clearly below the lower limit of 4.3 for STS compositions, indicating simultaneous presence of NAT and STS particles. Particles in the upper layer could be evaporating solid particles since the temperatures are relatively high, compared to T_{NAT} . A large degree of symmetry in particle properties is observed between the ascend and descend through the upper layers, indicating that nearly the same cloud particles are observed in both passages.

Flight #2, 25 January 2000.

In this flight three up/down maneuvers through PSC layers were performed. PSCs were observed at temperatures between 8 K below and 3 K above T_{NAT} , at altitudes between 480 and 530 K (Figure 5, using the same type of graphs as in Figure 4). The fine structure of particle layers within PSCs was clearly evident in all particle instruments. The water vapor concentrations varied quite substantially between 4.5 and 7 ppmv. For this flight, the chemical composition analysis has been completed as indicated by the horizontal bars giving the $\text{H}_2\text{O}:\text{HNO}_3$ molar ratios of the observed particles. Layers with molar ratios near 3 ± 0.5 indicate a NAT composition, consistent with high values of color indices, also showing the presence of solid particles. In these layers a relatively high concentration of large particles was observed. These types of particles are observed at temperatures close to T_{NAT} (or even above T_{NAT} around 78600 sec). Many of the NAT-composition particles were observed several times in same the altitude range around 500-510 K. Another type of particles were observed with $\text{H}_2\text{O}:\text{HNO}_3$ molar ratios from 4.3 to 7 (i.e. larger than the lower limit of STS particle compositions, indicated by the horizontal green line in the upper panel in Figure 5) and in agreement with ternary solution compositions. The layers are characterised by low colour index, also indicating liquid particles. Integrated particle volumes were consistent with theoretical predictions for STS. These particles were observed around 75100, 76000, and 77000 sec. These measurements were obtained near the ice point, approximately 5 K below T_{NAT} , and 1 K below the condensation temperature for supercooled ternary solutions, T_{STS} . Other layers had color indices of 6-8 with depolarization ratios > 3 suggesting some asphericity. Condensed volumes were consistent with both NAT and STS. The volume weighted molar ratios of 3.4 were near NAT. These observations at 5-6 K below T_{NAT} , the coldest temperatures observed during flight, were consistent in suggesting that the clouds consisted of mixtures of STS and NAT particles.

ARAT flights.

The LEANDRE backscatter lidar on board the ARAT/Fokker27, flew in evening of 25 January 2000 in coordination with the second PSC-analysis gondola. Two flights were performed as described in more detail in the CNRS_SA contribution to part B of this report.

The first flight, upwind before PSC Analysis launch, was made between Kiruna and Andoya, and lasted almost 2 hours (take off at 18:30 UT, landing at 20:15 UT). The ARAT flew almost parallel to the stratospheric winds at 50 hPa and 30 hPa. During this first flight, PSCs were observed between Kiruna and approximately the

Norwegian border, between about 21 and 25 km in altitude. They presented a layered structure and strongly depolarised the lidar signal. Backscatter ratio can roughly be estimated at values around 4-5 for the bottom layers and around 6-8 for the upper layers. The depolarisation seems stronger for the upper layers than for the bottom ones.

The second flight was made between Kiruna and South-East of Rovaniemi. The ARAT took off at 20:44 UT, which was one hour after the PSC Analysis balloon launch, and landed at 23:15 UT. The position of the balloon was communicated in real time to the ARAT through the VHF station in Esrange. During this second flight, PSCs were observed between Kiruna and the mid-distance between Kiruna and the Finnish border, between about 20 and 22 km in altitude. Meanwhile, the backscatter ratio may be slightly less than for the first PSC flight.

Meteorological mesoscale/microphysical modelling framework.

The Regional Atmospheric Modelling System (RAMS) has been installed at the DMI supercomputer, and an additional stream line model to derive air parcel trajectories has been added to the model. A non-equilibrium liquid type 1b PSC model has been developed as an extension of the existing DMI microphysical model. The modelling framework has been used for analysis of the test flight situation in January 1998 and for analysis of the observations during the THESEO-2000 campaign. More details can be found in the DMI contribution to part B of this report.

VI DISSEMINATION, USE, OR EXPLOITATION.

A large number of scientific publications have been published, submitted for publication, or being in preparation as results from the PSC-analysis project. This includes two very fast published/submitted papers on immediate results in one of the World's leading scientific journals, *Science*. Results from the projects have been and will be presented at various scientific conferences. Data from the various instruments in the PSC-analysis flights have been stored at the common European data base at NILU. Results from the project will be used to constrain microphysical models to describe the formation of polar stratospheric clouds. This includes both the microphysical model within the project (which is public available) and external microphysical models. More accurate knowledge of PSC formation is a prerequisite for better modelling and understanding of polar ozone depletion in a future stratospheric climate, possibly characterised by lower stratospheric temperatures, increased water vapour concentrations, and more widespread PSC formation and denitrification in the Arctic regions.

VII. CONCLUSIONS:

The rates of heterogeneous chemical reactions, activating chlorine species into ozone depletions substances, depend on the chemical composition and physical phase of the particles. In addition, only solid type PSC particles can introduce denitrification, which may prolong the ozone depletion from, activated halogen compounds. Therefore details of PSC formation are required for a more accurate prediction of ozone depletion in a future stratospheric climate². For more than a decade it has been known that nitric acid holding particles may form in the stratosphere at temperature above the ice frost point³. However, no detailed chemical composition measurements of PSC particles have been available. For the first time, the exact chemical composition of different PSC particle types (liquid and solid) has been measured in three balloonborne flights under different meteorological conditions. Although laboratory measurements have shown that nitric acid trihydrate would be the stable compound at stratospheric conditions⁴, the measurements in this project have for the first time confirmed the existence of NAT particles in the polar stratosphere.

² Waibel, A.E., Th. Peter, K.S. Carslaw, H. Oelhaf, G. Wetzal, P.J. Crutzen, U. Pöschl, A. Tsias, E. Reimer, and H. Fischer, Arctic ozone loss due to denitrification, *Science* 283, 2064-2069, 1999; Becker, G., R. Müller, D. S. McKenna, M. Rex, K.S. Carslaw, and Hermann Oelhaf, Ozone loss rates in the Arctic stratosphere in the winter 1994/1995: Model simulations underestimate results of the Match analysis, *J. Geophys. Res.* 105, 15175-15184, 2000.

³ Fahey, D.W., K.K. Kelly, G.V. Ferry, L.R. Poole, J.C. Wilson, D.M. Murphy, M. Loewenstein, and K.R. Chan, In Situ Measurements of Total Reactive Nitrogen, Total Water, and Aerosol in a Polar Stratospheric Cloud in the Antarctic, *J. Geophys. Res.* 94, 11299-11315, 1989.

⁴ Hanson, D., and K. Mauersberger, Laboratory Studies of the Nitric Acid Trihydrate: Implications for the South Polar Stratosphere, *Geophys. Res. Lett.* 15, 855-858, 1988.

The objectives of the project, namely to obtain and complete characterisation of PSC particles in terms of their chemical composition and optical properties, have successfully been fulfilled by the three balloonborne flights performed in the project. All specific objectives of the project have been successfully accomplished. The data analysis has not been fully completed only 6 months after the project officially terminated, but a series of publications are in preparation in addition to those scientific articles already published or submitted.

VIII. PUBLICATIONS ARISING FROM FROM THE PROJECT:

Scientific publications

- Cairo F., G. Di Donfrancesco, A. Adriani, L. Pulvirenti and F. Fierli, Comparison of various linear depolarization parameters measured by lidar, *Applied Optics*, vol. 38, No. 21, 4425-4432, 1999.
- de La Noë J., J. Ovarlez, H. Ovarlez, C. Schiller, N. Lautié, P. Ricaud, J. Urban, D. G. Feist, L. Zalesak, N. Kämpfer, M. Ridal, D. Murtagh, K. Lindner, U. Klein, K. Künzi, P. Forkman, A. Winnberg, P. Hartogh and A. Engel, Water vapor distribution inside and outside the polar vortex during THESEO, Proceedings of the Fifth European Symposium on Polar Stratospheric Ozone Research, St. Jean de Luz, France, September 1999, Air Pollution Research Report , European Commission, 2000.
- Deshler, T., C. Kröger, J. Rosen, A. Adriani, F. Cairo, and G. Di Donfrancesco, N. Larsen, C. Voigt, A. Kohlmann, J. Schreiner, K. Mauersberger, J. Ovarlez, H. Ovarlez, Index of Refraction of Polar Stratospheric Cloud Particles Inferred from Balloonborne Measurements of the Physical and Optical Properties of the Particles, *Journal of Geophysical Research*, abstract submitted, 2000.
- Knopf, D., Zink, P., Schreiner, J., Mauersberger, K.: Calibration of an Aerosol Composition Mass Spectrometer with Sulfuric Acid/Water Aerosol. *Aerosol Sci. Technol.*, submitted.
- Kohlmann, A.: Kalibration von Massenspektrometern zur Aerosol-Analyse durch dynamische Expansion von Wasserdampf, HNO₃ und HCl. Ph.D. Thesis, Heidelberg 2000.
- Larsen, N., I.S. Mikkelsen, B.M. Knudsen, J. Schreiner, C. Voigt, K. Mauersberger, J.M. Rosen, and N.T. Kjome, Comparison of chemical and optical in-situ measurements of polar stratospheric clouds, *Journal of Geophysical Research*, 105, 1491-1502, 2000.
- Larsen, N., Chemical understanding of ozone loss - heterogeneous processes: Microphysical understanding and outstanding issues, Proceedings of the Fifth European Symposium on Polar Stratospheric Ozone Research, St. Jean de Luz, France, September 1999, Air Pollution Research Report , European Commission, 2000.
- Larsen, N., Ib Steen Mikkelsen, Bjørn M. Knudsen, Jochen Schreiner, Christiane Voigt, Konrad Mauersberger, James M. Rosen, and Norman T. Kjome, Comparison of chemical and optical in-situ measurements of PSC particles, Proceedings of the Fifth European Symposium on Polar Stratospheric Ozone Research, St. Jean de Luz, France, September 1999.
- Larsen, N., Polar Stratospheric Clouds, Microphysical and Optical Models, DMI Scientific Report 00-06, 2000.
- Larsen, N., I. S. Mikkelsen, B. M. Knudsen, C. Voigt, A. Kohlmann, J. Schreiner, K. Mauersberger, T. Deshler, C. Kröger, J. Rosen, A. Adriani, F. Cairo, and G. Di Donfrancesco, J. Ovarlez, H. Ovarlez, Microphysical mesoscale simulations of polar stratospheric cloud formation over Northern Scandinavia on 25 January 2000 constrained by in-situ measurements of chemical and optical cloud properties, *Journal of Geophysical Research*, abstract submitted, 2000.
- Mikkelsen, I.S. and N. Larsen, Non hydrostatic simulations of leewaves over northern Scandinavia on 25 January 1998, in K.S Carslaw and G.T. Amanatidis (ed), Mesoscale processes in the stratosphere, Their effect on stratospheric chemistry and microphysics, Proceedings of the European workshop 8 to 11 November 1998, Bad Tölz, Bavaria, Germany, Air Pollution Research Report no. 69, European Commission, pp. 165-170, 1999.

- Mikkelsen, I. S. and N. Larsen, Non-hydrostatic modeling of steep leewaves over Northern Scandinavia on 25 January 2000, *Journal of Geophysical Research*, abstract submitted, 2000.
- Schiller, C., R. Bauer, J. Beuermann, F. Cairo, T. Deshler, A. Dörnbrack, G. Ehret, J. Elkins, A. Engel, A. Fix, N. Larsen, M. Müller, S. Oltmans, H. Ovarlez, J. Ovarlez, F. Stroh, G. Toon, H. Vömel, and T. Wetter, Dehydration in the Arctic stratosphere during the THESEO 2000 / SOLVE campaigns, *Journal of Geophysical Research*, abstract submitted, 2000.
- Schreiner, J., C. Voigt, A. Kohlmann, F. Arnold, K. Mauersberger, and N. Larsen, Chemical analysis of polar stratospheric cloud particles, *Science* 283, 968-970, 1999.
- Schreiner, J., Schild, U., Voigt, C., Mauersberger, K.: Focusing of aerosols into a particle beam at pressures from 10 to 150 torr. *Aerosol Sci. Technol.* 31, 373-382 (1999).
- Schreiner, J., Voigt, C., Zink, P., Kohlmann, A., Knopf, D., Mauersberger, K.: A mass spectrometer system for analysis of polar stratospheric aerosols. *Rev. Sci. Instrum.*, submitted.
- Schreiner, J., C. Voigt, A. Kohlmann, K. Mauersberger, T. Deshler, C. Kröger, J. Rosen, N. Larsen, A. Adriani, F. Cairo, and G. Di Donfrancesco, J. Ovarlez, H. Ovarlez, Chemical, physical and optical properties of polar stratospheric clouds in mountain waves, *Journal of Geophysical Research*, abstract submitted, 2000.
- Voigt, C., J. Schreiner, , A. Kohlmann, , P. Zink, F. Arnold, K. Mauersberger, N. Larsen, and A. Dörnbrack, Evidence of supercooled ternary solution PSCs, in K.S Carslaw and G.T. Amanatidis (ed), *Mesoscale processes in the stratosphere, Their effect on stratospheric chemistry and microphysics*, Proceedings of the European workshop 8 to 11 November 1998, Bad Tölz, Bavaria, Germany, *Air Pollution Research Report* no. 69, European Commission, pp. 255-258, 1999.
- Voigt, C., J. Schreiner, K. Mauersberger, A. Tsias, T. Peter, N. Larsen, A. Dörnbrack, A case study of PSC particle formation, *Proceedings of the Fifth European Symposium on Polar Stratospheric Ozone Research*, St. Jean de Luz, France, September 1999.
- Voigt, C., A. Tsias, A. Dörnbrack, S. Meilinger, B. Luo, N. Larsen, J. Schreiner, K. Mauersberger, and T. Peter, Non-equilibrium compositions of ternary polar stratospheric clouds in gravity waves, *Geophysical Research Letters*, submitted, 2000a.
- Voigt, C., J. Schreiner, A. Kohlmann, K. Mauersberger, N. Larsen, T. Deshler, C. Kröger, J. Rosen, A. Adriani, G. Di Donfrancesco, F. Cairo, J. Ovarlez, H. Ovarlez, C. David, and A. Dörnbrack, Nitric acid trihydrates in polar stratospheric cloud particles, *Science*, submitted, 2000b.
- Voigt, C. Ph.D. Thesis, in preparation, 2000c.

Presentations.

- Adriani, A., F. Cairo, F. Cardillo, G. Di Donfrancesco, R. Morbidini, M. Viterbini, J. Ovarlez, H. Ovarlez, T. Deshler, C. Kröger, J. Rosen, C. David, S. Bekki, K. Mauersberger, C. Voigt, A. Kohlmann, J. Schreiner, and N. Larsen, Balloon-borne Measurements of chemical, physical, and optical properties of polar stratospheric clouds. Part I: Instruments flown on 25 January 2000, THESEO-2000/SOLVE science team meeting, 25-29 September 2000, Palermo, Italy.
- Deshler, T., C. Kröger, J. Rosen, C. Voigt, A. Kohlmann, J. Schreiner, K. Mauersberger, N. Larsen, J. Ovarlez, A. Adriani, F. Cairo, G. Di Donfrancesco, C. David, and S. Bekki, Balloon-borne Measurements of chemical, physical, and optical properties of polar stratospheric clouds. Part II: Particles near the frost point temperature, THESEO-2000/SOLVE science team meeting, 25-29 September 2000, Palermo, Italy.
- Deshler, T., C. Kröger, J. Rosen, C. Voigt, A. Kohlmann, J. Schreiner, K. Mauersberger, N. Larsen, J. Ovarlez, H. Ovarlez, A. Adriani, F. Cairo, and G. Di Donfrancesco, Index of Refraction of Polar Stratospheric Cloud Particles Inferred from Balloonborne Measurements of the Chemical, Physical and Optical Properties of the Particles, American Geophysical Union Fall Meeting, San Francisco, USA, 15-19 December 2000.
- I. S. Mikkelsen, N. Larsen, and K.H. Fricke, Simulations of mountain waves observed over Northern Scandinavia using different model resolutions, Fifth European Symposium on Polar Stratospheric Ozone Research, St. Jean de Luz, France, September 1999, (poster).
- Larsen, N., I.S. Mikkelsen, C. Voigt, J. Schreiner, F. Arnold, A. Kohlmann, U. Schild, P. Zink, and K. Mauersberger, Microphysical mesoscale simulations of Scandinavian leewave PSCs, analysed for chemical composition and optical properties, International workshop on mesoscale processes in the stratosphere, Bad Tölz, Germany, 9-11 November 1998.
- Larsen, N., Chemical understanding of ozone loss - heterogeneous processes: Microphysical understanding and outstanding issues, Fifth European Symposium on Polar Stratospheric Ozone Research, St. Jean de Luz, France, September 1999.
- Larsen, N., Ib Steen Mikkelsen, Bjørn M. Knudsen, Jochen Schreiner, Christiane Voigt, Konrad Mauersberger, James M. Rosen, and Norman T. Kjome, Comparison of chemical and optical in-situ measurements of PSC particles, Fifth European Symposium on Polar Stratospheric Ozone Research, St. Jean de Luz, France, September 1999.
- Larsen, N., Arctic ozone depletion: The role of polar stratospheric clouds in a colder climate, Danish Society for Atmospheric Research, 1st conference, Copenhagen, October 1999.
- Schiller C., J. Beuermann, R. Müller, F. Stroh, A. Engel, M. Müller, N. Larsen, and J. Ovarlez, Dehydration in the Arctic stratosphere during the THESEO2000 / SOLVE campaigns, Proceedings of the THESEO2000 / SOLVE Workshop, Palermo, September 2000.
- Schreiner J., A. Kohlmann, C. Voigt, P. Zink, K. Mauersberger, N. Larsen, Composition measurements of polar stratospheric cloud particles, EGS, 19-23. April 1999, Den Haag, Nethland
- Schreiner J., A. Kohlmann, C. Voigt, P. Zink, K. Mauersberger, Composition measurements of polar stratospheric cloud particles, EGS, 25-29 April 2000, Nice, France.
- Schreiner, J. A. Kohlmann, C. Voigt, P. Zink and K. Mauersberger, T. Deshler., C. Kröger, J. Rosen, C. David and N. Larsen, Characterisation of polar stratospheric clouds, AGU, 25-29 September 2000, Washington, USA
- Voigt, C., J. Schreiner, F. Arnold, A. Kohlmann, U. Schild, P. Zink, K. Mauersberger, and N. Larsen, First in-situ measurements of the chemical composition of polar stratospheric cloud particles, International workshop on mesoscale processes in the stratosphere, Bad Tölz, Germany, 9-11 November 1998.

- Voigt, C., J. Schreiner, K. Mauersberger, A. Tsias, T. Peter, N. Larsen, A. Dörnbrack, A case study of PSC particle formation, Fifth European Symposium on Polar Stratospheric Ozone Research, St. Jean de Luz, France, September 1999.
- Voigt, C., J. Schreiner, A. Kohlmann, K. Mauersberger, T. Deshler, C. Kröger, J. Rosen, N. Larsen, A. Adriani, G. Di Donfrancesco, F. Cairo, J. Ovarlez, H. Ovarlez, C. David, and S. Bekki, Balloon-borne Measurements of chemical, physical, and optical properties of polar stratospheric clouds. Part II: Particles at temperatures near TNAT, THESEO-2000/SOLVE science team meeting, 25-29 September 2000, Palermo, Italy.
- Voigt, C., J. Schreiner, A. Kohlmann, P. Zink, F. Arnold, K. Mauersberger and N. Larsen, Ternary solution PSCs Measured in Leewaves. EGS, 19-23. April 1999, Den Haag, Nethland
- Voigt, C. J. Schreiner, A. Kohlmann, U. Schild, P. Zink, F. Arnold, N. Larsen, K. Mauersberger, First in situ measurements of the chemical composition of PSCs, Theseo project meeting July 1999, Heidelberg, Germany
- Voigt, C., J. Schreiner, P. Zink, A. Kohlmann, K. Mauersberger, Messung der Komposition polarer stratosphärischer Wolkenteilchen Bunsentagung, May 1999, Dortmund, Germany

PART B: INDIVIDUAL REPORT.

Contractor (coordinator): Danish Meteorological Institute (DMI.RDD.MAR)

Leading scientist: Niels Larsen

Scientific and technical staff: Ib Steen Mikkelsen
Bjørn Knudsen

Address: Lyngbyvej 100
DK-2100 Copenhagen
Denmark

Telephone. +45-3915-7414

Fax: +45-3915-7460

E-Mail: nl@dmi.dk
ism@dmi.dk
bk@dmi.dk

I. OBJECTIVES

- i) Co-ordination of the project.
- ii) Installation of a non-hydrostatic meteorological mesoscale model (Regional Atmospheric Modelling System; RAMS-3b), and addition of a 3D streamline integration module for trajectory calculations.
- iii) Development of a non-equilibrium microphysical model for liquid type 1b polar stratospheric cloud particles. Inclusion of a module for homogeneous freezing of liquid particles in the model.
- iv) Participation in the test flight campaign in Kiruna, January 1998 and in the THESEO-2000 campaign by backscatter sonde measurements, provision of stratospheric PV and temperature forecast.
- v) Meteorological mesoscale analysis in connection with the PSC observations.
- vi) Microphysical analysis of observations.
- vii) Presentation of results at international meetings

II. MAIN RESULTS OBTAINED:*Project coordination.*

Four regular project meetings have taken place, all at the Max-Planck-Institut für Kernphysik in Heidelberg. In addition two major project meeting took place at Esrange in January/February 1999. Three of the project meetings in Heidelberg concerned the specification of instrument integration, instrument assembly, instrument and TM testing, and flight planning while the final meeting concerned the scientific analysis and discussions of the measurements obtained in January 2000. The project meetings in Esrange mainly concerned count down planning and logistics and plans for postponing the experiments for one year due to unfavourable meteorological conditions for PSC formation in winter 1998/99. Minutes from all project meetings are available from the coordinator. In addition to the project meetings, a few consultation meetings between the coordinator and MPI have taken place.

Backscatter sonde measurements.

Part of the DMI / University of Wyoming-PA national funded contribution to the project has been directed into participation of the flight experiment from Esrange using the University of Wyoming backscatter sondes. The backscatter sonde has been mounted on the common gondolas together with the other PSC-analysis instruments and has also been flown on independent small balloons prior to the launch of the PSC-analysis gondola in PSC survey flights. These first backscatter sounding provide information about the approximate altitude of PSC occurrence.

The University of Wyoming backscatter sonde¹ is equipped with a xenon flash lamp, emitting collimated horizontal light pulses about once every 7 second. The backscattered light from the aerosol and cloud particles is detected by two silicon photodiodes on the sonde, each equipped with filters transmitting in two wavelengths around 480 and 940 nm. The sonde detects the backscattered signal at an angle about 173° with respect to the beam forward direction from an air volume of app. 1 m³ within a few meters in front of the instrument and can be used up to at least 30 km. Air pressure and temperature are measured simultaneously with the optical signals. The sonde can also be equipped with an ozone sensor. The basic measurement is the aerosol backscatter ratio, i.e. ratio between the particulate and molecular volume backscattering coefficients at the two wavelengths (B_{940} and B_{480}) from which a colour index C ($C = B_{940}/B_{480}$) is derived. The colour index gives an indication of the presence of liquid ($C < 6$) or solid phase particles ($C > 9$)². In Figure 1 is shown the backscatter sonde.

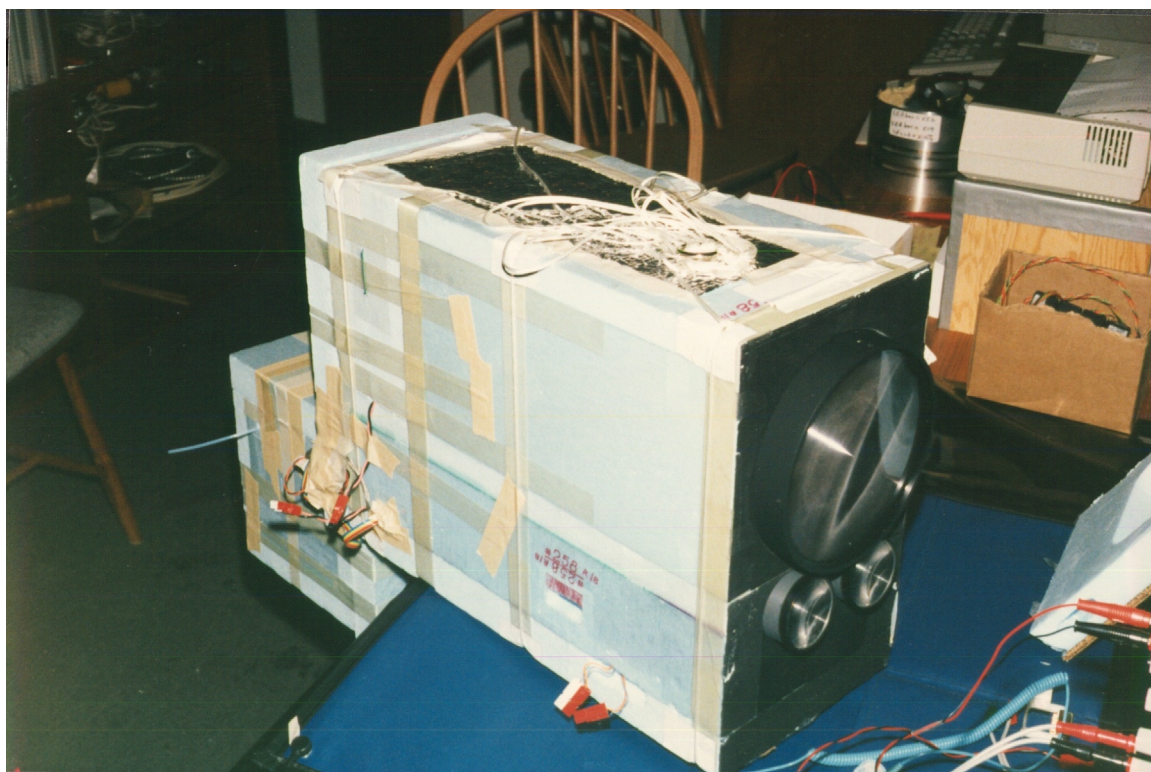


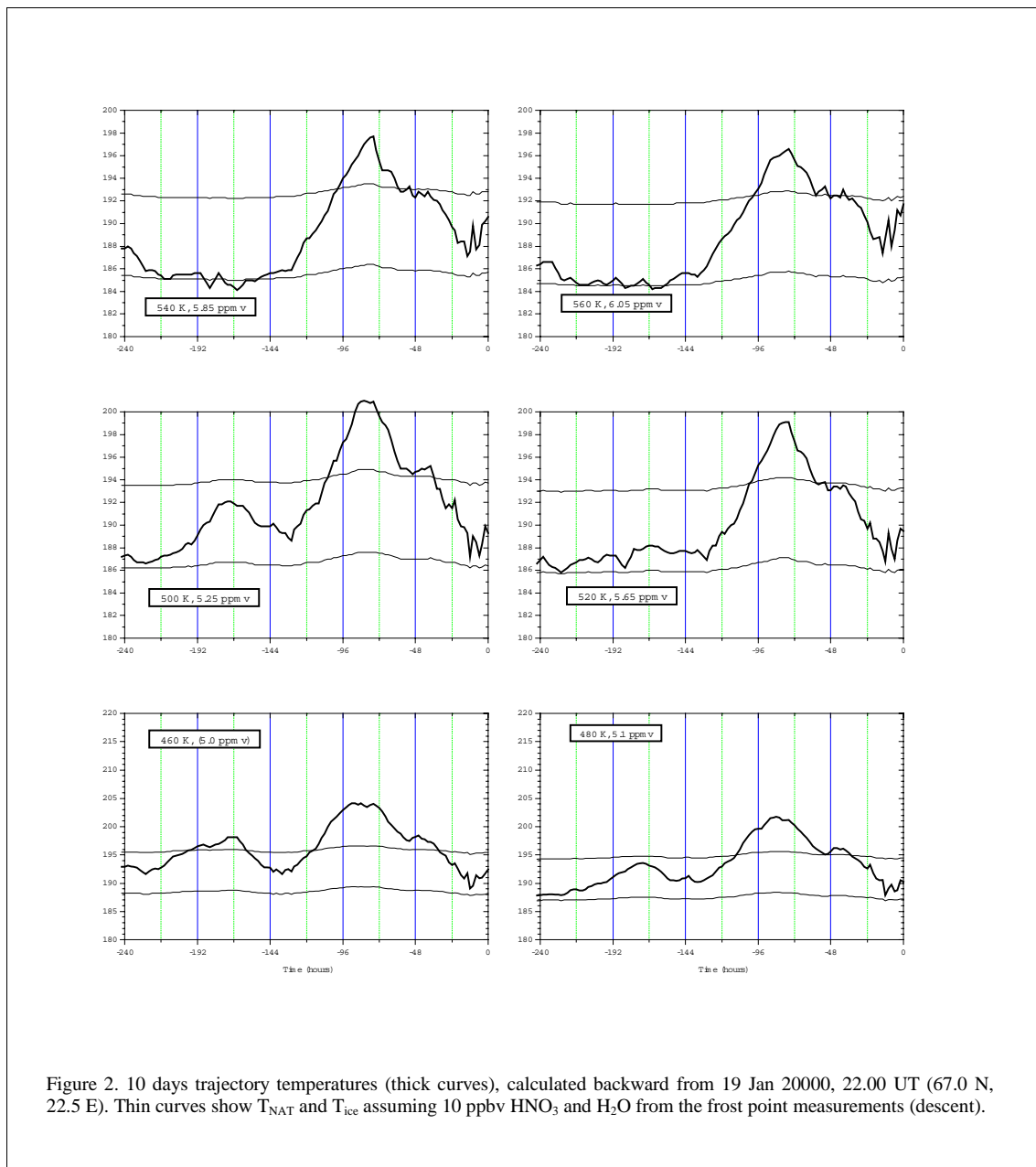
Figure 1. University of Wyoming backscatter sonde.

Meteorological synoptic scale analysis of the observations.

During the campaigns, the DMI have provided 10-days forecasts of stratospheric temperatures and maps of potential vorticity and temperatures, used for flight planning. Synoptic 10-days backward isentropic trajectories, based on ECMWF analyses, have been calculated, giving the temperature histories of the observed particles prior to entering the Scandinavian mountain region where the detailed RAMS model provide the high resolution temperature histories. The synoptic 10-days temperature histories of the 19 January and 25 January 2000 observational cases appear in Figure 2 and 3, calculated at potential temperatures 460,480,500,520, 540, and 560 K.

¹ Rosen, J.M. and N.T. Kjome, Backscattersonde: a new instrument for atmospheric aerosol research, *Appl. Opt.* 30, 1552-1561, 1991

² Larsen, N., B.M. Knudsen, J.M. Rosen, N.T. Kjome, R. Neuber, and E. Kyrö: Temperature histories in liquid and solid polar stratospheric cloud formation, *J. Geophys. Res.* 102, 23505-23517, 1997.



In the 19 January case it can be seen that temperatures at the highest altitudes have been close to the ice frost point 6-10 days prior to the observations and freezing could have taken place during this period. Any solid particles would probably remain in the solid phase since temperatures do not rise above the sulphuric acid tetrahydrate (SAT) melting temperature (≈ 215 K). On the other hand, nitric acid in the particles would have evaporated in the warming 3-4 days prior to the observations since temperature rise well above T_{NAT} . If the process of melting upon cooling takes place³, solid particles might turn into liquid STS particles in the subsequent cooling prior to entering the mountain region.

³ Koop, T. and K.S. Carslaw, Melting of $\text{H}_2\text{SO}_4 \cdot 4\text{H}_2\text{O}$ Particles upon cooling: Implications for Polar Stratospheric Clouds, *Science* 272, 1638-1641, 1996.

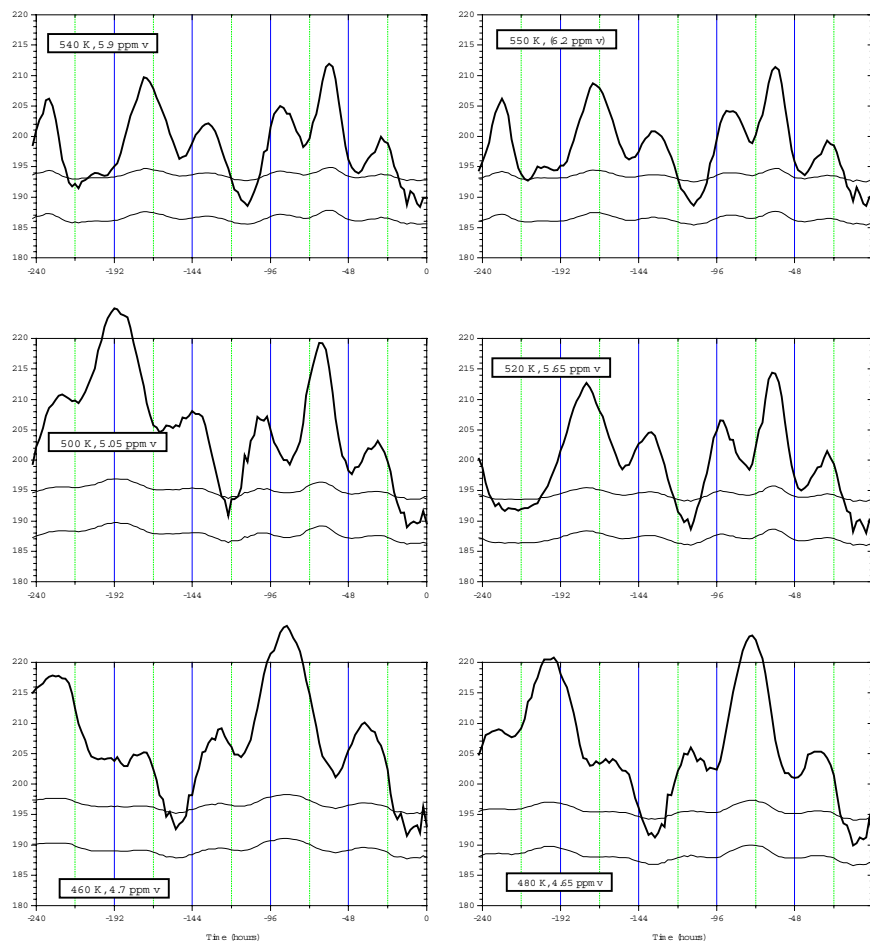


Figure 3. 10 days trajectory temperatures (thick curves), calculated backward from 25 Jan 2000, 21.00 UT (66.8 N, 23.8 E). Thin curves show T_{NAT} and T_{ice} assuming 10 ppbv HNO_3 and H_2O from the frost point measurements (descent).

The synoptic temperature histories of the particles observed on 25 January 2000 are much different. In this case temperatures were very high at all altitudes 2-3 days prior to observations. Any solid particles would probably have turned into the liquid state during this warming, and any freezing would probably have taken place in the mountain wave perturbations shortly before observation.

The modified potential vorticity has also been calculated along the 10-days backward trajectories. The modified potential vorticity is defined here as

$$MPV = PV \left(\frac{475\text{K}}{\theta} \right)^{4.5}$$

where PV is the potential vorticity and θ is the potential temperature. The 10-days backward MPV values of the calculated trajectories appear in Figure 4. Whereas the MPV values in the 19 January case stay nearly constant, the MPV values in the 25 January case vary considerably backward in time, indicating a mixture of external air into the polar vortex around 500 K. This could be the reason for the highly variable H_2O mixing ratios observed this day, compared to the 19 January case.

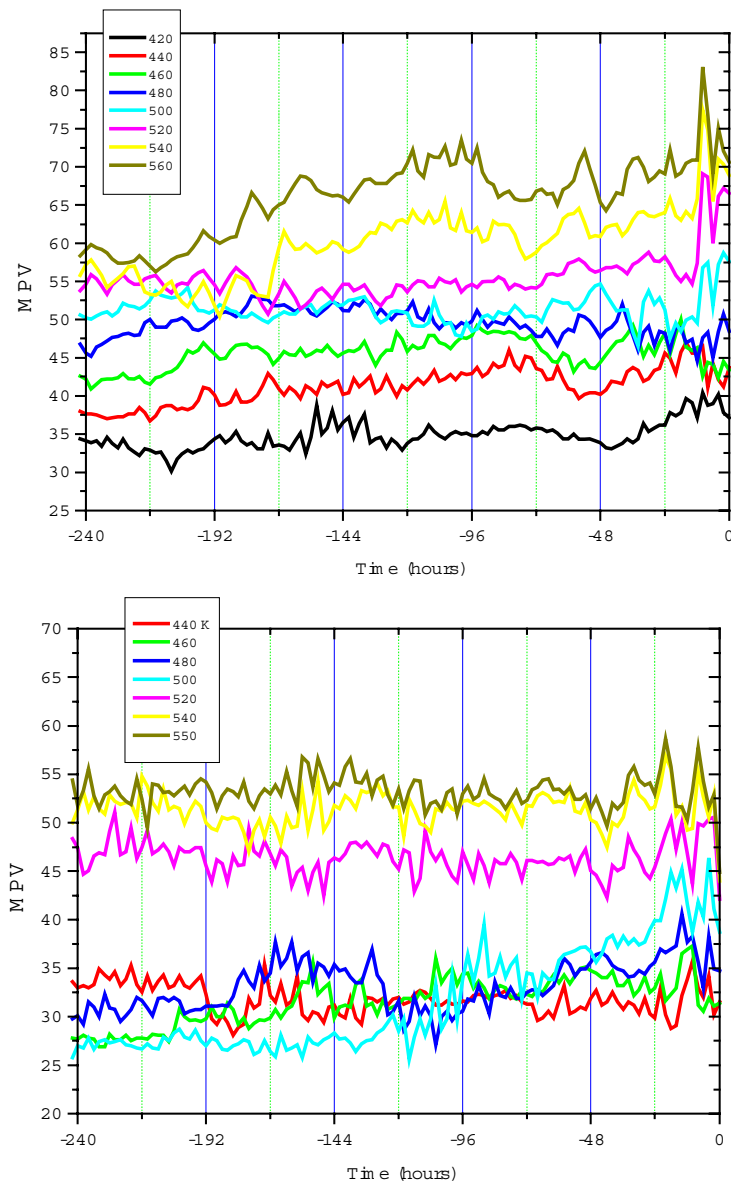


Figure 4. Modified potential vorticity of the same trajectories as in Figures ?? and ?? for the 19 January (upper panel) and 25 January 2000 case (lower panel), calculated at the potential temperature levels as indicated in the legend. MPV units: $10^{-6} \text{K m}^2 \text{s}^{-1} \text{kg}^{-1}$.

Meteorological mesoscale analysis of the observations.

Non-hydrostatic simulations of leewaves over Northern Scandinavia on 25 January, 1998.

Nonhydrostatic simulations of the moderate lee waves in the area surrounding Kiruna in connection with the 25 January 1998 test balloon flight have been performed using the first installation-version of the RAMS-model. The meteorological simulations have been described in detail by *Mikkelsen and Larsen* [1999]. The main grid of the model in this first version was centered at 21°E, 68°N and covered an area of 2400 × 2400 km with a horizontal grid size of 16 km. A nested grid, cocentered with the main grid, had a grid size of 4 km, and for both grids the vertical spacing was between 100 and 300 m. Analysis fields from the ECMWF and UKMO were used to start the integration of the model at January 24, 1998, 2000 UT. Air parcel trajectories were computed on the nested grid to coincide with the balloon as it reached the floating height. Isentropic temperature histories on the 491 K potential temperature surface, derived from the air parcel trajectories, were used as input to the microphysical/optical model to calculate the particle sizes, chemical compositions, and optical properties as the particles move over the mountains. Before January 24, 2000 UT, when the air parcels are located over the North Atlantic, a linear temperature decrease were approximated from synoptic temperature analysis.

Non-hydrostatic simulations of leewaves over Northern Scandinavia on 25 January, 2000

The purpose of these simulations is to establish the temperature and pressure history of the stratospheric air parcels of which the polar stratospheric cloud (PSC) contents was observed during the balloon flight on 25 January, 2000, 19:47-23:25 UT. We first summarize the meteorological situation and the waves present in the balloon data including the standard radiosoundings. The 'European Centre for Medium-Range Weather Forecasts' (ECMWF) analysis and forecast fields were used to initialize and force the high-resolution simulations. The model θ -level fields are used directly to interpolate the RAMS fields. With the T319 resolution of the ECMWF fields this has the advantage that gravity waves of 300 km wavelengths and larger already are present in the starting fields of the RAMS integration.

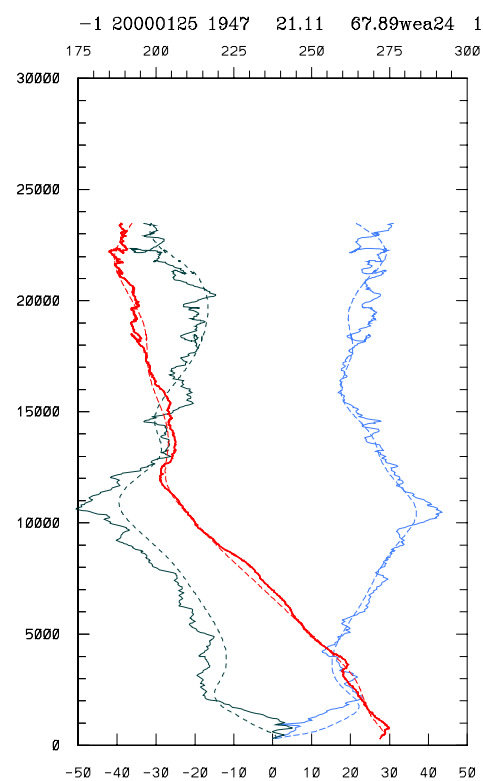


Figure 5. Temperature (K, red, top scale), zonal (blue), and meridional (green) wind (ms^{-1} , bottom scale) as function of altitude (m). Dashed profiles based upon ECMWF fields.

The balloon, launched at Esrange (21.08E,67.89N) at 19:47 UT on 25 January, 2000 covered the stratosphere 100-500 km downstream of - and in a southeastward direction normal to the ridge .

Figure 5 shows the temperature and wind profiles observed during the upleg. A bottom inversion 400 m above groundlevel is present in the temperature, a warm front at 4 km, a thermal tropopause at 12 km, a warm layer at 13-16 km altitude and the stratospheric temperature minimum at 22 km altitude where the solid PSC are observed. A low level jet is present at 2-4 km altitude, the jetstream is at 11 km altitude. The three dashed curves are the corresponding profiles interpolated in space and time from the ECMWF fields at 18, 21, and 00 UT (25-26 January) to be discussed later.

Figure 6 is a vertical cross section of the ECMWF potential temperature and temperature at 21 UT in a plane containing the complete balloon trajectory. The qualitative features of the ECMWF fields do not change during the balloon flight, and the comparison shall be limited to the 21 UT plot, although it applies in time to the first part of the flight shown in Figure 5 only.

wea24 2000-01-25-2100.g1

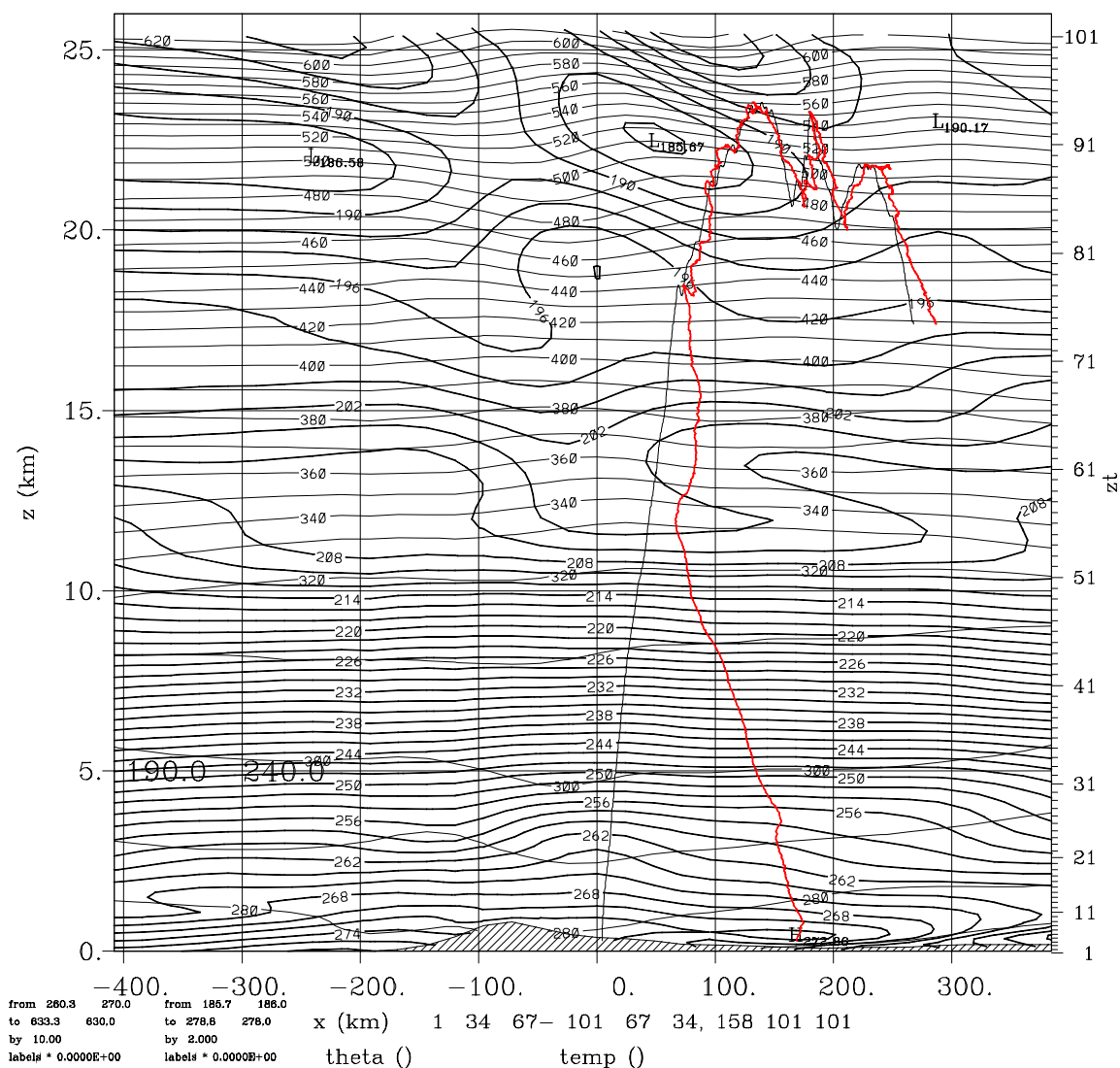


Figure 6. Vertical cross-section of the ECMWF fields at 21 UT in a plane containing the balloon trajectory. The abscissa is zonal displacement (km) with respect to 21°E, 68°N. Height (km) is shown on the left axis. Potential temperature (light black) is contoured in 10 K, and the regular temperature (heavy black) in 2 K intervals. The Scandinavian mountains are cross-hatched. The balloon trajectory is shown as a black light curve, and the balloon temperature as a red curve. (See text for explanation).

The balloon temperature profile in Figure 6 is plotted as a function of the height along a horizontal temperature axis, the origin of which is placed at the trajectory. The scale is such that a point at the trajectory corresponds to 190 K and the separation between the vertical grid lines drawn every 100 km corresponds to 50 K. The bottom inversion 400 m above ground level (see also Figure 6) is not well reproduced in the ECMWF temperature field. The hot, Foehn effect, is seen 100-200 km to the east 300 m above ground level. The high thermal tropopause is due to the large scale lee waves forming over the Scandinavian mountain ridge, lifting and adiabatically cooling the air around 12 km altitude. A horizontal plot shows indeed that these waves form parallel to the ridge. This orientation may also be seen in satellite pictures of the tropospheric clouds. The cooling in the lee wave extends the tropospheric lapse rate upward by 1-2 km. The warmer region above the thermal tropopause is not quite well reproduced in the ECMWF field as seen in Figures 5 and 6.

The upper part of the trajectory shows that the lowest temperatures (the red curve to the left of the trajectory) are placed near the top of a wave in the ECMWF fields. The agreement however breaks

down in the subsequent down- and uplegs. At the top of the first upleg a temperature minimum in the data coincide with a hot region in a wave valley and at the bottom of the first downleg the temperatures are in opposite phases. The 00 UT at 26 January ECMWF fields are different from the 21 UT fields, but the agreement with the last part of the data is not better.

As explained above, the RAMS model is initialized and forced using the ECMWF fields. We have made two runs, starting at 00, and 12 UT, 25 January. The RAMS model is formulated in polar stereographic coordinates, in this case with the pole placed at 21°E, 68°N. The grid points are equidistant in the projection plane with a separation of 24 km. This should be compared to the T319 ECMWF truncation corresponding to a minimum wavelength of $360/319=1.1^\circ$ greatcircle or 42 km gridspacing if three points are required to resolve a wavelength. In practice we apply the ECMWF fields at a T213 truncation as little information is present in the shorter wavelengths. At the start time the RAMS fields are identical to the ECMWF fields except for the differences in the orography. During the integration the RAMS fields are nudged along the boundary of the 2400 km times 2400 km model region using a linear interpolation of the 3-hourly ECMWF fields. The run for the first part of the day is tested against two radiosoundings from Esrange made during the morning that reached 35-37 km altitude. The data are interesting because of the very strong wave activity. The problems seen in comparing to the ECMWF fields are seen as well, but the RAMS model simulates more of the height variations because of the much better vertical resolution.

Figure 7 shows the comparison with the PSC balloon flight in the same format as Figure 6. In comparing Figures 6 and 7 it is seen that the lee behind the Scandinavian mountain range is stronger in the ECMWF simulation whereas more Atlantic air is swept over the range in the RAMS simulation. The stronger winds over the range cause the waves to form nearer to the range. It is seen in the tropopausal wave and in the stratospheric waves. Until we understand why the RAMS model is behaving like this it is of less value to make simulations with higher resolutions. The RAMS model uses a climatological sea-surface temperature, which has a slightly warmer Gulf Stream than the actual sea surface temperatures from the ECMWF analysis for 25-26 January, 2000. The higher temperatures make the Atlantic troposphere more unstable allowing the air to easier pass the mountains. The actual SST shall be used in the RAMS simulations. In the RAMS simulations presented here, the thickness of the model layers is 100 m in the troposphere which should be compared to a higher layer density in the ECMWF model. RAMS simulations with 50 m layer thickness at the surface shall be performed. The simulations have been made with two nested grids, both centred at Esrange, having the same vertical resolution and 8 and 2 km horizontal resolutions. This was to test if the drag from smaller scale gravity waves could create the reduced wind speed over the mountains, but this is not the case. The 2-km fields show very large cooling rates resulting in temperatures of 179 K. These are however earlier in the day and do not affect the air parcels that are observed during the PSC balloon flight. Trajectories have been integrated using the RAMS field values at each model integration step for all simulations and made available to the PSC modelling.

In conclusion, much can be learnt from the ECMWF fields using the full information available in the ECMWF model level data. These have been used as well to initialize and force the RAMS simulations. The RAMS simulations contain lee waves of a different, and incorrect nature, having larger wind speeds over the mountains. There is qualitative agreement only with the observed stratospheric temperature variations in both ECMWF and RAMS.

aej24 2000-01-25-2100.g1

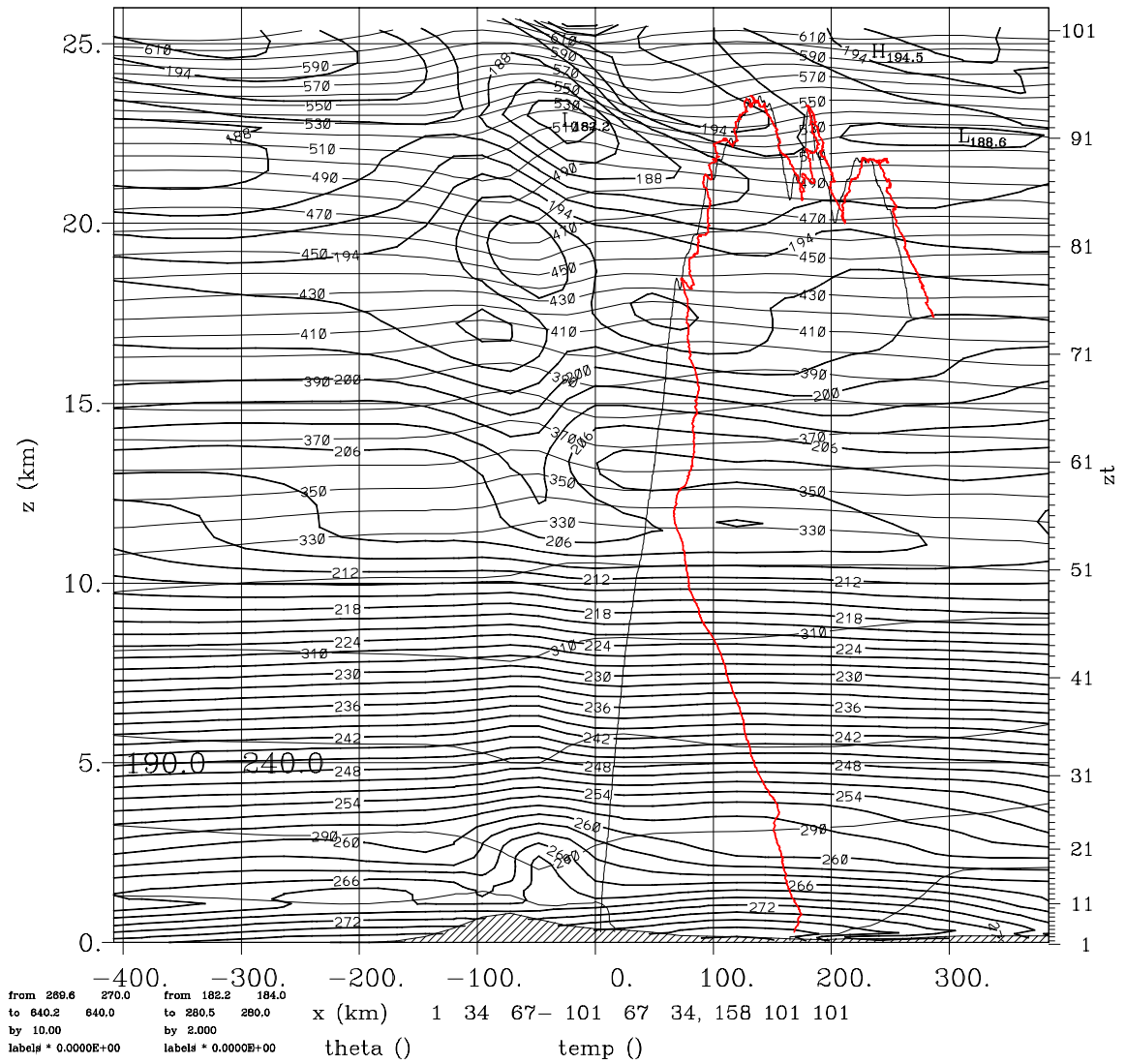


Figure 7. RAMS simulations in the same format as Figure 6.

Microphysical model developments.

Polar stratospheric cloud particles, observed in the lee of mountains as in this project, could be exposed to strong temperature fluctuations as the air passes over the mountain ridge. Liquid type 1b PSC particles are generally believed to be composed of supercooled ternary solutions (STS) ($\text{HNO}_3/\text{H}_2\text{O}/\text{H}_2\text{SO}_4$). When the temperature decreases nitric acid and water condenses on the particles, changing the composition into a nearly binary nitric acid solution at very low temperatures. Due to slow diffusion of nitric acid in the gas phase, the rapid temperature fluctuations imply that only the smallest cloud particles in the size distribution will obtain equilibrium with the gas phase. Thereby the composition of the liquid particles is expected to depend on their radius with the smallest particles obtaining the highest HNO_3 concentration at low temperatures.

A new version of the DMI microphysical PSC model has been developed which allows for the non-equilibrium simulation of liquid type 1b PSC particles [Larsen, 2000a]. The model takes as input the time-dependent ambient air temperature, pressure, and mixing ratios (partial pressures) of H_2O and HNO_3 , and calculates the time-dependent PSC size distributions and gas phase concentrations, assuming an initial size distribution of background sulphate aerosols. The exchange of mass between the gas and condensed phase during particle growth and evaporation is calculated by the basic vapour diffusion equation⁴. The model uses STS vapour pressures⁵ and takes into account kinetic surface, latent heat, and the Kelvin effects. The model applies “Lagrangian” particle growth in radius space; that is, the model calculates the time-dependent radius of individual particles in a number of size classes, each size class having a fixed number of particles per kilogram of air. This eliminates problems with numerical diffusion when using fixed size bins, and the calculation of the particle size distribution is exactly reversible in repeated condensation-evaporation cycles. The Lagrangian approach allows for non-equilibrium simulation of particle growth in fast changing temperature conditions where slow HNO_3 diffusion in the gas phase will imply that only the smallest particles quickly obtain equilibrium with the gas, giving rise to a size-dependent composition of the STS particles. This is particularly important for simulation of PSCs in mountain lee wave conditions⁶. The model also simulates the growth and evaporation of type 1a PSC particles (assumed to be composed of NAT) and type 2 PSC ice particles once these particles are formed by homogeneous freezing of liquid type 1b PSC particles below the ice frost point⁷. The optical model takes as input the liquid particle size distributions from the microphysical model and calculates from Mie theory⁸ the expected aerosol backscatter ratios at 940 and 480 nm and thereby the colour index as observed by the University of Wyoming backscatter sonde. The calculations take account of the angular distribution of the reflected light into the backscatter sonde. The composition-dependent (and thereby size-dependent) real parts of refractive indices of STS are calculated⁹, assuming a negligible imaginary part (10^{-7}). For the calculations shown below, 500 size classes have been applied in the microphysical model

⁴ Pruppacher, H.R., and J.D. Klett, *Microphysics of Clouds and Precipitation*, 2.ed., Kluwer Academic Publishers, Dordrecht, Boston, London, 954 pp., 1997.

⁵ Luo, B., K.S. Carslaw, T. Peter, and S.L. Clegg, Vapour pressures of $\text{H}_2\text{SO}_4/\text{HNO}_3/\text{HCl}/\text{HBr}/\text{H}_2\text{O}$ solutions to low stratospheric temperatures, *Geophys. Res. Lett.* 22, 247-250, 1995.

⁶ Meilinger, S., T. Koop, B.P. Luo, T. Huthwelker, K.S. Carslaw, U. Krieger, P.J. Crutzen, and T. Peter, Size-dependent stratospheric droplet composition in mesoscale temperature fluctuations and their potential role in PSC freezing, *Geophys. Res. Lett.*, 22, 3031-3034, 1995.

⁷ Tabazadeh, A., S.T. Martin, and J.S. Lin, The effect of particle size and nitric acid uptake on homogeneous freezing of sulfate aerosols, *Geophys. Res. Lett.*, 27, 1111-1114, 2000.

⁸ Bohren, C.F. and D.R. Huffman, 1983, *Absorption and Scattering of Light by Small Particles*, J. Wiley & Sons, New York, 530 pp.

⁹ Krieger, U.K., J.C. Mössinger, B. Luo, U. Weers, and T. Peter, Measurements of the refractive indices of $\text{H}_2\text{SO}_4/\text{HNO}_3/\text{H}_2\text{O}$ solutions to stratospheric temperatures, *Appl. Opt.*, 39, 3691 – 3703, 2000.

Microphysical analysis of the observations.

The DMI microphysical model was used, so far, for analysis of the results from the test flight in January 1998 (cf. Figure 1 in Part A of this report) [Larsen *et al.*, 2000] and of the PSC-analysis flight on 25 January 2000 (Figure 5 in Part A of this report).

25 January 1998 case.

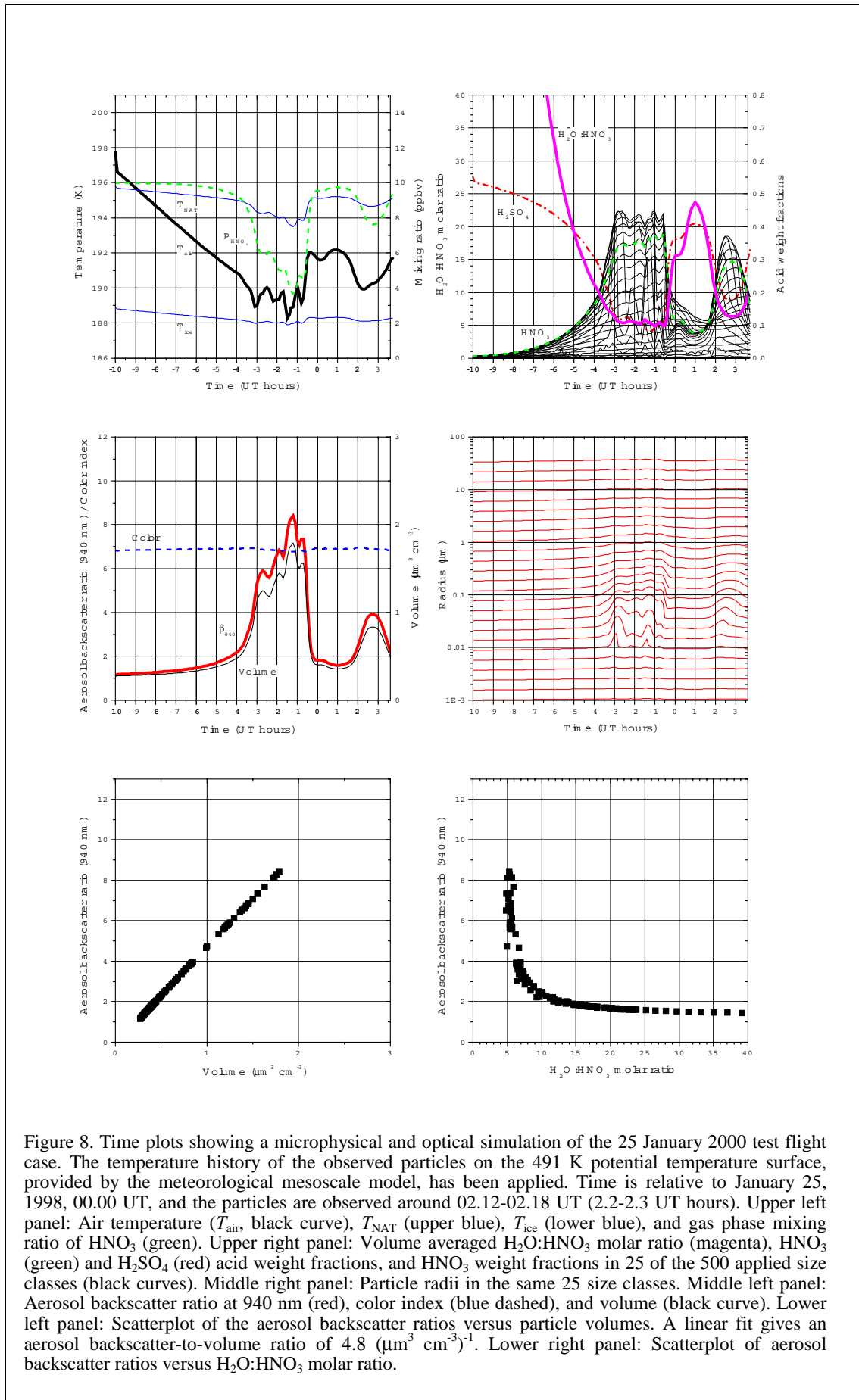
The temperature histories, calculated by the RAMS model for the 25 January 1998 case have been used as input to the microphysical model. Result appear in Figure 8. The upper left panel of Figure 8 shows as functions of time the air temperature (T_{air}), T_{NAT} , T_{ice} , and gas phase mixing ratio of HNO_3 . The upper right panel shows as functions of time the volume-averaged $\text{H}_2\text{O}:\text{HNO}_3$ molar ratio, approaching a value of 6 at temperatures lower than 190 K, the volume averaged HNO_3 and H_2SO_4 weight fractions, and the HNO_3 weight fraction of particles in every 20 of the applied 500 individual size classes, where the smallest activated particles obtain the largest HNO_3 weight fractions. The middle right panel shows as functions of time the radii in the same size classes. Particles with radii smaller than $\approx 0.005 \mu\text{m}$ do not grow due to the Kelvin effect, while the smallest of the activated particles with radii between approximately 0.01 and $0.1 \mu\text{m}$ show the fastest response to changes in temperature. The curves in the middle left panel show as functions of time the aerosol backscatter ratio at 940 nm, the colour index, and the total particle volume. The aerosol backscatter ratio and volume display the characteristic sharp increases in a narrow temperature range, with the colour index staying nearly constant between 6.5 and 7. The solid square symbols in the lower left panel show a scatterplot of the calculated aerosol backscatter versus volume, and those in the lower right panel show the aerosol backscatter ratio versus $\text{H}_2\text{O}:\text{HNO}_3$ molar ratio (results shown for every 0.1 hours throughout the simulation). The backscatter ratios increase significantly above the background levels only when the molar ratios are lower than ≈ 10 . In the actual volume and temperature range, a nearly linear relationship between aerosol backscatter and volume in the lower left panel is derived with an aerosol backscatter-to-volume ratio of $4.8 (\mu\text{m}^3 \text{cm}^{-3})^{-1}$ at 940 nm wavelength. At the time of the measurements (0212-0218 UT, or 2.2-2.3 UT hours) the model calculates aerosol backscatter ratios around 3 and $\text{H}_2\text{O}:\text{HNO}_3$ ratios around 7, both significantly lower than measured.

For representative stratospheric sulphate concentrations and gas phase mixing ratios of nitric acid and water vapour, the measured chemical composition of the particles with $\text{H}_2\text{O}:\text{HNO}_3$ values between 10 and 30 (cf. Figure 1 in Part A) would correspond to particle volumes lower than $0.7 \mu\text{m}^3 \text{cm}^{-3}$, assuming the particles to be composed of STS in equilibrium with the gas phase. Using the derived aerosol backscatter-to-volume ratio, $4.8 (\mu\text{m}^3 \text{cm}^{-3})^{-1}$, this particle volume would be expected to give rise to an aerosol backscatter ratio around 3.4. This also seems to contradict the measured aerosol backscatter with values up to 11 in the PSC at 8000 s.

Taken separately, the chemical and optical measurements could be explained assuming that the PSC particles are composed of supercooled ternary solutions. However, the particles are very dilute in HNO_3 , so, according to both equilibrium and microphysical model results, they would be interpreted as STS particles with a low volume, corresponding to a relatively small uptake of HNO_3 and H_2O . The predicted low STS particle volume would give rise to a much smaller aerosol backscatter ratio than actually observed. Non-equilibrium effects induced by mountain lee wave temperature perturbations do not seem to explain the discrepancy. Uncertainties in the assumed refractive indices of the particles could be a straightforward explanation, but the required high values of the real part refractive indices (>1.50 at 940 nm) are in disagreement with previous laboratory experiments and theoretical predictions¹⁰, although more consistent with recent Arctic observations¹¹.

¹⁰ Luo, B., U.K. Krieger, and T. Peter, Densities and refractive indices of $\text{H}_2\text{SO}_4/\text{HNO}_3/\text{H}_2\text{O}$ solutions to stratospheric temperatures, *Geophys. Res. Lett.* 23, 3707-3710, 1996.

¹¹ Deshler, T., B. Nardi, A. Adriani, F. Cairo, G. Hansen, F. Fierli, A. Hauchecorne, and L. Pulvirenti, Determining the index of refraction of polar stratospheric clouds above Andoya (69°N) by combining size-resolved concentration and optical scattering measurements, *J. Geophys. Res.*, 105, 3943-3953, 2000.

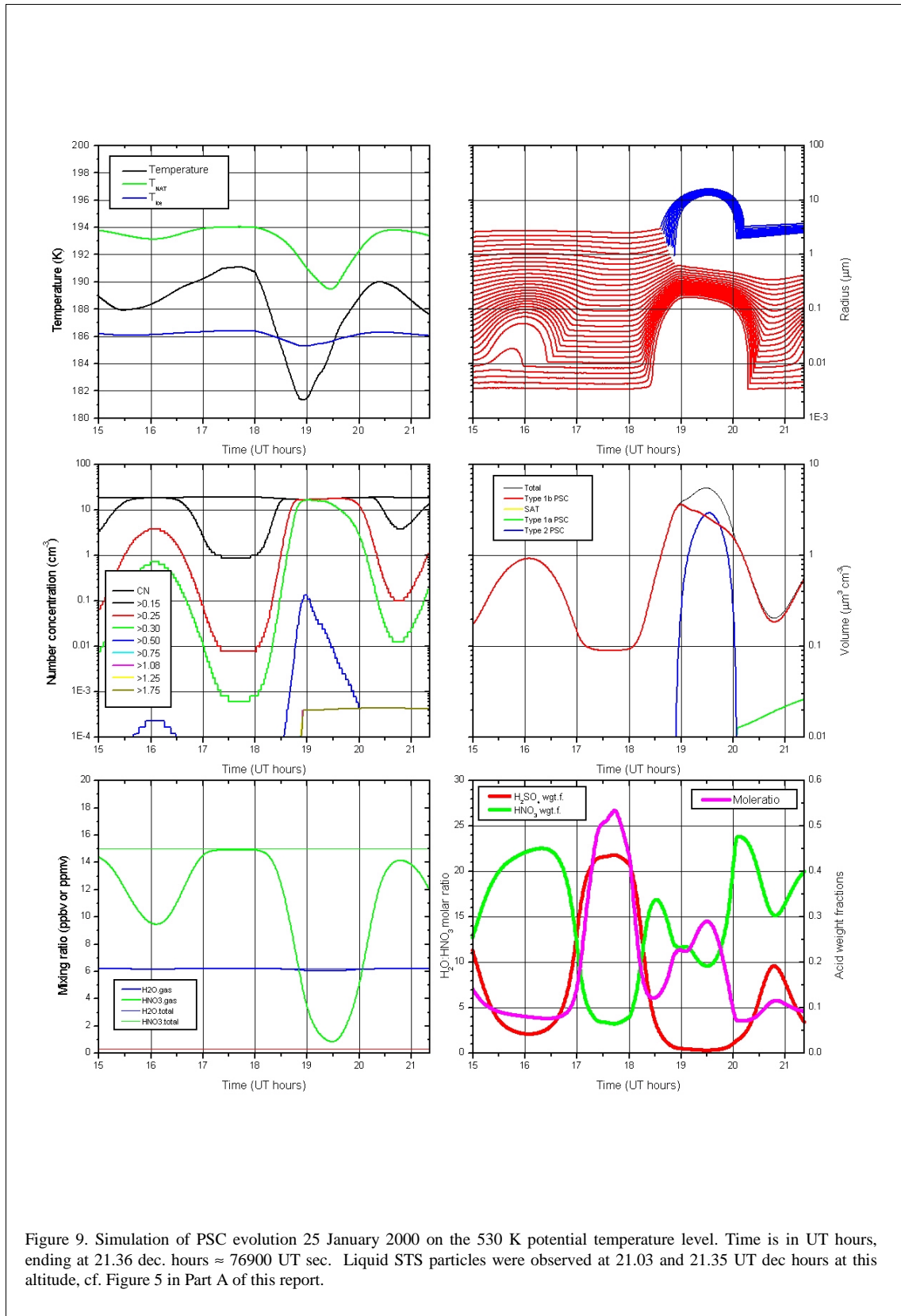


25 January 2000 case.

Two layers of particle observations are of particular interest in this case, namely the layer of liquid STS particles observed around 530-535 K at 76100 and 76900 UT seconds (21.14 and 21.36 UT dec. hours) and the layer around 500-510 K with solid NAT particles (cf. Figure 5 in Part A of this report). The latter particles were encountered several times during the flight at 75700 (21.03), 77500 (21.53), 78400 (21.78), 79700 (22.14), and 81000 (22.50) UT seconds (UT dec. hours). The mesoscale trajectory analysis indicate that in fact the balloon hit nearly the same airparcels during these encounters, i.e. for each encounter the mesoscale model indicates the same airparcel. Temperature histories from the mesoscale model at these two altitudes were extended backward in time from a location west of the Scandinavian mountains well outside the mountain wave region and combined with synoptic temperature histories (cf. Figure 3) backward in time until the maximum temperatures were met 2-3 days prior to observation. This will give a good starting point for the microphysical simulations as the particles under these warm conditions could be assumed to be liquid sulphate aerosols.

The upper left panel of Figures 9 and 10 shows as functions of UT time (dec. hours) the air temperature, T_{NAT} , and T_{ice} . The upper right panel shows the radii of particles in every 20 of the applied 500 individual size classes; red curves for liquid and blue curves for solid particles. The middle right panel shows the total particle volume densities of different types of particles. The curves in the middle left panel shows total number of particles (CN, upper curve) and the integral (accumulated) particle size distributions $N(>r)$ in radii classes corresponding to the University of Wyoming optical particle counter, i.e. the number concentration of particles with radii $> r$ (cf. lower panel in Figure 5 in Part A of this report). The lower left panel shows the gas phase and total concentrations of nitric acid (HNO_3 , green, ppbv) and water (H_2O , blue, ppmv) and the total condensed sulphuric acid (H_2SO_4 , red, ppbv). The lower right panel shows the volume-averaged $\text{H}_2\text{O}:\text{HNO}_3$ molar ratio (magenta), and the volume averaged HNO_3 (green) and H_2SO_4 (red) weight fractions.

Figure 9 shows a simulation of the PSC evolution on the 530 K potential temperature surface where liquid STS particles were observed. The results are shown as function of UT dec. hours, ending at 21.36 dec. hours \approx 76900 UT seconds. Only the time interval after 15.00 dec. hours is shown where the airparcel passed over the mountain area before observation. The model was initialised at -39 hours, where temperatures were above 210 K, with a sulphate aerosol unimodal lognormal size distribution, characterised by a total number concentration of $N_t=25 \text{ cm}^{-3}$, median radius $r_m=0.075 \text{ }\mu\text{m}$, and geometric standard deviation $\sigma=1.35$, consistent with the OPC heated inlet measurements. The model simulates a total particle volume of $0.3\text{-}0.5 \text{ }\mu\text{m}^3 \text{ cm}^{-3}$ in good agreement with the observations (cf. Figure 5 in Part A of this report) and calculates $\text{H}_2\text{O}:\text{HNO}_3$ molar ratios between 4 and 7, consistent with the measurements. In Figure 11 are shown the calculated integral size distributions at 76100 (21.14) and 76900 (21.36) UT sec. (dec. hours), compared with the measurements (dots). The total number of particles and the size distributions are in good agreement with the measurements. The temperature reaches 3-4 K below the ice frost point around 19.00 UT dec. hours which induces freezing only among the few largest particles. After the temperature increases above T_{ice} , the ice evaporates, leaving behind a small concentration of relatively large NAT particles, which do not contribute significantly to the total particle volume and the average particle composition. However, these large particles do show up as a shoulder in the measured and simulated accumulated size distributions. The observed slight increase in particle sizes between the two measurements, separated by 800 seconds, is reflected in the simulations.



The simulation of the particle formation around 500-510 K where solid NAT particles were observed is shown in Figure 10. Only the time interval after UT dec. hours is shown where the airparcel passed over the mountain area before observation. In this simulation an initial bimodal lognormal size distribution of sulphate aerosols, existing at temperatures around 220 K 2-3 days prior to observation, was assumed. Consistent with the OPC heated inlet measurements the following bimodal lognormal parameters $N_i=(20.0 \text{ cm}^{-3}; 8.0 \cdot 10^{-3} \text{ cm}^{-3})$, $r_m=(0.045 \text{ }\mu\text{m}; 0.5 \text{ }\mu\text{m})$, and $\sigma=(1.68; 1.15)$ were adopted. The model simulates a total particle volume of $1\text{-}2 \text{ }\mu\text{m}^3 \text{ cm}^{-3}$ in good agreement with the observations (cf. Figure 5 in Part A of this report). The model calculates $\text{H}_2\text{O}:\text{HNO}_3$ molar ratios of 3, consistent with the measurements of NAT particle compositions. The temperature drops more than 8 K below the ice frost point around 19-20 dec. hours which induces a freezing into type 2 ice PSC particles of a substantial fraction of the liquid particles. The type 2 PSC particle volume rises shortly to values above $100 \text{ }\mu\text{m}^3 \text{ cm}^{-3}$ before the ice evaporates above T_{ice} , leaving behind a relative large concentration of type 1a PSC particles, composed of NAT which dominate the total particle volume. In Figure 11 is shown a comparison between the measured (dots) and calculated accumulated size distributions at time 75700 (21.03), 77500 (21.53), 78400 (21.78), 79700 (22.14), and 81000 (22.50) UT seconds (UT dec. hours). The model simulates the size distribution a radius between 0.3 and 1.25 μm reasonably well. However, it is difficult for the model to represent the small concentrations of larger particles with radii $> 1.75 \text{ }\mu\text{m}$, and the model tends to underestimate the concentrations of small particles. The freezing process depends strongly on the temperature history going through the temperature minimum and small errors in the mesoscale temperatures may introduce large changes in calculated size distributions. Also the adopted initial sulphate aerosol size distribution has an influence on the calculated PSC sizes. In this and the above example, a parameterised model for the homogeneous freezing process has been used. In this model version volume-proportional freezing is assumed to take place in a $\Delta T=8.8 \text{ K}$ symmetric temperature interval around T_{ice} . At the upper temperature end ($T_{\text{ice}}+4.4\text{K}$), freezing is assumed to be extremely slow (100 days to freeze a $1\text{ }\mu\text{m}$ STS particle) while at the low-temperature end ($T_{\text{ice}}-4.4\text{K}$), freezing takes place instantaneously (1 sec). The freezing temperature is variable since the first formed ice particles take up water vapour by condensation further reducing the water partial pressure and the ice frost point. Using this parameterisation, the calculated size distributions become strongly dependent on ΔT , and ΔT has been adjusted to make the best representation of the measured size distributions in the two cases, measured at 530 and 508 K potential temperature altitude. The modelling of homogeneous freezing, based on parameterisations from laboratory measurements¹², has also been attempted. However, using this (presumably more physically correct model) generates an even smaller concentration of large particles and the concentration of small particles would be too high, compared to the observations. Further work on improvements in the modelling of the freezing process is in progress.

¹² Tabazadeh, A., S.T. Martin, and J.S. Lin, The effect of particle size and nitric acid uptake on homogeneous freezing of sulfate aerosols, *Geophys. Res. Lett.*, 27, 1111-1114, 2000.

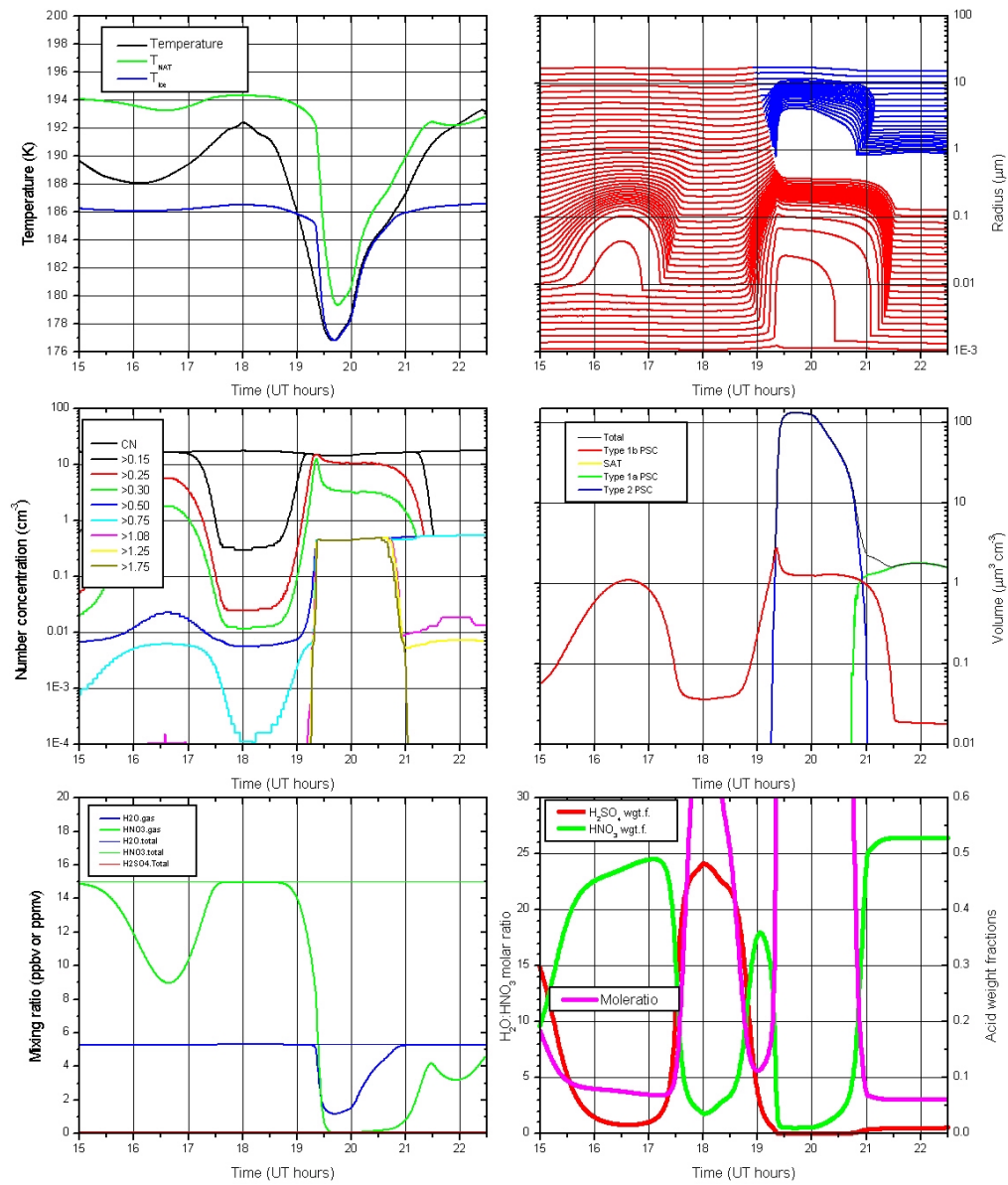
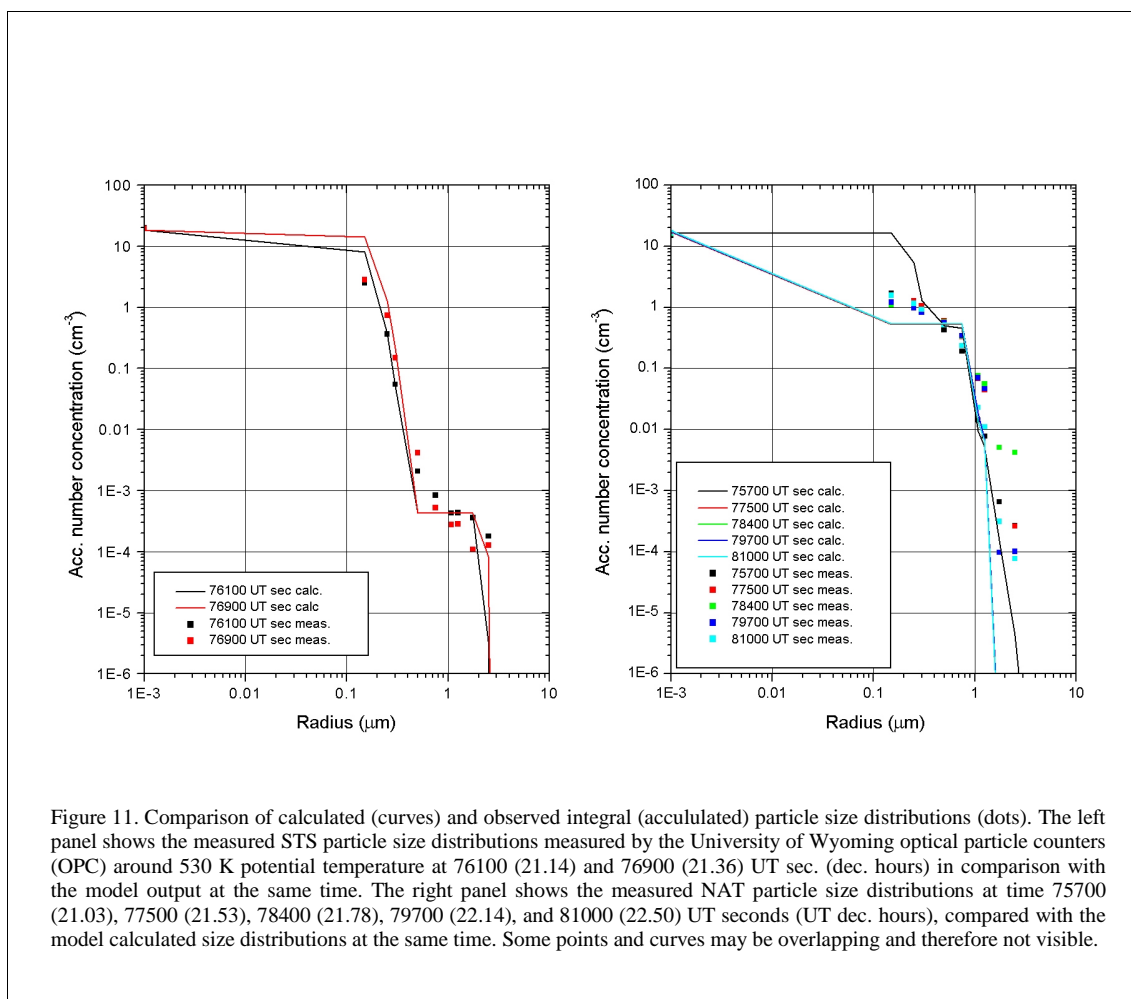


Figure 10. Simulation of PSC evolution 25 January 2000 on the 508 K potential temperature level. Time is in UT hours, ending at 22.50 UT dec. hours \approx 81100 UT sec. Solid NAT particles were observed around 21.03, 21.53, 21.78, 22.14, and 22.50 UT dec. hours cf. Figure 5 in Part A of this report.



III DEVIATIONS FROM TECHNICAL ANNEX AND REASONS.

There are no deviations from the technical annex in the DMI tasks.

V. CONCLUSIONS:

The objectives of the project have all been achieved. Modelling tools are now available and are being used for further analysis of the comprehensive data set obtained throughout the balloon flights. The unique data set offers outstanding possibilities to obtain new in-depth knowledge about the PSC formation processes. Due to the relatively short period between the field experiments and the formal termination of the project, the data analysis has not been fully completed. However, work is in progress for further analysis, and a number of papers are in preparation for the special issue of Journal of Geophysical Research about results from the THESEO-2000/SOLVE campaign.

Publications

- Carslaw, K.S., H. Oelhaf, B. Carli, M. Chipperfield, J.-N. Crowley, F. Goutail, B.M. Knudsen, N. Larsen, W. Norton, M. Rex, R. Ruhnke, and M. Volk, Polar Ozone Depletion, cp. 3, in Second Assessment of European Research on the Stratosphere, European Commission, submitted 2000.
- Carslaw, K.S., H. Volkert, P. Haynes, N.R.P. Harris, N. Larsen, G. Amanatidis, Th. Peter, The European Workshop on Mesoscale Processes in the Stratosphere – Overview and outcomes, in K.S. Carslaw and G.T. Amanatidis (ed), Mesoscale processes in the stratosphere, Their effect on stratospheric chemistry and microphysics, Proceedings of the European workshop 8 to 11 November 1998, Bad Tölz, Bavaria, Germany, Air Pollution Research Report no. 69, European Commission, pp. 1-6, 1999.
- Larsen, N., Ib Steen Mikkelsen, Bjørn M. Knudsen, Jochen Schreiner, Christiane Voigt, Konrad Mauersberger, James M. Rosen, and Norman T. Kjome, Comparison of chemical and optical in-situ measurements of PSC particles, Proceedings of the Fifth European Symposium on Polar Stratospheric Ozone Research, St. Jean de Luz, France, September 1999.
- Larsen, N., I.S. Mikkelsen, B.M. Knudsen, J. Schreiner, C. Voigt, K. Mauersberger, J.M. Rosen, and N.T. Kjome, Comparison of chemical and optical in-situ measurements of polar stratospheric clouds, *Journal of Geophysical Research*, 105, 1491-1502, 2000.
- Larsen, N., Polar Stratospheric Clouds, Microphysical and Optical Models, DMI Scientific Report 00-06, 2000a.
- Larsen, N., Chemical understanding of ozone loss - heterogeneous processes: Microphysical understanding and outstanding issues, Proceedings of the Fifth European Symposium on Polar Stratospheric Ozone Research, St. Jean de Luz, France, September 1999, Air Pollution Research Report, European Commission, 2000b.
- Larsen, N., I. S. Mikkelsen, B. M. Knudsen, C. Voigt, A. Kohlmann, J. Schreiner, K. Mauersberger, T. Deshler, C. Kröger, J. Rosen, A. Adriani, F. Cairo, and G. Di Donfrancesco, J. Ovarlez, H. Ovarlez, Microphysical mesoscale simulations of polar stratospheric cloud formation over Northern Scandinavia on 25 January 2000 constrained by in-situ measurements of chemical and optical cloud properties, *Journal of Geophysical Research*, abstract submitted, 2000.
- Mikkelsen, I.S. and N. Larsen, Non hydrostatic simulations of leewaves over northern Scandinavia on 25 January 1998, in K.S. Carslaw and G.T. Amanatidis (ed), Mesoscale processes in the stratosphere, Their effect on stratospheric chemistry and microphysics, Proceedings of the European workshop 8 to 11 November 1998, Bad Tölz, Bavaria, Germany, Air Pollution Research Report no. 69, European Commission, pp. 165-170, 1999.
- Mikkelsen, I. S., N. Larsen, and K.H. Fricke, Simulations of mountain waves observed over Northern Scandinavia using different model resolutions, Proceedings of the Fifth European Symposium on Polar Stratospheric Ozone Research, St. Jean de Luz, France, September 1999.
- Mikkelsen, I. S. and N. Larsen, Non-hydrostatic modeling of steep leewaves over Northern Scandinavia on 25 January 2000, *Journal of Geophysical Research*, abstract submitted, 2000.
- Rivière, E.D., N. Huret, J.-B. Renard, F.T.-Goffinont, M. Pirre, N. Larsen, S. Eckermann, C. Camy-Peyret, S. Payan, and F. Lefevre, Chlorine associated with mesoscale solid polar stratospheric clouds on February 26 1997 above Kiruna, Proceedings of the Fifth European Symposium on Polar Stratospheric Ozone Research, St. Jean de Luz, France, September 1999.
- Rivière, E., N. Huret, F.G. Taupin, J.B. Renard, M. Pirre, S. Eckerman, N. Larsen, T. Deshler, F. Lefèvre, S. Payan and C. Camy-Peyret, Role of leewave in the formation of solid PSCs: case studies from February 1997, *J. Geophys Res.*, 105, 6845-6853, 2000.

Schreiner, J., C. Voigt, A. Kohlmann, F. Arnold, K. Mauersberger, and N. Larsen, Chemical analysis of polar stratospheric cloud particles, *Science* 283, 968-970, 1999.

Voigt, C., A. Tsias, A. Dörnbrack, S. Meilinger, B. Luo, N. Larsen, J. Schreiner, K. Mauersberger, and T. Peter, Non-equilibrium compositions of ternary polar stratospheric clouds in gravity waves, *Geophysical Research Letters*, submitted, 2000.

Voigt, C., J. Schreiner, A. Kohlmann, K. Mauersberger, N. Larsen, T. Deshler, C. Kröger, J. Rosen, A. Adriani, G. Di Donfrancesco, F. Cairo, J. Ovarlez, H. Ovarlez, C. David, and A. Dörnbrack, Nitric acid trihydrates in polar stratospheric cloud particles, *Science*, submitted, 2000.

Presentations.

Adriani, A., F. Cairo, F. Cardillo, G. Di Donfrancesco, R. Morbidini, M. Viterbini, J. Ovarlez, H. Ovarlez, T. Deshler, C. Kröger, J. Rosen, C. David, S. Bekki, K. Mauersberger, C. Voigt, A. Kohlmann, J. Schreiner, and N. Larsen, Balloon-borne Measurements of chemical, physical, and optical properties of polar stratospheric clouds. Part I: Instruments flown on 25 January 2000, THESEO-2000/SOLVE science team meeting, 25-29 September 2000, Palermo, Italy.

Deshler, T., C. Kröger, J. Rosen, C. Voigt, A. Kohlmann, J. Schreiner, K. Mauersberger, N. Larsen, J. Ovarlez, A. Adriani, F. Cairo, G. Di Donfrancesco, C. David, and S. Bekki, Balloon-borne Measurements of chemical, physical, and optical properties of polar stratospheric clouds. Part II: Particles near the frost point temperature, THESEO-2000/SOLVE science team meeting, 25-29 September 2000, Palermo, Italy.

Deshler, T., C. Kröger, J. Rosen, C. Voigt, A. Kohlmann, J. Schreiner, K. Mauersberger, N. Larsen, J. Ovarlez, H. Ovarlez, A. Adriani, F. Cairo, and G. Di Donfrancesco, Index of Refraction of Polar Stratospheric Cloud Particles Inferred from Balloonborne Measurements of the Chemical, Physical and Optical Properties of the Particles, American Geophysical Union Fall Meeting, San Francisco, USA, 15-19 December 2000.

Larsen, N., I.S. Mikkelsen, C. Voigt, J. Schreiner, F. Arnold, A. Kohlmann, U. Schild, P. Zink, and K. Mauersberger, Microphysical mesoscale simulations of Scandinavian leewave PSCs, analysed for chemical composition and optical properties, International workshop on mesoscale processes in the stratosphere, Bad Tölz, Germany, 9-11 November 1998.

Larsen, N., Chemical understanding of ozone loss - heterogeneous processes: Microphysical understanding and outstanding issues, Fifth European Symposium on Polar Stratospheric Ozone Research, St. Jean de Luz, France, September 1999, (invited).

Larsen, N., Ib Steen Mikkelsen, Bjørn M. Knudsen, Jochen Schreiner, Christiane Voigt, Konrad Mauersberger, James M. Rosen, and Norman T. Kjome, Comparison of chemical and optical in-situ measurements of PSC particles, Fifth European Symposium on Polar Stratospheric Ozone Research, St. Jean de Luz, France, September 1999.

Larsen, N., Arctic ozone depletion: The role of polar stratospheric clouds in a colder climate, Danish Society for Atmospheric Research, 1st conference, Copenhagen, October 1999.

Rivière, E.D., N. Huret, J.-B. Renard, F.T.-Goffinont, M. Pirre, N. Larsen, S. Eckermann, C. Camy-Peyret, S. Payan, and F. Lefevre, Chlorine associated with mesoscale solid polar stratospheric clouds on February 26 1997 above Kiruna, Fifth European Symposium on Polar Stratospheric Ozone Research, St. Jean de Luz, France, September 1999.

Voigt, C., J. Schreiner, A. Kohlmann, K. Mauersberger, T. Deshler, C. Kröger, J. Rosen, N. Larsen, A. Adriani, G. Di Donfrancesco, F. Cairo, J. Ovarlez, H. Ovarlez, C. David, and S. Bekki, Balloon-borne Measurements of chemical, physical, and optical properties of polar stratospheric clouds. Part II: Particles at temperatures near TNAT, THESEO-2000/SOLVE science team meeting, 25-29 September 2000, Palermo, Italy.

PART B: INDIVIDUAL REPORT.

Contractor: Max-Planck-Gesellschaft zur Förderung der Wissenschaften e.V.,
represented by the Max-Planck-Institut für Kernphysik (MPIK)

Leading Scientist: Prof. Dr. K. Mauersberger

Scientific Staff: Dr. J. Schreiner, C. Voigt, Dr. A. Kohlmann

Address: Max-Planck-Institute for Nuclear Physics, Atmospheric Physics Division
PO.-Box 103980, D69029 Heidelberg
Saupfercheckweg 1, D69117 Heidelberg

Telephone: ++49 6221 516286
Fax: ++49 6221 516553
E-mail: konrad.mauersberger@mpi-hd.mpg.de
jochen.schreiner@mpi-hd.mpg.de

OBJECTIVES

Polar stratospheric clouds (PSCs) grow in the winter polar vortex from the stratospheric background sulfate aerosol at sufficiently low temperatures, i.e., below about 195 K, by condensation of mainly H₂O and HNO₃. Both liquid and solid PSC particles provide surfaces for the heterogeneous reactions leading to active chlorine- and bromine-containing species, which under the action of sunlight form catalytically ozone-destroying radicals. The only in-situ measurement of the chemical composition of PSCs before the present project has been performed in January 1998 during a flight from Kiruna with the balloon-borne apparatus developed for the THESEO campaign. The PSCs probed had formed in lee waves east of the Scandinavian mountains. The molar ratios H₂O/HNO₃ were consistently found above 10 at temperatures between 189 and 192 K, indicating supercooled ternary solution (STS) droplets of H₂O, HNO₃, and H₂SO₄ [1].

The main objective of MPIK within the framework of the present THESEO project was to accomplish more detailed analyses of PSC particles during two balloon flights. This required several modifications of the PSC-analysis instrument to improve its sensitivity, and to build a second duplicate instrument. Integration of the instruments of the partners (particle counters, backscatter sondes, hygrometer, temperature sensors) into two identical common balloon gondolas was also a task of MPIK. Two complete flight-ready gondolas enable two balloon flights without re-calibration and check-up of the instruments.

Due to the unfavorable weather conditions in January 1999, the planned balloon flights had to be cancelled. But in late January 2000, the Arctic stratosphere was unusually cold with the polar vortex above the North Atlantic and Scandinavia, so that there were a lot of PSCs above Kiruna and the flights could be performed successfully. Meanwhile further technical improvements of the PSC-analysis instruments were realized and extensively tested.

MAIN RESULTS OBTAINED

The PSC-Analysis Instrument

The instrument, depicted in **Figure 1**, combines an aerodynamic lens [2, 3] which collimates the aerosol particles into a narrow beam providing a separation of gaseous and condensed matter, a small particle evaporation sphere to convert the aerosol into a gas, and a mass spectrometer to measure the composition of the evaporated particles. High-speed differential pumping, provided by two LHe pumps, increases the aerosol-to-ambient-air ratio by a factor of $>3 \times 10^5$ [4].

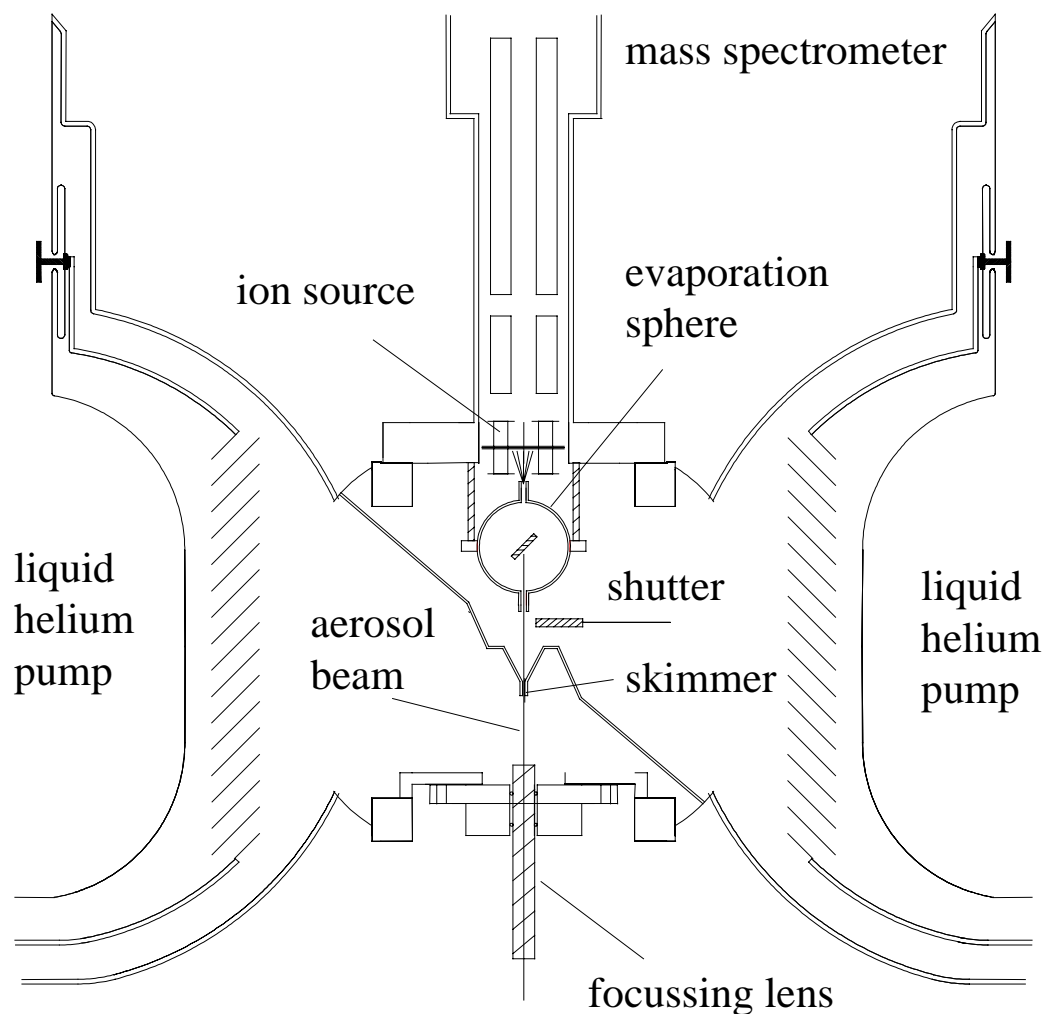


Figure 1: Schematic drawing of the PSC-analysis instrument. For explanations see the text.

Aerosols are drawn into a 100 mm long cylindrical tube with an inner diameter of 6 mm containing, at regular distances, seven circular orifices with diameters decreasing from 1.4 to 0.5 mm. These orifices concentrate aerosol particles with diameters of 0.1 to 4 μm towards the optical centerline so that a tightly collimated aerosol beam will be formed. At the exit the particles pass through a nozzle of 0.45 mm diameter where they become accelerated into the first vacuum chamber. This nozzle acts as a critical orifice controlling the gas flux through the lens of 15 cm^3/s . The lens is held in a manipulator to adjust the beam. The width of the aerosol beam is 1-2 mm in diameter at a distance of 95 mm so that a capillary tube (skimmer), 30 mm behind the lens is able to separate the aerosols from most gas molecules, which are rapidly dispersed after leaving the nozzle and condensed on the surface of the first LHe pump which will provide, at a pumping speed of more than 2000 L/s, a pressure of about 10^{-3} to 10^{-4} mbar. The skimmer is 30 mm long with an entrance opening of 0.8 mm and an exit of 1.6 mm in diameter.

Through the skimmer, the aerosol beam enters a second vacuum chamber also containing a LHe pump which provides a pressure of 5×10^{-8} mbar. (The pressure within the mass-spectrometer chamber should be as low as possible to reach a low detection limit for the signals produced by the evaporated aerosol particles.) Finally, 95 mm behind the lens exit inside the second chamber, the particle beam enters, through a capillary of 5 mm length and 2.5 mm diameter, a small heated gold sphere of 10 mm diameter where the aerosols are stopped and immediately evaporate. The evaporation sphere is thermostatted at 80 $^{\circ}\text{C}$ (better than ± 0.1 $^{\circ}\text{C}$). The gas leaves the sphere through another small capillary tube with a length of 4.5 mm and a diameter of 3.5 mm which focuses the gas molecules towards the

ion source, a crossing electron beam of 70 eV. The ions formed are drawn into a magnetic mass spectrometer equipped with two channeltron multipliers for mass separation.

Due to the capillaries, about 70% of the evaporated aerosols leave the evaporation sphere towards the ion source, while 30% will be lost through the aerosol entrance and are not available for analysis. The residence time for inert gases within the evaporation sphere is about 1 ms. For molecules such as H₂O and HNO₃ that adsorb easily, the residence time is as large as hundreds of milliseconds to even seconds. A shutter in front of the sphere can either be retracted or block the beam from entering the sphere. In the latter position background-gas measurements are made.

The mass spectrometer is operated in a stepping mode where the height of selected mass peaks is monitored sequentially. This mode allows a higher time resolution compared to a scanning mode. The measuring time for each data point is ~250 ms. During a balloon flight, every 2 s a set of peaks due to HNO₃ and H₂O, and every 17 s a set of peaks due to other aerosol components is monitored; gas-phase and background peaks follow every 2 min. At a balloon descent/ascent velocity of 1 m/s, this corresponds to a vertical resolution of a few meters for HNO₃ and H₂O and approximately 20 m for other aerosol components.

The aerosol particles need about 30 ms to traverse the lens. During this time, the particles remain under almost the same environmental conditions (pressure, temperature) as present in the atmosphere. During the balloon flight, both thermal isolation of the gondola and placement of the lens entrance 80 mm outside of the gondola reduce the heat transfer between experiment and lens keeping the latter as close as possible to the outside temperature. Calculations with a non-equilibrium model [5, 6] indicate that the composition change within the lens is negligible. The main pressure drop within the nozzle accelerates the aerosol particles to about 200 m/s. With such a high speed, PSC particles will reach the spherical collector at a distance of 95 mm within 0.5 ms. During this very short transition time, a perceptible change in chemical composition of the very fragile PSC particles in vacuum is unlikely.

The entire PSC-analysis system was extensively tested in the laboratory either using synthetic H₂SO₄/H₂O [17], H₂SO₄/HNO₃/H₂O, and (NH₄)₂CO₃/H₂O aerosols or with N₂ to characterize the influence of background gas; see [4].

The mass spectrometers were calibrated by a pressure-related dynamic expansion procedure providing a known and constant gas flow of H₂O or HNO₃ at pressures as low as during PSC analysis. The desired gas is supplied to a volume at an accurately determined pressure and allowed to expand through a small orifice (under molecular flow conditions) into a sphere held at ultrahigh vacuum by LHe pumps and connected to the mass spectrometer. The pressure-related sensitivity for water, i.e., the background-corrected count rate at mass 18 divided by the H₂O partial pressure immediately before the orifice is plotted in **Figure 2** vs. the H₂O partial pressure immediately before the orifice. The values are approximately constant showing that the ion detectors work linearly in this range. The first data point with its large uncertainty was obtained at a pressure in the sphere below 10⁻⁹ mbar, the lower limit of realizable pressures. For the calibration of nitric acid, thermal decomposition in vacuum according to $4 \text{HNO}_3 \rightarrow 4 \text{NO}_2 + 2 \text{H}_2\text{O} + \text{O}_2$, probably occurring mainly at the walls of the vacuum system, and adsorption at the walls have been considered. The resulting molar sensitivities (counts/mol) are accurate to about ±1% for H₂O or ±8% for HNO₃ when molar ratios are determined; if absolute amounts are required, the respective accuracies are only ±8% or ±11%. Details are outlined in [7].

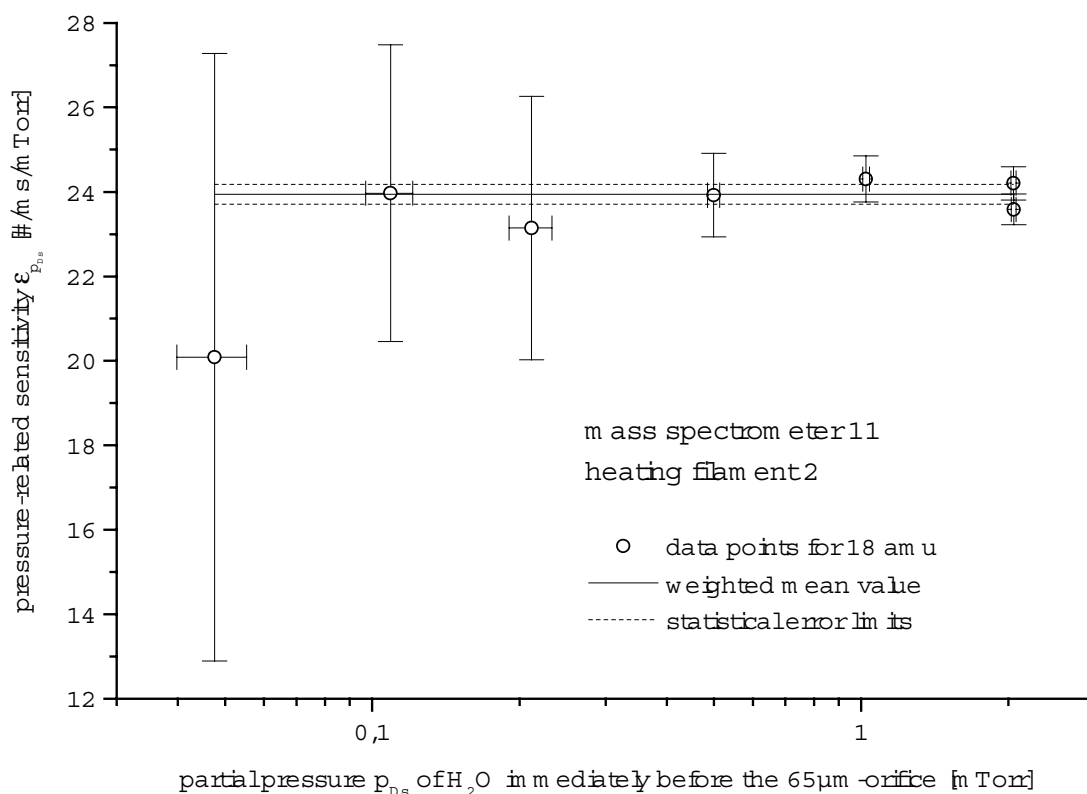


Figure 2: Pressure-related sensitivity of one of the mass spectrometers at 18 amu vs. the H_2O partial pressure immediately before the orifice. Also indicated is the weighted mean value (solid line) with its statistical error (dotted lines). The heating filament is one of two redundant ones of the ion source.

Major improvements of the instrument compared to the version used for the previous flight, which resulted in an about 50 times higher sensitivity, comprise replacement of the quadrupole mass spectrometer by a more sensitive magnetic instrument, improvement of the mass-spectrometer electronics, and optimization of the instrument's geometry. Furthermore, the gondola was modified and enlarged to carry the additional instruments, and the protective frame surrounding the gondola was redesigned to reduce its weight substantially.

The Balloon Flights

The two gondolas were launched on January 19, 2000 at 20:43 UT and January 25, 2000 at 19:46 UT from Esrange near Kiruna, Sweden, in the framework of the THESEO 2000 campaign. The balloons were equipped with valves and ballast, so that the operators of CNES were able to perform repeated ascent and descent maneuvers of the balloons at altitudes between 20 and 24 km. The instruments worked very well during all the PSC penetrations of both flights.

Figure 3 shows a vertical cross section of the temperature distribution along the flight track (black line) of the second flight (25.01.2000) at 22:00 UT, simulated with a mesoscale meteorological model [8, 9]. The balloon encountered the extension of a cold that had developed over the Scandinavian mountains due to adiabatic expansion of ascending air masses in mountain-induced gravity waves. The measured temperatures agree well with the simulated values but showing small-scale fluctuations. The very low simulated temperatures within the cold suggest that a fraction of the particles observed onboard the balloon gondola could have nucleated above the Scandinavian mountains.

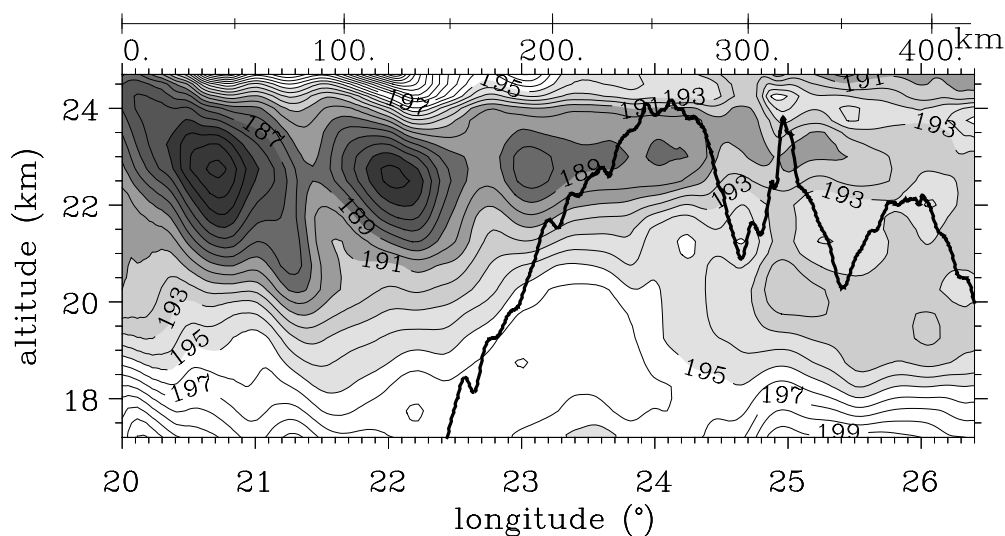


Figure 3: Simulated temperatures during the balloon flight on January 25, 2000; the calculation was performed using the mesoscale MM5-model [8, 9] by A. Dörnbrack of DLR-Institute for Physics of the Atmosphere, Oberpfaffenhofen/Germany. The balloon trajectory (black line) shows the ascents and descents during the 2½ h period when measurements were taken. The air parcels encountered by the balloon experienced very low temperatures above the Scandinavian mountains.

The mass-spectrometric count rates due to condensed water and nitric acid obtained during this flight are displayed in **Figure 4** together with backscatter ratios at two wavelengths (measured by DMI and CNR), particle number densities for three size classes (measured by UW), atmospheric temperature, and altitude. A close correlation is visible between H_2O , HNO_3 , backscatter ratios (being markers for the presence of PSCs), and particle counts. In contrast to the previous measurement [1, 18], however, a close correlation between low temperatures and the presence of PSCs is absent; this reflects the different meteorological situations in January 1998 and January 2000.

A layer of particles with median diameters of 1.5 to 2 μm and concentrations of less than 0.5 cm^{-3} was penetrated several times around 75700, 77500, 78400, 79700 and 81000 s UT. In the clouds, strong fluctuations of the H_2O and HNO_3 signals result from low particle number counting statistics, given each data point corresponds to particles contained in 4 cm^3 air; i.e., each point represents only a few (or even no) incoming particles. Particularly between 77500 and 78300 s, the H_2O data demonstrates that single particles can be resolved individually. The H_2O signal response is fast and shows no influence of the previous measurement 2 s before, while the response for HNO_3 is slower and the signals are slightly smoothed. There are water measurements, however, which do not show such a strong variation in the count rates. Around 75000, 76000, and particularly near 77000 s UT, a smooth H_2O signal distribution was recorded, resulting from the measurement of high concentrations ($1\text{-}10 \text{ cm}^{-3}$) of small particles with a median diameter between 0.3 and 1 μm .

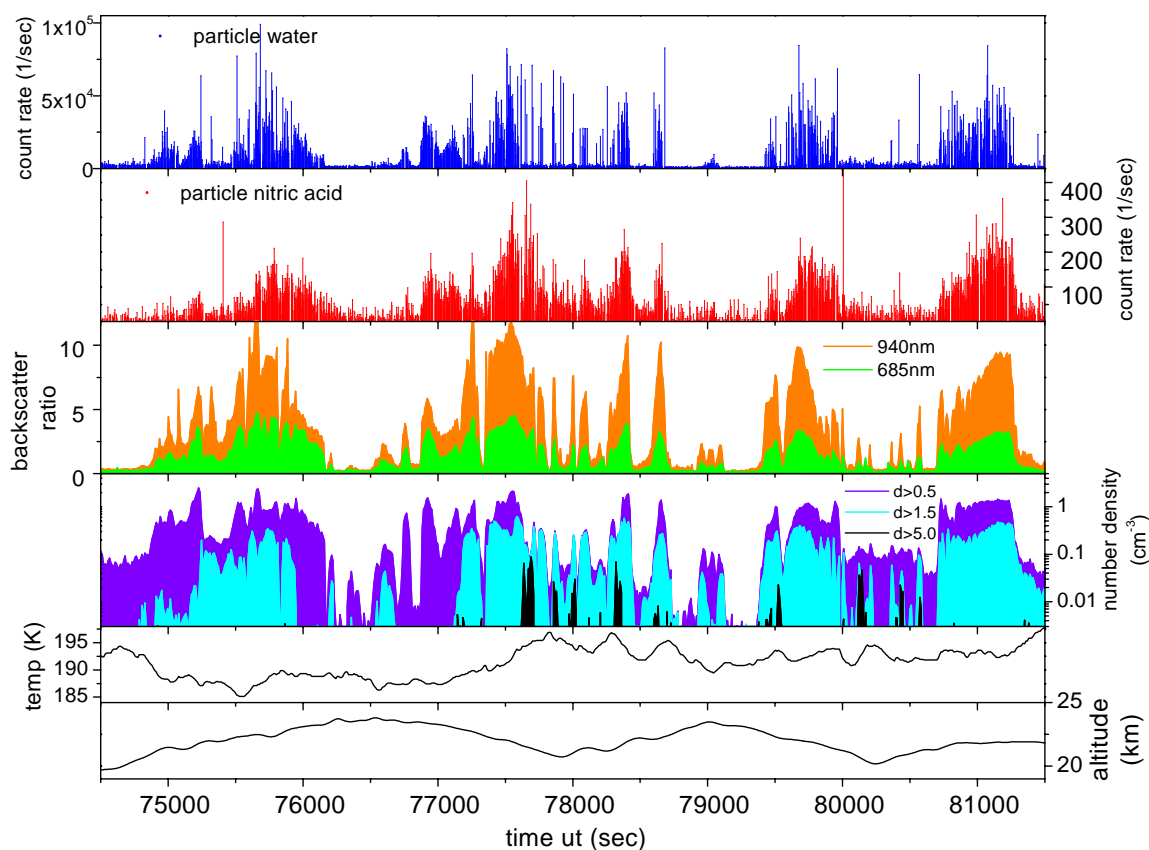


Figure 4: Summary of the data obtained during the flight on January 25, 2000. The two upper panels show the condensed water and nitric acid mass-spectrometric count rates, measured at masses 18 and 63 amu, respectively. The third panel displays backscatter-ratio measurements at 940 and 685 nm. In the fourth panel the integrated number densities of three selected particle size classes, i.e., >0.5 , >1.5 , and >5.0 μm , are presented. The lowest panels show the atmospheric temperature and the altitude of the gondola.

With the aid of the laboratory calibrations, the count rates of H_2O and HNO_3 were converted to molar ratios of $\text{H}_2\text{O}/\text{HNO}_3$ and averaged over longer periods to minimize the statistical error. The resulting molar ratios are plotted in **Figure 5** together with the particle volume and the difference of the measured temperature both to T_{ICE} (the frost point of H_2O , determined by CNRS-LMD) and T_{NAT} (the calculated equilibrium temperature of $\text{HNO}_3 \cdot 3\text{H}_2\text{O}$). Most of the molar ratios are found to be $\text{H}_2\text{O}/\text{HNO}_3 = 3 \pm 0.5$, proving these particles to consist of $\text{HNO}_3 \cdot 3\text{H}_2\text{O}$ (nitric acid trihydrate, NAT). The corresponding clouds exhibit particle volumes of 1 to 2 $\mu\text{m}^3/\text{cm}^3$ air in close agreement with model calculations [10]. In clouds producing a smooth water signal distribution, the particles have molar ratios of $\text{H}_2\text{O}/\text{HNO}_3 \geq 4.5$ and volumes of <0.5 $\mu\text{m}^3/\text{cm}^3$ air at temperatures up to ~ 3 K above T_{ICE} , consistent with calculations for supercooled ternary solution droplets [10, 11]. At 78600 s UT, $\text{HNO}_3 \cdot 3\text{H}_2\text{O}$ particles are present despite $T > T_{\text{NAT}}$; this may indicate that solid $\text{HNO}_3 \cdot 3\text{H}_2\text{O}$ particles evaporate rather slowly [12].

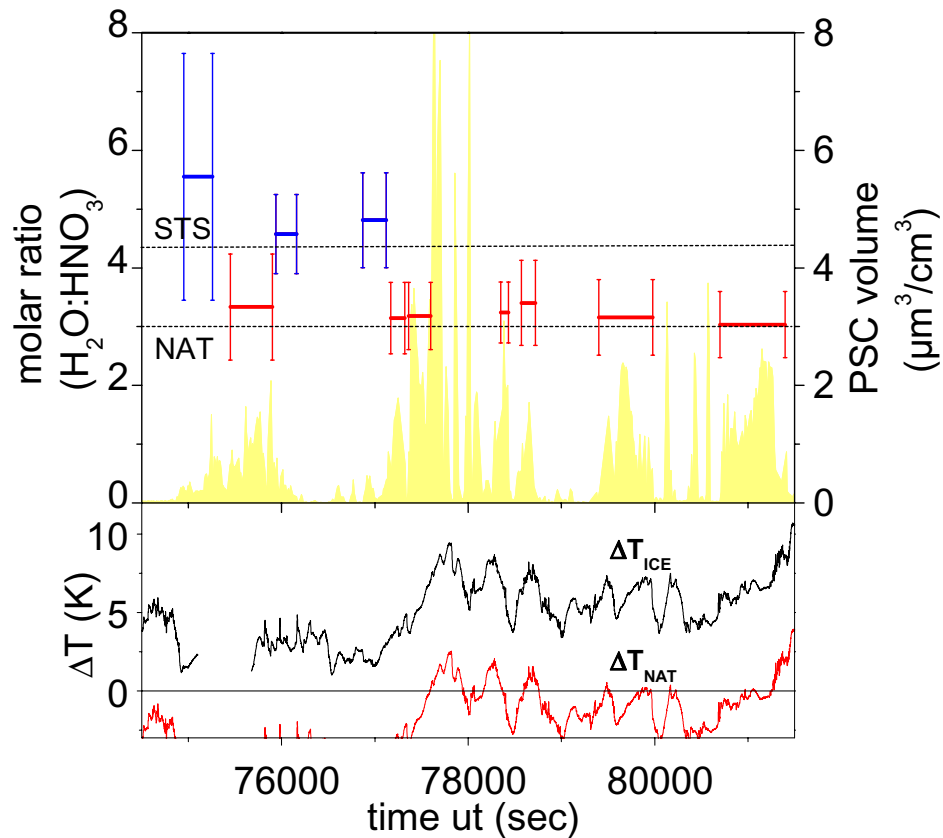


Figure 5: Measured molar ratios $\text{H}_2\text{O}/\text{HNO}_3$ of PSC particles together with the total particle volume (per cm^3 air) (upper panel). The total volume is calculated from a bimodal lognormal particle size distribution fitted to the data set. The dotted line indicates the molar ratio of 3 for NAT particles and the dashed line the lowest possible molar ratio for STS droplets according to model predictions [10, 11]. The lower part of the figure shows the difference of the measured temperatures both to T_{ICE} and to T_{NAT} assuming 8 ppbv HNO_3 in the gas phase (based on data obtained on board of the NASA DC-8 aircraft operating from Kiruna in the framework of the SOLVE campaign and in cooperation with THESEO 2000). NAT particles are stable at temperatures below T_{NAT} .

The air parcels encountered during the first flight on January 19, 2000 had experienced minimum temperatures that were somewhat higher than six days later, but the temperatures met by the gondola were in the same range. Due to adiabatic cooling on traversing the Scandinavian mountains, lee waves had developed which induced the formation of PSCs. The upper panel of **Figure 6** shows the mass-spectrometric count rate due to H_2O , registered during a part of the flight covering two PSC penetrations. The high count-rate peaks most probably correspond to individual large NAT particles, the calculated diameter of which ranges between about 1 and $2.5 \mu\text{m}$ and is displayed in the second panel. The averaged molar ratios $\text{H}_2\text{O}/\text{HNO}_3$ for the two cloud penetrations are above 3 but clearly below the lower limit of 4.3 for supercooled ternary solution droplets suggesting the simultaneous presence of NAT particles and STS droplets. The lower count rates measured between the high peaks also indicate small STS droplets or background aerosol. This interpretation is consistent with the relatively low backscatter ratios registered by the partners. During the part of the flight not shown in figure 6, mainly STS droplets were observed.

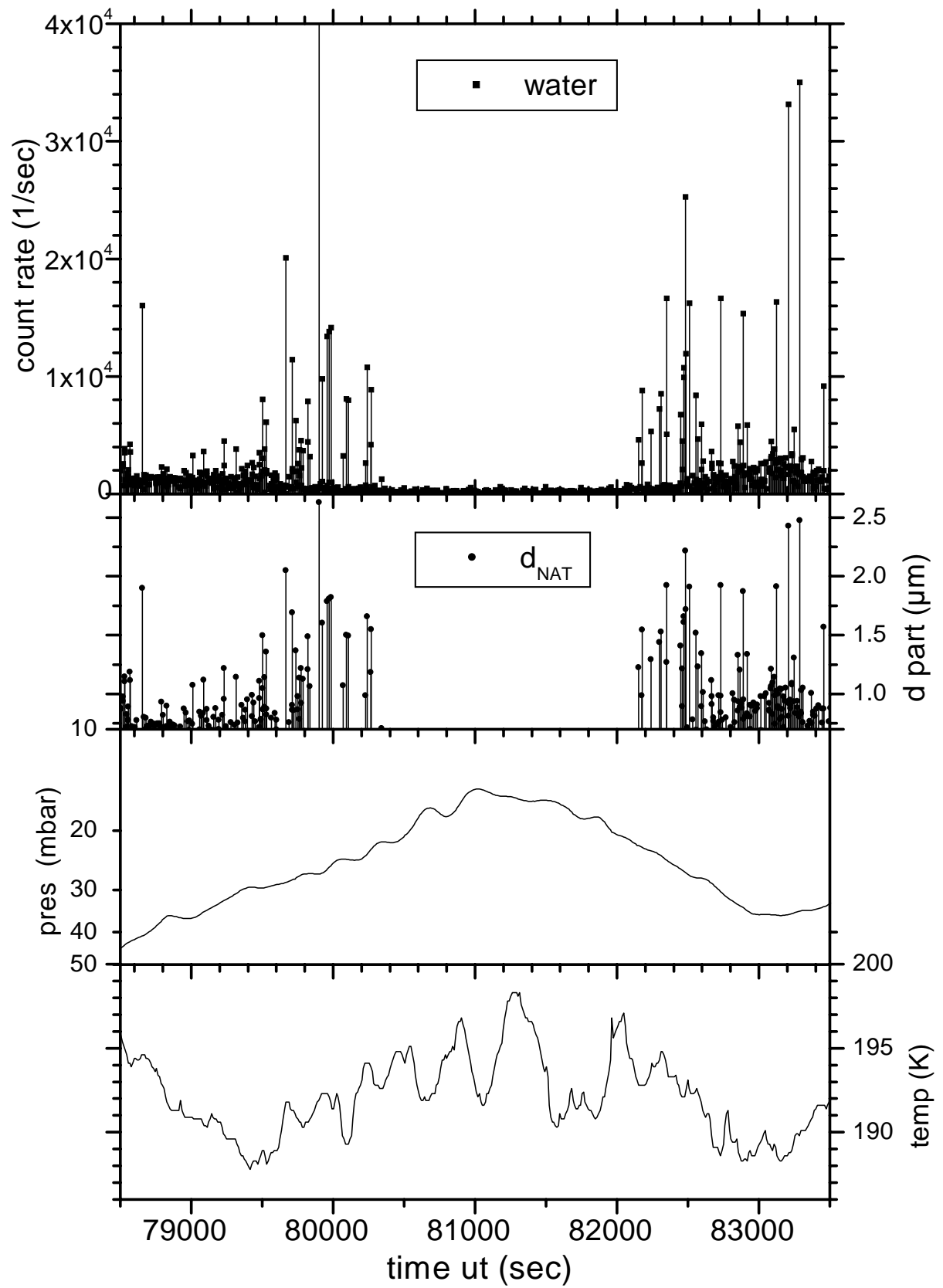


Figure 6: Data obtained during the flight on January 19, 2000, top to bottom: mass-spectrometric count rate at 18 amu (H₂O), NAT single-particle diameter calculated using absolute calibration results, ambient pressure, and temperature vs. time.

Data evaluation in collaboration with the partners is not yet fully completed. More details will be outlined in a forthcoming Ph.D. thesis [13].

DEVIATIONS FROM THE TECHNICAL ANNEX AND REASONS

As already explained in the progress report, the initially planned measurements of gaseous nitric acid were dropped. After the meteorological situation in January 1999 had prevented balloon flights, it was decided to postpone the campaign by one year to December 1999/ January 2000. This required a half-year extension of the project duration.

CONCLUSIONS

The in-situ chemical analysis of polar stratospheric clouds, performed in January 2000 with balloon-borne instruments above Scandinavia, revealed the presence of particles consisting of nitric acid trihydrate (NAT, HNO₃·3H₂O) in the Arctic stratosphere. Besides these NAT particles, liquid supercooled ternary solution (STS) droplets were registered with H₂O/HNO₃ molar ratios above 5 as predicted by model calculations. A temperature hysteresis in the PSC particles' life cycle is demonstrated by the detection of STS droplets at lower temperatures than NAT particles.

Thus, our measurements confirm the prediction [14-16], originally made for the Antarctic stratosphere, that solid NAT particles exist in polar stratospheric clouds at temperatures above the frost point of water and near the equilibrium temperature of NAT.

References and Publications from the Project (*)

- [1]* Schreiner, J., Voigt, C., Kohlmann, A., Arnold, F., Mauersberger, K., Larsen, N.: Chemical analysis of polar stratospheric cloud particles. *Science* **283**, 968-970 (1999).
- [2] Schreiner, J., Voigt, C., Mauersberger, K., McMurry, P., Ziemann, P.: Aerodynamic lens system for producing particle beams at stratospheric pressures. *Aerosol Sci. Technol.* **29**, 50-56 (1998).
- [3]* Schreiner, J., Schild, U., Voigt, C., Mauersberger, K.: Focusing of aerosols into a particle beam at pressures from 10 to 150 torr. *Aerosol Sci. Technol.* **31**, 373-382 (1999).
- [4]* Schreiner, J., Voigt, C., Zink, P., Kohlmann, A., Knopf, D., Mauersberger, K.: A mass spectrometer system for analysis of polar stratospheric aerosols. *Rev. Sci. Instrum.*, submitted.
- [5] Tsias, A., Prenni, A.J., Carslaw, K.S., Onasch, T.P., Luo, B.P., Tolbert, M.A., Peter, T.: Freezing of polar stratospheric clouds in orographically induced strong warming events. *Geophys. Res. Lett.* **24**, 2303-2306 (1997).
- [6] Meilinger, S.M., Koop, T., Luo, B.P., Huthwelker, T., Carslaw, K.S., Krieger, J., Crutzen, P.J., Peter, T.: Size-dependent stratospheric droplet composition in lee-wave temperature fluctuation and their potential role in PSC freezing. *Geophys. Res. Lett.* **22**, 3031-3034 (1995).
- [7]* Kohlmann, A.: Kalibration von Massenspektrometern zur Aerosol-Analyse durch dynamische Expansion von Wasserdampf, HNO₃ und HCl. Ph.D. Thesis, Heidelberg 2000.
- [8] Leutbecher, M., Volkert, H.: Stratospheric temperature anomalies and mountain waves: A three-dimensional simulation using a multi-scale weather prediction model. *Geophys. Res. Lett.* **23**, 3329-3332 (1996).
- [9] Dörnbrack, A., Leutbecher, M., Kivi, R., Kyrö, E.: Mountain-wave induced record-low stratospheric temperatures above Northern Scandinavia. *Tellus* **51A**, 951-963 (1999).
- [10] Carslaw, K.S., Luo, B.P.; Clegg, S.L.; Peter, T.; Brimblecombe, P.; Crutzen, P.J.: Stratospheric aerosol growth and HNO₃ gas phase depletion from coupled HNO₃ and water uptake by liquid particles. *Geophys. Res. Lett.* **21**, 2479-2482 (1994).

-
- [11] Tabazadeh, A., Turco, R.P., Jacobson, M.Z.: A model for studying the composition and chemical effects of stratospheric aerosols. *J. Geophys. Res.* **99D**, 12897-12914 (1994).
- [12]* Voigt, C., Schreiner, J., Kohlmann, A., Zink, P., Mauersberger, K., Larsen, N., Deshler, T., Kröger, C., Rosen, J., Adriani, A., Di Donfrancesco, G., Cairo, F., Ovarlez, J., Ovarlez, H., David, C., Dörnbrack, A.: Nitric acid trihydrate (NAT) in polar stratospheric cloud particles. *Science*, submitted.
- [13]* Voigt, C. Ph.D. Thesis, in preparation.
- [14] Crutzen, P.J., Arnold, F.: Nitric acid cloud formation in the cold Antarctic stratosphere: a major cause for the springtime "ozone hole". *Nature* **324**, 651-654 (1986).
- [15] Toon, O.B., Hamill, P., Turco, R.P., Pinto, J.: Condensation of HNO₃ and HCl in the winter polar stratosphere. *Geophys. Res. Lett.* **13**, 1284-1287 (1986).
- [16] Hanson, D.R., Mauersberger, K.: Laboratory studies of the nitric acid trihydrate: implications for the south polar stratosphere. *Geophys. Res. Lett.* **15**, 855-858 (1988).
- [17]* Knopf, D., Zink, P., Schreiner, J., Mauersberger, K.: Calibration of an Aerosol Composition Mass Spectrometer with Sulfuric Acid/Water Aerosol. *Aerosol Sci. Technol.*, submitted.
- [18]* Voigt, C., Tsias, A., Dörnbrack, A., Meilinger, S., Luo, B., Schreiner, J., Larsen, N., Mauersberger, K., Peter, T.: Non-Equilibrium Polar Stratospheric Cloud Compositions Measured in Lee Waves. *Geophys. Res. Lett.*, submitted.

PART B: INDIVIDUAL REPORT.

Contractor: Laboratoire de Météorologie Dynamique (LMD), UMR 8539

Leading scientist : Joëlle Ovarlez
Scientific staff: Henri Ovarlez, Jacques Crespin, Bertrand Gaubicher

Address : Ecole Polytechnique, 91128 Palaiseau cedex, France.
Tel : 33 (0)1 69 33 48 00
Fax : 33(0)1 69 33 30 05
E-Mail : joelle.ovarlez@polytechnique.fr

I. OBJECTIVES

The amount of water vapour has a strong influence on the threshold temperatures for the existence of Polar Stratospheric Clouds (PSC). The knowledge of the stratospheric water content profile is essential for the determination of the temperatures at which the Polar Stratospheric Clouds may form and persist, and is necessary for the modelling of the mechanism of formation of the different types of PSC particles. From the water vapour measurement in the polar stratosphere, the threshold temperature for ice particles existence (“the frost-point temperature”), and the threshold temperature for the condensation of Nitric Acid Trihydrate (T_{NAT}) can be known to be compared to the air temperature. So the possibility of the formation and persistence of PSC particles can be deduced (Hanson and Mauersberg, 1988, Larsen et al, 1997).

To perform the necessary water vapour content measurement the PSC Analysis gondola was equipped with a frost-point hygrometer designed and operated by LMD.

II. MAIN RESULTS OBTAINED:

The LMD payload, as part of the PSC Analysis gondola, is composed of a cryogenic frost-point hygrometer, and an air pressure and an air temperature sensor. These instruments have been used for several times during previous balloon campaigns, and among those the European experiments EASOE and SESAME, as described by Ovarlez and Ovarlez, 1994, 1996, and have been used also during the WAVE/THESEO program (de La Noe et al, 2000). The air temperature is measured by a micro bead thermistor from Victory Engineering Corporation and the air pressure is measured by a sensor from Paroscientific instruments. The frost-point hygrometer is designed by LMD and is based on the chilled-mirror technique. In this technique a layer of condensate is detected by an optical system, and the temperature of the mirror at which this layer is detected is measured and represents the frost-point of the air passing over the mirror. The mirror temperature is controlled cryogenically: the mirror is cooled through a copper rod immersed in a liquid nitrogen bath enclosed in a dewar container, and the heating is produced by a resistance wire wrapped around the copper rod. Then, the hygrometer measures directly the frost-point temperature, which is an important parameter to be compared to the air temperature for the study of the occurrence of the different types of PSCs. The measurement of the air pressure allows the determination of the water vapour volume mixing ratio. The 2σ uncertainty is 0.3C for the frost-point temperature, and 5% on the mixing ratio.

For an easy integration in the whole gondola, the LMD payload is set as a parallelepiped box 120x45x45 cm, for a weight of 40 kg including batteries. In the frame of THESEO/PSC Analysis program, the data transmission was performed through the common telemetry of the gondola as set up by MPIK. To prevent contamination of the water vapour measurements, the LMD payload is arranged so that the air inlet for the water vapour measurement is below and far from the whole gondola, and the measurements are made during night-time.

Two balloon flights of the common gondola were scheduled during the THESEO winter 1998-1999 campaign from Kiruna, Sweden. Then two complete gondola have been prepared on the field on the beginning of 1999 to be ready to fly as soon as there were conditions for occurrence of PSCs. However, there was no opportunity to have a flight in the conditions propitious to Polar Stratospheric Clouds occurrence as the stratospheric mean temperature inside the vortex during winter 1998/1999

were the warmest that have been observed from the 10 previous years (EORCU, 1999). Consequently the instruments returned from KIRUNA after the THESEO winter campaign, and new tests and calibration checks have been made in the laboratory, before the instruments were sent again to Kiruna for the 1999-2000 winter campaign (THESEO 2000). During the winter 1999-2000 the stratospheric vortex was very cold and a lot of PSCs events occurred (EORCU 2000). Then the two flights of the PSC Analysis gondola were performed in lee wave-induced PSCs above Scandinavia, respectively on 19 and 25 January 2000.

General observations:

During the first flight, on 19 January, water vapour measurements were made during the first ascent, first descent and beginning of second ascent inside the cloud, then a failure of the main telemetry - telecommand system occurred at the beginning of the second ascent, so that water vapour measurements could no be made from that time. The air temperature profile from the LMD payload compared to the air temperature profiles from the temperature sensors operated by the other partners of the projects shows a systematic difference of about 2C all over the altitude range, from the ground level to the upper altitude level. As the thermistor used for the temperature measurement is broken when the payload is recovered, a calibration of this sensor could not be made. A careful error analysis let us conclude that this can be explained only by a human error by using bad calibration coefficients. However the air temperature data from the second flight were in agreement with the data from the other sensors within less than 0.5C.

The air temperature profiles for the 2 flights are very fluctuating, particularly inside the clouds, and the temperature minima inside the clouds was about -85C on 19 January and -88C on 25 January. The temperature was always above the frost point temperature except in a thin layer at around 22 km (500K) on 25 January.

The water vapour profiles for the two flights show very different features:

For the 19 January flight, ascent and descent profiles are similar together, showing that the way of integration of the hygrometer and associated air inlet prevents any pollution from the whole gondola. Moreover the mean H₂O profile is similar to the inside the vortex profiles as measured without PSCs during previous years, as it is shown on figure 1.

Considering the water vapour content of 25 January, many perturbations occur inside the cloud, together with air temperature perturbations, but the mean mixing ratio lays in the range of the more stable inside the vortex profiles that are shown on figure 1. In fact the PSC investigated on 25 January was very inhomogeneous.

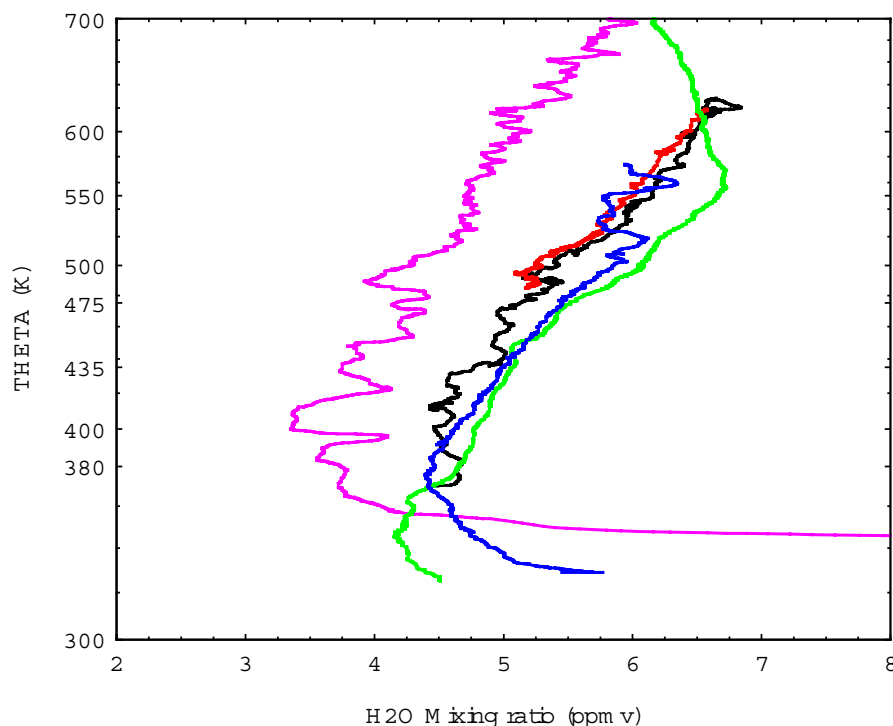


Figure 1. The water vapour profile during ascent (black) and first descent (red) on 19 January 2000 flight are very similar together with a mean slope similar to the one of previous profiles measured inside the vortex with the same instrument but without PSCs (green line, Winter 94/1995 - SESAME; blue line, Winter 1998/1999 - WAVE). The water vapour profile on 25 January 2000 (not shown) is much more fluctuating, but also around the inside the vortex profiles. The purple line is the mid latitude profile measured during spring 1999 from Aire sur l'Adour (WAVE/THESEO program)

Detailed flight 19 January:

During the balloon flight of 19 January 2000, a PSC has been investigated in a large altitude range, between about 17,5 and 23,5 km (420k and 560K). A time series of the water vapour and air temperature data for this flight is displayed on figure 2, where the time series of potential temperature shows the ascent and descent inside the cloud. The time period when the balloon is inside the PSC are deduced from the measured backscatter ratio (DMI and CMR Part B reports). As explained above the water vapour measurements were not made in the last part of the balloon flight.

The air temperature is very changeable inside as well outside the PSC investigated. Inside the cloud, the air temperature is always above the frost-point temperature and even, for thin layers, around and slightly above the equilibrium temperature for NAT particles. A detailed study on the composition of the particles of that PSC is given in the Part B-report from MPI.

A decrease of the water vapour mixing ratio occurs at around 21 km (~500K on figure 1, around 83000 seconds on the upper panel of Figure 2). Though very small this decrease could be attributed to dehydration as shown, by Schiller et al (2000) as similar decrease has been measured at the same altitude level from other in situ measurements inside the vortex during that cold winter.

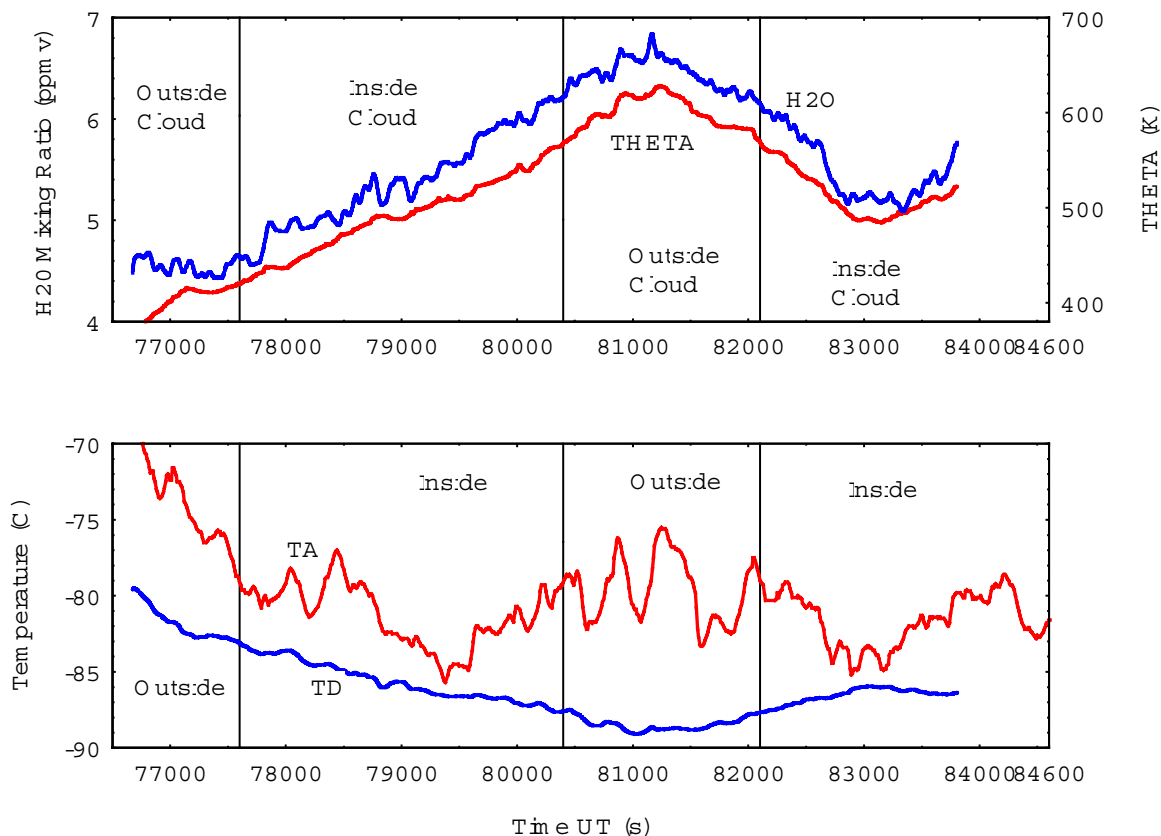


Figure 2. The upper panel displays the water vapour mixing ratio together with the potential temperature THETA. The lower panel displays the air temperature TA compared to the frost-point temperature TD. TA is from the Vaisala radiosonde onboard the gondola, as the LMD temperature sensor shows some discrepancies as explained in 3.1. The penetrations inside the Polar Stratospheric clouds during the first ascent and descent are shown.

Detailed Flight 25 January

On 25 January the observed PSC from the balloon flight laid between about 20 and 24 km (between $\sim 475\text{K}$ and 530K). A time series of the water vapour and air temperature data from this balloon flight is displayed on Figure 3. The corresponding potential temperature is also shown in order to locate the ascent and descent inside the PSC. In agreement with the other partners of the project, the cloud has been separated in 5 parts, corresponding to different layers investigated separately with respect to the particle composition analysis, as it appeared that the cloud had a very complex structure. The time series of potential temperature, on Figure 3, shows how the control of the piloting of the balloon was done with high accuracy by the CNES team in order to make several ascents and descents inside the cloud.

Compared to the data from the 19 January flight on Figure 2, the water vapour content is very perturbed inside the cloud, but stays always in the range of the expected stratospheric content from previous observations, that is to say below ~ 7 ppmv. At the same time a lot of large variations occur on the air temperature measurements. The air temperature variability is such that the difference between the air temperature and the frost-point temperature, inside the cloud, varies in a large range. Inside the PSC, the air temperature ranges from about 1C below the frost-point to about 2C above T_{NAT} . Then many layers containing different types of particles can be investigated, and it is shown that NAT particles were surviving above T_{NAT} .

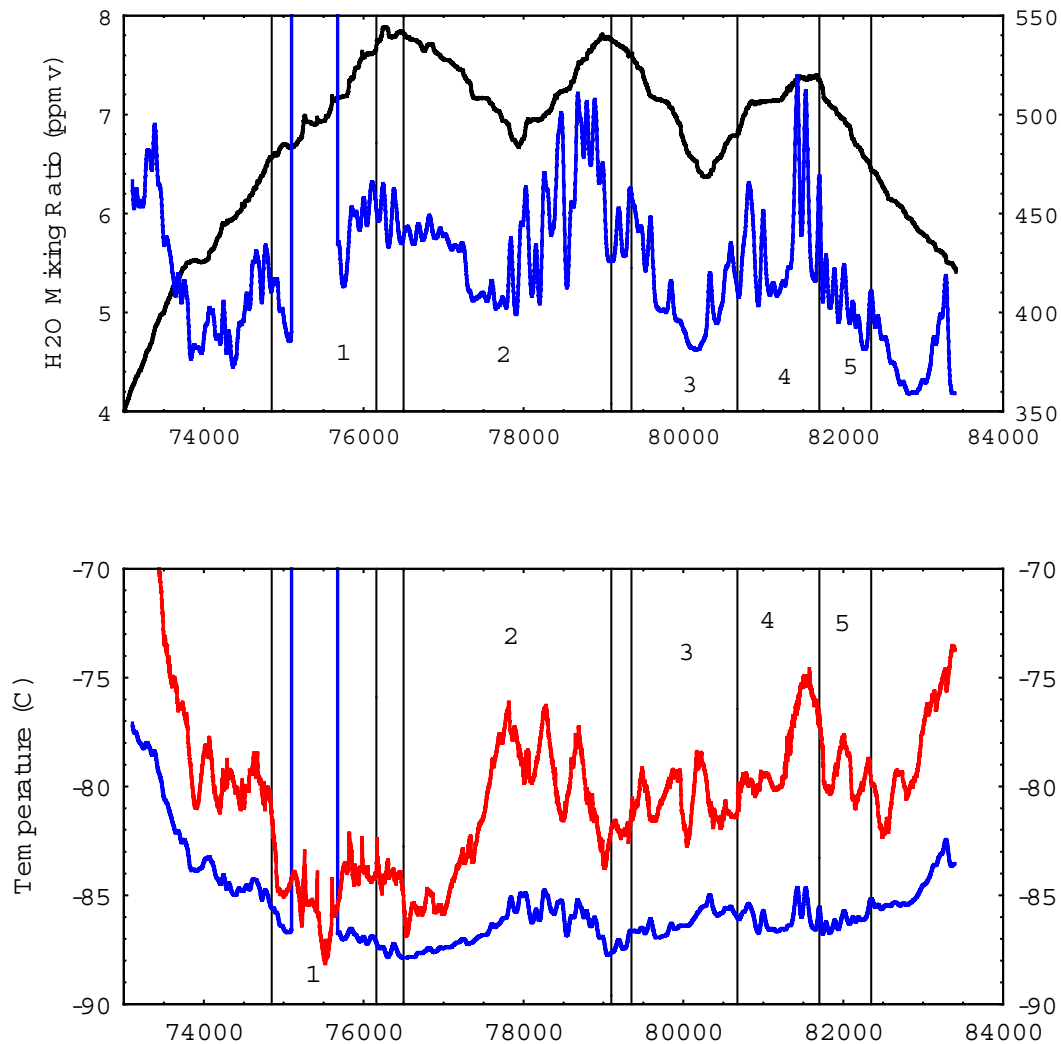


Figure 3. The upper panel displays the water vapour mixing ratio (blue line) together with the potential temperature (black line) for the flight of 25 January. The lower panel displays the air temperature (red line) compared to the frost point temperature (blue line). The time when the balloon was inside the PSC are marked by 1 to 5; and it is seen that from about 75000 to 82300 seconds, the measurements were almost always made inside the PSC except at the 2 first ceilings of the balloon (between 1 and 2 and between 2 and 3)

During the first ascent the air temperature was as low as -88°C (cloud 1 on Figure 3) and possibly below the frost-point temperature at around 22km (500 K). Unfortunately as seen on Figure 3, the hygrometer was unable to make measurement at that time, as a disequilibrium of the control loop of the instrument occurred, perhaps because of the large perturbations encountered in that layer. However the extrapolation of the data let us think that the air temperature was about 1 to 2C below the frost-point temperature. However the data from the particle detector and backscatter sondes do not indicate the presence of ice particles in the corresponding thin layer. This is not surprising as the back trajectory calculations, in the layers in the altitude range where the PSC was encountered by the balloon, indicate that the temperature of the corresponding air masses has not been low enough to form ice particles, but has been below T_{NAT} for 20 hours prior to sampling (Voigt et al, 2000).

III DEVIATIONS FROM TECHNICAL ANNEX AND REASONS.

There are no deviations from the technical annex.

IV. CONCLUSIONS.

The water vapour measurements performed with the LMD frost-point hygrometer, together with air temperature and air pressure sensor, on board the PSC Analysis gondola during 2 flights in January 2000 allowed the determination of the threshold temperature for ice and NAT particle existence, and help to the study of the particle properties. The air temperature inside the PSCs investigated was very changeable. The mean water vapour mixing ratio profile inside the PSC of 19 January is quite smooth and similar to those measured without the occurrence of PSCs. However, on 25 January, the water vapour profile is much perturbed inside the investigated PSC. That PSC has a very inhomogeneous structure and is composed of many layers with different particles properties. The data from the LMD payload have been put very early after the field campaign in the data-base available to the other partners of the project.

References:

- Adriani, F. Cairo, F. Cardillo, G. Di Donfrancesco, N. Larsen, K. Mauersberger, C. Voigt, J. Schreiner, J. Ovarlez, H. Ovarlez, T. Deshler, C. Kröger, J. Rosen, C. David and S. Bekki, Multi-instrumental in situ observations on polar stratospheric clouds by balloon-borne experiment at Kiruna, Sweden, during winter 1999-2000, *Proceedings of the THESEO2000 / SOLVE Workshop*, Palermo, September 2000.
- de La Noë J., J. Ovarlez, H. Ovarlez, C. Schiller, N. Lauté, P. Ricaud, J. Urban, D. G. Feist, L. Zalesak, N. Kämpfer, M. Ridal, D. Murtagh, K. Lindner, U. Klein, K. Künzi, P. Forkman, A. Winnberg, P. Hartogh and A. Engel, Water vapor distribution inside and outside the polar vortex during THESEO, *Proceedings of the fifth European Workshop on Stratospheric Ozone*, St Jean de Luz, France, CEC publication, 2000.
- Deshler Terry, Chris Kröger, James Rosen, Christiane Voigt, Andreas Kohlmann, Jochen Schreiner, Konrad Mauersberger, Niels Larsen, Joelle Ovarlez, Henri Ovarlez, Alberto Adriani, Francesco Cairo, Guido Di Donfrancesco, Christine David and Slimane Bekki Balloonborne measurements of chemical, physical and optical properties of PSC particles. Part II: Temperatures near TICE on 25 January 2000, *Proceedings of the THESEO2000 / SOLVE Workshop*, Palermo, September 2000.
- EORCU, The Northern Hemisphere Stratosphere in the winter 1998/99, *report from the European Ozone Research Coordinating Unit*, Cambridge, 1999
- EORCU, The Northern Hemisphere Stratosphere in the winter and spring 1999/2000, *report from the European Ozone Research Coordinating Unit*, Cambridge, 2000.
- Hanson D., And K. Mausberger, Laboratory studies of the nitric acid trihydrate: Implications for the south polar stratosphere, *Geophys. Res. Lett.*, 15, 855-858, 1988.
- Larsen N., B. M. Knudsen, J. M. Rosen, N. T. Kjome, R. Neuber, and E. Kyro, Temperature histories in liquid and solid stratospheric cloud formation, *J. Geophys. Res.*, 102, D19, 23,505-23,517, 1997.
- Ovarlez Joelle and Henri Ovarlez, Stratospheric water vapor content evolution during EASOE, *Geophys. Res. Lett.*, 21, 13, 1235-1238, 1994.
- Ovarlez Joelle and Henri Ovarlez, Water vapour and aerosols measurements during SESAME, and the observation of low water vapour content layers, *Air Pollution report 56 on Polar stratospheric ozone*, European Commission Brussels, 205-208, 1996.
- Schiller C., J. Beuermann, R. Müller, F. Stroh, A. Engel, M. Müller, N. Larsen, and J. Ovarlez, Dehydration in the Arctic stratosphere during the THESEO2000 / SOLVE campaigns, *Proceedings of the THESEO2000 / SOLVE Workshop*, Palermo, September 2000.
- Voigt C., J. Scheiner, A. Kohlmann, K. Mausberger, T. Deshler, C. Kröger, J. Rosen, N. Larsen, A. Adriani, G. Di Donfrancesco, F. Cairo, J. Ovarlez, H. Ovarlez, C. David, and S. Bekki, Balloonborne measurements of chemical, physical and optical properties of Polar Stratospheric Clouds, Part III: Particles at Temperature near TNAT, *Proceedings of the THESEO2000 / SOLVE Workshop*, Palermo, September 2000.

PART B: INDIVIDUAL REPORT.

Contractor: Consiglio Nazionale delle Ricerche,
Istituto di Fisica dell' Atmosfera (CNR.IFA)

Leading scientist: Alberto Adriani

Scientific and technical staff: Francesco Cairo
Francesco Cardillo
Guido Di Donfrancesco
Roberto Morbidini
Lucio Pulvirenti
Maurizio Viterbini

Address: Via del Fosso del Cavaliere 100
00133 Roma
Italy

Telephone. +39 06 49 93 43 48
Fax: +39 06 20 66 02 91
E-Mail: alberto.adriani@ifa.rm.cnr.it

OBJECTIVES FOR THE PROJECT

To contribute to the project's multi-instrumental study of polar stratospheric clouds in terms of measurements of their optical properties.

To use optical techniques to measure the structure of the cloud, its optical density and its thermodynamic phase (i.e. if constituted by liquid or solid particles).

In order to achieve this main scientific goal, a LAser Backscatter Sonde in a new version had to be designed, built and flown on the PSC-Analysis gondola along with the other instruments contributing to the project.

*II. MAIN RESULTS OBTAINED**II.1. INSTRUMENTATION*

The design of the new version of LABS has been developed during the first months of the first year of the contract.

The new LABS can use 2 lasers at the wavelengths of 532 and 685 nm: a miniaturised polarised Nd-YAG laser and a laser diode respectively. The sonde has three receiving channels: two at the 532 nm wavelength for polarised (polarisation parallel to the laser emission) and cross-polarised backscattered light. A third channel is for the 685 nm wavelength. The laser emissions are modulated with a frequency of 0.5 Hz for an acquisition period of 2 s. Both backscattered signal and atmospheric background signal plus electronic noise are acquired in successive times within the acquisition period. The spatial vertical resolution depends on the balloon speed. The LABS is shown in the photograph below.

The new LABS can give measurements of backscattering ratios and the backscattering coefficients of the particles along with depolarisation and colour ratio 685/532. The primary information is the backscattering ratio (BR) which gives a measurement of the amount of light backscattered from the particles with respect to that one backscattered from the molecular atmosphere. The backscattering ratio, BR, is proportional to the concentration and the size of the particles. It depends on the altitude and it can be considered as a particle mixing ratio. From this parameter it is possible to get direct information about the cloud structure and its optical density. BR is defined by the formula:

$$BR = \frac{\beta_p + \beta_m}{\beta_m}$$

where β_p and β_m are the particle and molecular volume backscattering coefficients respectively.

The backscattering coefficient, β_p , is approximately proportional to the surface of the particles and it does not depend on the altitude at which it is calculated. It is also directly related the extinction of the cloud. The molecular backscattering coefficient depends on the atmospheric pressure and temperature and on the laser wavelength. It can be calculated by the formula:

$$\beta_m = \frac{5}{K} \times \frac{P}{T} \times (\lambda[\mu m])^{-4} \times 10^{-33} m^{-1} sr^{-1}$$

where K is the Boltzman constant. Then, the backscattering coefficient is:

$$\beta_p = \beta_m \times (BR - 1)$$

The depolarised backscattered light from particles is particularly important in the study of polar stratospheric clouds. In fact, through the depolarisation measurements it can be assessed if the polar stratospheric cloud under study contains solid particles inside. Also the colour ratio can give a complementary information on the phase of the cloud particles and a rough information about the size of the particles. Moreover, the use of the 532 nm wavelength can permit a direct comparison of LABS data with ground-based and airborne lidars using such wavelength during the THESEO campaign.

Depolarisation can be defined in different ways [Cairo et al., 1999], although volume depolarisation ratio or aerosol depolarisation ratio are mainly used from the scientific community. The aerosol depolarisation ratio δ_p is probably the most suitable depolarisation parameter for inter-comparison among different lidars and LABS. In terms of volume backscattering coefficients, it is defined as:

$$\delta_p = \frac{\beta_p^\perp}{\beta_p^\parallel}$$

where the subscript p refers to particles, and the superscripts \perp and \parallel refer respectively to the cross and parallel component of the volume backscattering coefficient, with respect to the polarisation plane of the output laser beam. δ_p has the advantage of giving a specific description of the particle, since it does not vary with respect to changes in the number density of the particles, as long as the average shape of the particles is not changed. On the other hand, δ_p tends to become noisy when the aerosol burden is low.

In terms of quantities of common usage in the lidar practice, δ_p assumes the form:

$$\delta_p = \delta_m \times \frac{\Delta \times BR^\perp - 1}{BR^\parallel - 1}$$

where Δ is the ratio of the background corrected raw signal from the cross and parallel channels, normalized to 1 in regions where no aerosol are present,

$$\Delta = \frac{S^\perp}{S^\parallel} \times K$$

$S^{\perp,\parallel}$ are the lidar raw signals from cross and parallel channels,

$K : \Delta = 1 \Leftrightarrow$ no aerosols

and R^\parallel is the Backscatter Ratio of the parallel channel: $BR^\parallel = \frac{\beta_A^\parallel + \beta_m^\parallel}{\beta_m^\parallel}$

$\delta_m = \frac{\beta_m^\perp}{\beta_m^\parallel}$ is the depolarisation expected from a purely molecular atmosphere.

It has often been assumed, following theoretical considerations of Young (1980), a value of 1.4% for δ_m . That value has been confirmed both theoretically and experimentally (Bridge and Buckingham, 1960; Bates, 1984; Cohen and Low, 1969).

However, the most commonly used parameter is the total volume depolarisation, D, defined as

$$D = \frac{\beta_p^\perp + \beta_m^\perp}{\beta_p^\parallel + \beta_m^\parallel} = \frac{\beta^\perp}{\beta^\parallel} = C \frac{S^\perp}{S^\parallel}$$

The calibration constant, C, is calculated assuming a pure molecular atmospheric depolarisation ratio equal to 1.4% where the signal is coming from a range of the atmosphere free of particles, $BR=1$ [Young, 1980]. In this report we are going to use the definition of the volume depolarisation D.

The relative error on BR can be estimated on the order of 5% with an absolute minimum value of ± 0.05 for every BR. The relative error on the depolarisation can be estimated to be on the order of 10-15% with an absolute minimum value of ± 0.25 for every D below 20 km and ± 0.5 for every D above that level.

After completing the design, a first prototype of the sonde was built. The prototype was flown twice to test the functionality on the optical and mechanical components and the electronics as single parts and the all instrument as a whole. The first test of the new LABS was hold in Leon, Spain, in late March and the second from Laramie, Wyoming, USA, in early August. The first test revealed the necessity of a better conditioning of the photomultipliers (used in the detection of the signal) for low-pressure working conditions. Modifications of the photomultipliers were operated in our laboratories. From the point of view of the other components, the prototype worked properly. The second flight was done with upgraded photomultipliers and all worked successfully. During such flight, the interface for telemetry with University of Wyoming optical particle counter (OPC) was also tested. During the experiments, LABS used the OPC telemetry for transmitting data to the ground station.

Three instruments had been prepared for the experiment which had to be held during the 1998-1999 winter from Kiruna, Sweden. However, the unfavourable stratospheric condition during that winter did not permit to carry out the experiment. The stratosphere was generally too warm for stratospheric cloud formations.

The instruments were then flow during the successive winter, 1999-2000, in the frame of the THESEO 2000 programme.

II.2. THE EXPERIMENT

The general description of the experiments in which the two LABS instruments had been flown is given in the general part of this report. Only the observations performed by LABS are then reported and described hereafter.

LABS was flown twice on 19 and 25 January 2000. In both flights the payload was flown inside a polar stratospheric cloud. Preliminary results are respectively reported in Figure 1 and Figure 2. In those figures the backscattering ratios at 685 nm and the volume depolarisation ratios calculated at 532 nm are depicted.

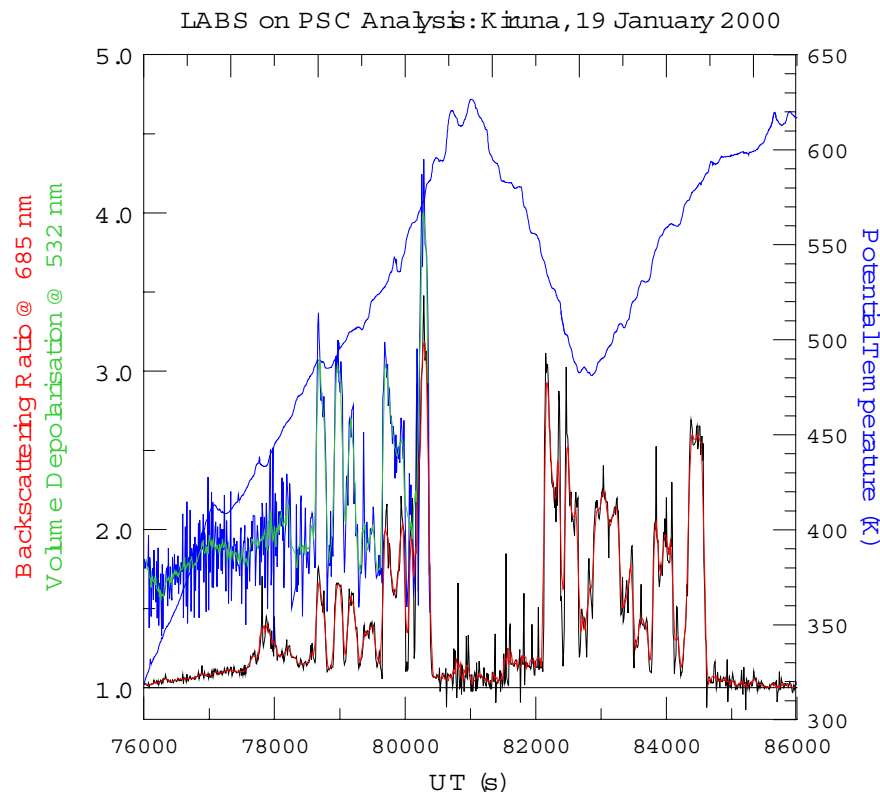


Figure 1

As the accuracy of the green laser power monitors was poor in both flights, the backscattering ratios at 532 nm are not given in the figures. Moreover, as the no-reliability of the emitted laser power measurements yield to a poor accuracy of the absolute calibration on the green channel, a calculation of the colour ratios is not possible. The same issue applies to the aerosol depolarisation ratio calculations. On the other hand, the calculation of the volume depolarisation ratios is not depending on the accuracy of the laser power monitoring because the laser power fluctuations weight in the same way on both polarised and depolarised channels. Therefore, the depolarisation is reliable inside the clouds, where the signal to noise ratio is significantly high also in the receiving channel for depolarised signal (for a pure molecular atmosphere the depolarised signal is of the order of 1/100 of the polarised channel). Finally, a failure of the photomultiplier receiving depolarised signal occurred in both flights. Then, it was not possible to calculate the depolarisation ratios for all the flights. The cause of the failures was attributed to the influence of electromagnetic fields generated by the electronics inside the sonde on that specific photomultiplier. Such failures never occurred during ground tests preceding the field experiments. In fact the failure was strictly connected to the physical position of the photomultiplier inside the sonde. Solutions to solve such a problem have been already studied for the next experiments.

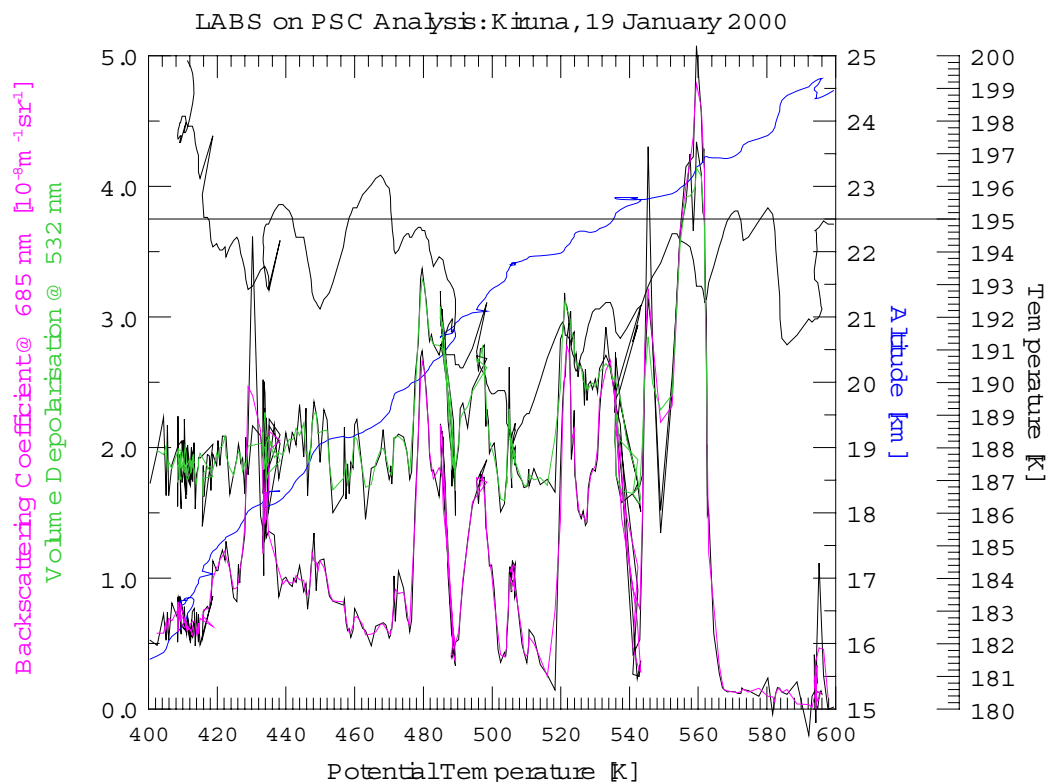


Figure 2

During the first flight (Figure 1) the payload crossed a stratospheric cloud approximately located between 480 and 590 K (approx 20-24 km) for 3 times (2 ascents and 1 descent). Looking at the combination of backscattering ratio and depolarisation during the first ascent, this cloud looks quite homogeneous in terms of particles contented. The cloud was probably constituted of solid NAT particles in all level. However, the structure of the cloud was very layered. In the second part of the flight the payload partially crossed the same cloud which was presumably formed by the same kind of particles (depolarisation measurement are not available in the second part of the cloud).

At lower potential temperatures (altitudes), just below the main layered cloud and between 420 and 460 K (approx. 17.5-19 km), a thin liquid cloud was observed.

Figure 2 zooms the first part of the flight where depolarisation measurements were available. Backscattering coefficient and depolarisation are plotted versus potential temperature. Atmospheric temperature and geometrical altitude are also given for comparison. β_p is more sensitive to the particle concentration variation and it can better use to identify the fine structure of the cloud. The cloud was quite optically thin as the backscattering ratios reach a maximum of 3 at 560 K but it is usually lower than 2 (Figure 1). The backscattering coefficient varies between 1 and $5 \cdot 10^{-8} \text{ m}^{-1} \text{ sr}^{-1}$ (Figure 2). It can be noticed that the cloud is present only when the temperatures is lower than 195 K and their optical thickness is higher at higher temperatures. Also volume depolarisation values are low and range between 2% and 4%.

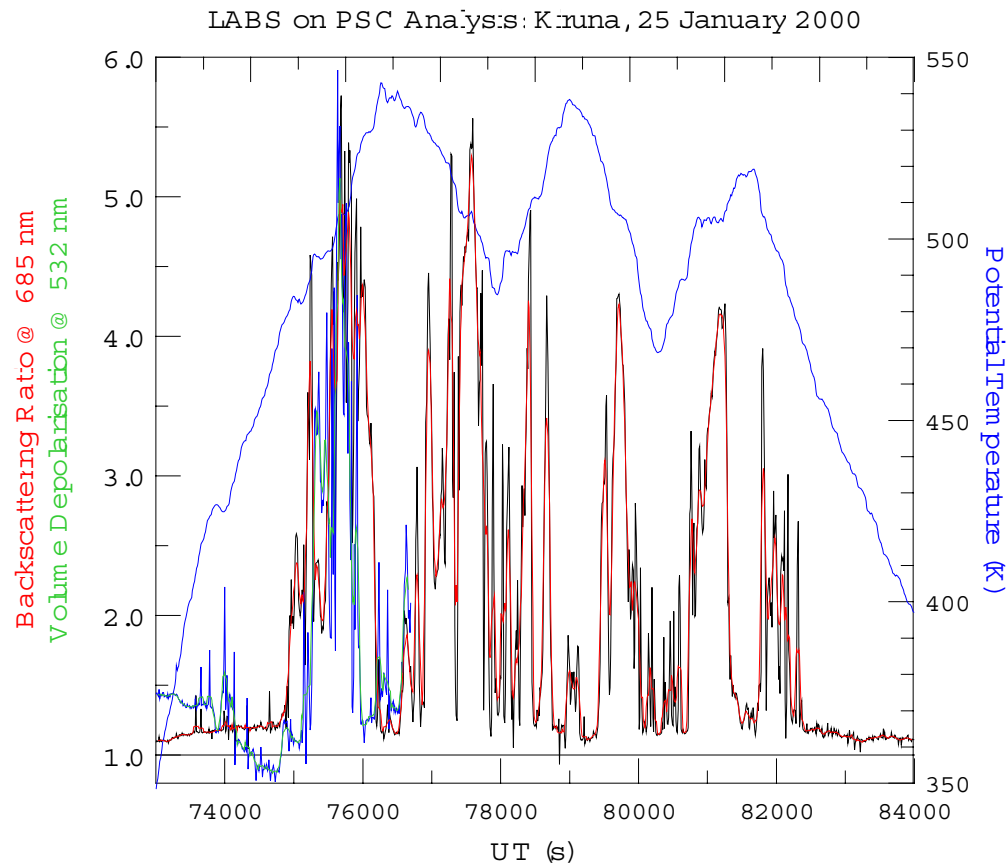


Figure 3.

The interaction of low tropospheric winds with the Scandinavian Alps can create mesoscale perturbations which propagate up to the middle atmosphere. In particular, the observation of 25 January was done on a PSC which formed under the temperature anomalies induced by such a mesoscale perturbation. The second flight is depicted in Figures 3 and 4. During this flight the payload crossed a polar stratospheric clouds for 6 times (3 ascents and 3 descents). Unfortunately, the depolarisation measurements were available only during the first crossing (see Figure 3). Also in this case the cloud looks quite stratified and the stratification was induced by the mesoscale perturbation. This flight was particularly most favourable than the first one and all the instruments on the payload were performing in their best conditions. The cloud was observed between 470 and 540 K of potential temperature (approximately 21-23 km). It was confined in only 2 km and

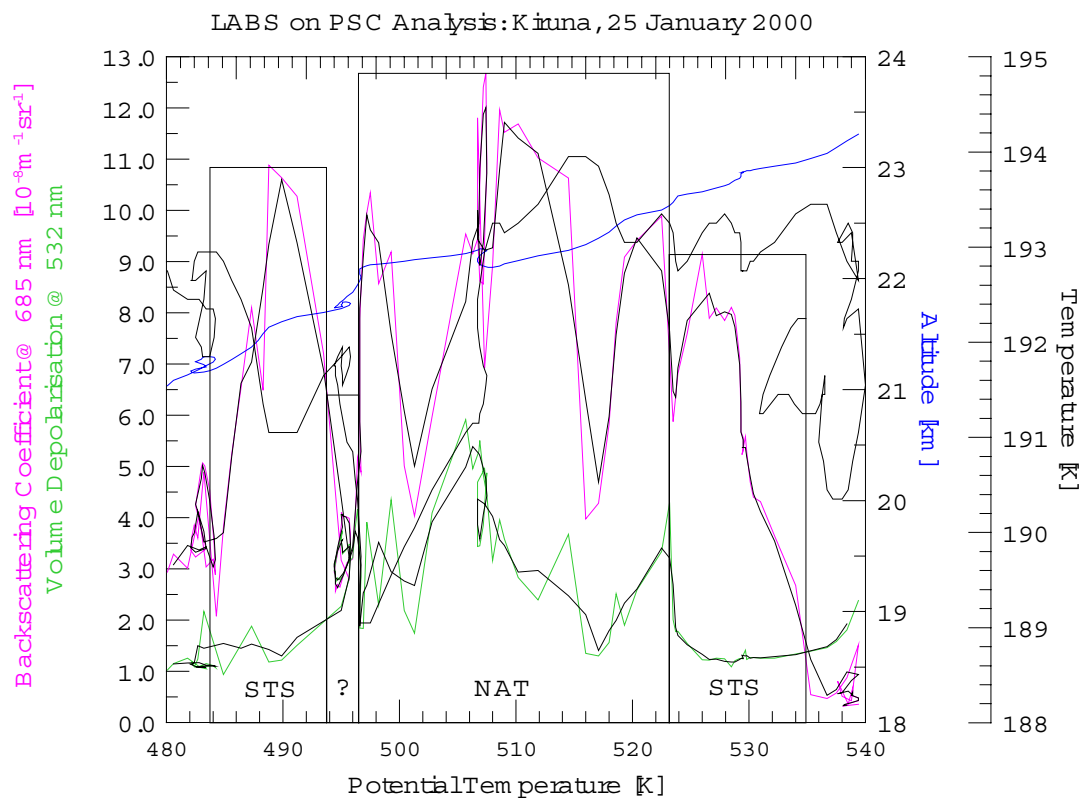


Figure 4.

its vertical structure was very stratified. The cloud was optically thicker than that one observed during the first flight. Some layer presented a vertical thickness of few hundred meters. A detail of the first part of the flight, where the LABS data set was complete, is reported in Figure 4. Backscattering coefficient and depolarisation are depicted versus potential temperature. Air temperature and geometrical temperature are given as reference. In this case the temperature is lower than the first flight and the cloud is structured with layer of different type of particles. Four type-layers are encircled in square boxes. The cloud appear like a sandwich: solid particles in the central part surrounded by liquid particles on top and at the bottom. The signature of this is in the comparison of backscattering coefficients and depolarisation. In the boxes identified by STS (Supercooled Ternary Solution), the depolarisation is lower than pure molecular atmosphere and the backscattering coefficient reaches values between 9 and $11 \times 10^{-8} \text{m}^{-1} \text{sr}^{-1}$. Moderate high depolarisation (values between 3 and 6%) are measured in the inner part of the cloud identified by NAT (Nitric Acid Tetrahydrate) due to the presence of solid particles. The identification of the composition was given by the MPI mass spectrometer mounted on the payload. Backscattering coefficients are scattered in a range 8 - $13 \times 10^{-8} \text{m}^{-1} \text{sr}^{-1}$. There is a thin layer at the interface between the STS and the NAT layers, identified by the "?", which present a no-clear signature and cannot be either in NAT or in STS typology. This fact is confirmed by mass spectrometer measurements as well. This part of the cloud would need a more detailed analysis by the comparison among the different instruments.

References

Bates, D. R., Rayleigh scattering by air, *Planet. Space Sci.*, 32, 785-791, 1984.

Bridge N. J. and A. D. Buckingham, The polarization of laser light scattered by gases, *Proc. R. Soc. London Ser. A* 295, 334-349, 1960.

Cairo F., G. Di Donfrancesco, A. Adriani, L. Pulvirenti and F. Fierli, Comparison of various linear depolarization parameters measured by lidar, *Applied Optics*, vol. 38, No. 21, 4425-4432, 1999.

Cohen A. J. and W. Low, An experimental determination of the depolarisation of scattered laser light by atmospheric air, *J. Appl. Meteor.* 8, 952-954, 1969.

Young, A. T., Rayleigh scattering, *Appl. Opt.* 20, 533-535, 1980.

III. DEVIATION FROM THE WORK PLAN

No deviations.

IV. CONCLUSIONS

In this report preliminary results have been reported. A more multi-instrumental data analysis is now in progress. A certain number of publications have been already planned to be submitted for publication in the next 1-2 years.

Publications.

So far, the activity in the framework of this project has produced the following publications and congress presentations:

Voigt C., J. Schreiner, A. Kohlmann, P. Zink, *K. Mauersberger, N. Larsen, T. Deshler, C. Kröger, J. Rosen, A. Adriani, F. Cairo, G. Di Donfrancesco, M. Viterbini, J. Ovarlez, H. Ovarlez, C. David, and A. Dörnbrack Nitric Acid Trihydrate (NAT) in Polar Stratospheric Clouds, Submitted to *Science*, 2000

Cairo F., G. Di Donfrancesco, A. Adriani, L. Pulvirenti and F. Fierli, Comparison of various linear depolarization parameters measured by lidar, *Applied Optics*, vol. 38, No. 21, 4425-4432, 1999.

Adriani A., F. Cairo, F. Cardillo, G. Di Donfrancesco, R. Morbidini, M. Viterbini, J. Ovarlez and H. Ovarlez, T. Deshler, C. Kröger, J. Rosen, C. David, S. Bekki, K. Mauersberger, C. Voigt, A. Kohlmann, J. Schreiner, and N. Larsen, Balloon-borne Measurements of Chemical, Physical, and Optical Properties of Polar Stratospheric Clouds. Part I: Instruments Flown on 25 January 2000, SOLVE-THESEO 2000 Science Meeting, Palermo, Italy, 25-29 September 2000.

Terry Deshler, Chris Kröger, James Rosen, Christiane Voigt, Andreas Kohlmann, Jochen Schreiner, Konrad Mauersberger, Niels Larsen, Joelle Ovarlez, Alberto Adriani, Francesco Cairo, Guido Di Donfrancesco, Christine David and Slimane Bekki, Balloon-borne Measurements of Chemical, Physical, and Optical Properties of Polar Stratospheric Clouds. Part II: Particles near the Frost Point Temperature, SOLVE-THESEO 2000 Science Meeting, Palermo, Italy, 25-29 September 2000.

C. Voigt, J. Schreiner, A. Kohlmann, K. Mauersberger, T. Deshler, C. Kröger, J. Rosen, N. Larsen, A. Adriani, G. Di Donfrancesco, F. Cairo, J. Ovarlez and H. Ovarlez, C. David and S. Bekki, Balloon-borne Measurements of Chemical, Physical, and Optical Properties of Polar Stratospheric Clouds. Part III: Particles at Temperatures near T_{NAT} , SOLVE-THESEO 2000 Science Meeting, Palermo, Italy, 25-29 September 2000.

PART B: INDIVIDUAL REPORT.

Contractor (coordinator): Service d'Aéronomie du CNRS - IPSL

Leading scientist: Dr. Christine David

Scientific and technical staff: Dr. Slimane Bekki
Prof. Gérard Mégie

Address: Université Paris 6 - B102
4, place Jussieu
75252 Paris Cedex 05
FRANCE

Telephone: +33 1 44 27 74 48 / +33 1 44 27 37 53

Fax: +33 1 44 27 37 76

E-Mail: Christine.David@aero.jussieu.fr
Slimane.Bekki@aero.jussieu.fr
Gerard.Megie@aero.jussieu.fr

OBJECTIVES FOR THE REPORTING PERIOD

In this project, Service d'Aéronomie was responsible for the deployment of the airborne lidar LEANDRE, mounted on the French « Avion de Recherche Atmosphérique et de Télédétection » (ARAT), a Fokker 27. The measured parameters, backscatter and depolarisation ratios at 532 nm, are complementary to the balloon data. As for the balloon-borne instrumentation, LEANDRE operation during THESEO included three different kinds of activities :

1. Preparation of the instruments and of campaign logistics
2. THESEO campaign
3. Data interpretation

The reporting period corresponds to the THESEO campaign and data interpretation. During the preparation phase, the instrument was tested and settled up for an optimal running and was installed in the aircraft. Flight procedures were defined, in terms of flight authorisations for the aircraft and co-ordination with the balloon flights. Then, during the campaign, data were acquired.

II. MAIN RESULTS OBTAINED: (methodology, results and discussions)

LEANDRE (Pelon et al., 1990) is a backscatter lidar. The Nd:Yag laser is frequency-doubled to emit 10 pulses per second at a wavelength of 532 nm. The beam is emitted at 20° to the vertical and perpendicular to the flight direction. The backscattered signal is collected on a 30 cm diameter telescope and split into components polarised parallel and perpendicular to the laser emission, which allows to distinguish between spherical and non-spherical scatterers. Each component is then detected by a photomultiplier tube. Pulse energy and receiver gains are monitored. The signals are time resolved using waveform transient recorders with a 2.5 Hz bandwidth and a resolution time of 200 ns. The data is stored on magnetic tape for further analysis. Real time visualisation is available during flight.

During the preparation phase, both the LEANDRE instrument and the ARAT logistics were prepared. The ARAT with LEANDRE on board arrived in Kiruna on 18 January 1999. Two ARAT flights were planned in connection with each balloon flight : one upwind flight before balloon launch, and a second flight tracking the balloon after launch.

The LEANDRE backscatter lidar on board the French research aircraft, ARAT/Fokker27, flew in coordination with the PSC Analysis gondola on 25/01/2000 evening. Two flights were performed. The first flight, upwind before PSC Analysis launch, was made between Kiruna and Andoya, and lasted almost 2 hours (take off at 18:30 UT, landing at 20:15 UT). The ARAT flew almost parallel to the stratospheric winds at 50 hPa and 30 hPa (cap ~110-120, wind coming from cap ~300). During this first flight, PSCs were observed between Kiruna and approximately the Norwegian boarder, between

about 21 and 25 km in altitude. They presented a layered structure and strongly depolarized the lidar signal. Backscatter ratio reached values up to 63 for the bottom layers and 120 for the upper layers (see figure 1). The depolarization, despite a higher backscatter ratio on perpendicular channel for the upper layers was stronger for the bottom layers, respectively around 17% and 23% (see figure 2). Above and after the Norwegian mountains, the signal was dominated by tropospheric clouds (between 8 and up to 12 km, likely the tropopause level). Nevertheless, between approximately the Norwegian boarder and the region where tropospheric clouds were observed, no PSC was detected.

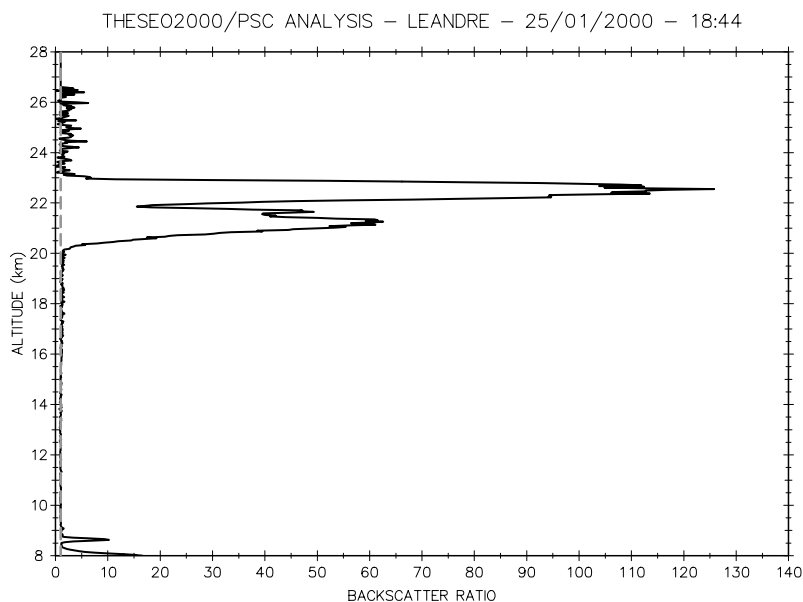


Figure 1: Backscatter ratio at 18:44 UT during the first LEANDRE/ARAT flight on 25/01/2000

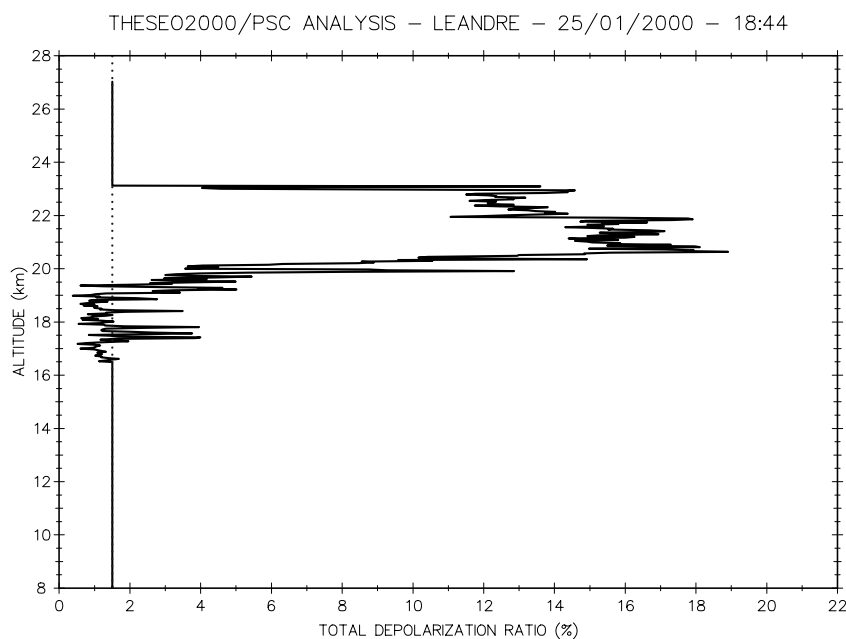


Figure 2: Depolarization ratio at 18:44 UT during the first LEANDRE/ARAT flight on 25/01/2000

The second flight was made between Kiruna and South-East of Rovaniemi. The ARAT took off at 20:44 UT, that is, one hour after the PSC Analysis balloon launch, and landed at 23:15 UT. The

position of the balloon was communicated in real time to the ARAT through the VHF station in Esrange. The ARAT caught the balloon position at 21:05 UT, then reduced its flight speed in order to follow the balloon at best. One track back was made slightly before reaching Rovaniemi. The tracking of the balloon was very efficient. The "go back" decision was taken for safety reasons at 21:55 (landing in Rovaniemi for refuelling would have been dangerous, due to bad surface meteorological conditions). During this second flight, PSCs were observed on a very short distance, between Kiruna and the mid-distance between Kiruna and the Finnish boarder, between about 20 and 22 km in altitude. As for the PSCs observed during the first flight, they presented a layered structure. Meanwhile, the backscatter ratio may be slightly less than for the first flight PSC. On the main part of this flight, PSC observation was precluded by a more than 5 km thick layer of tropospheric clouds.

DEVIATIONS FROM TECHNICAL ANNEX AND REASONS

During a previous campaign, one of the air-screw of the ARAT was blasted by a lightning. The time to repair and the ARAT only arrived in Kiruna the day of the first PSC Analysis gondola flight, but too late in the evening to accompany the balloon.

V. CONCLUSIONS

The objectives for the reporting periods have been partly reached. Due to unexpected technical problems on the aircraft, the ARAT was not able to make first coordinated flight with the PSC Analysis balloon. For the second flight the procedures and the co-ordination were very good, in particular the tracking of the balloon through VHF communication was very efficient. Unfortunately, meteorological conditions were not suitable to provide good measurements during the downwind flight. Therefore, during the upwind flight, strong PSCs were observed. Data were delivered to the Nilu database.

PART B: INDIVIDUAL REPORT

Contractor	Group de Physique Appliquée, Université de Geneve (GAP UNIGE)
Leading Scientist	Cristina Flesia
Scientific Staff	Andrei Starkov
Address	20 Rue de l'Ecole de médecine, 1211 Genève 4, Switzerland
Tel	+ 41 22 702 68 73
Fax	+ 41 22 702 68 63
E-Mail	Cristina.Flesia@physics.unige.ch

I. OBJECTIVES

The main objective for the first reporting period was to prepare the modelling algorithms for the analysis of the data of the THESEO Campaign. The responsibility of the University of Geneva lies in the provision of analysis algorithms to investigate the micro-physical characteristics of the PSC particles. During this preparation stage, the algorithms had to be updated for the analysis of lidar depolarisation data in conjunction with in-situ measurements for the validation of the results of the lidar retrieval.

The second period corresponds to the central part of the THESEO Campaign. The lidar depolarisation data will be analysed in detail using non spherical scattering calculations. The particle size distribution, calculated using the OPC data results will be used for the validation of the retrieval of the micro physical characteristics of the PSC particles obtained using the lidar data.

MAIN RESULTS OBTAINED

The work of the University of Geneva have been centred on the update of the already existing algorithms and on the development of new numerical tools for the analysis of the non spherical scattering from the PSC particles. Particular attention has been devoted to the development of algorithms for the estimation/ retrieval of the particle size from depolarisation measurements. The relative influence of the refractive index and the particle shape, which is of a particular importance for the joint analysis of the chemical and micro-physical properties of the PSC's particles have been studied in detail. Numerical simulation of the scattering properties have been performed for small non-spherical particles up to 2 μm and big ice crystals up to 100 μm . The non spherical scattering calculations for small particles in a range between 0.1 and 2 μm have been carried out using algorithms based on "Extended Boundary Condition Method". The scattering properties of big ice crystal particles have been performed using a geometrical optics. In both cases, a great variety of particles have been used. Results show that a mixture of different shape is the best approximation of the micro-physical properties of the atmospheric cloud particles

DANISH METEOROLOGICAL INSTITUTE

Scientific Reports

Scientific reports from the Danish Meteorological Institute cover a variety of geophysical fields, i.e. meteorology (including climatology), oceanography, subjects on air and sea pollution, geomagnetism, solar-terrestrial physics, and physics of the middle and upper atmosphere.

Reports in the series within the last five years:

No. 95-1

Peter Stauning and T.J. Rosenberg:
High-Latitude, day-time absorption spike events
1. morphology and occurrence statistics
Not published

No. 95-2

Niels Larsen: Modelling of changes in stratospheric ozone and other trace gases due to the emission changes : CEC Environment Program Contract No. EV5V-CT92-0079. Contribution to the final report

No. 95-3

Niels Larsen, Bjørn Knudsen, Paul Eriksen, Ib Steen Mikkelsen, Signe Bech Andersen and Torben Stockflet Jørgensen: Investigations of ozone, aerosols, and clouds in the arctic stratosphere : CEC Environment Program Contract No. EV5V-CT92-0074. Contribution to the final report

No. 95-4

Per Høeg and Stig Syndergaard: Study of the derivation of atmospheric properties using radio-occultation technique

No. 95-5

Xiao-Ding Yu, **Xiang-Yu Huang** and **Leif Laurssen** and Erik Rasmussen: Application of the HIRLAM system in China: heavy rain forecast experiments in Yangtze River Region

No. 95-6

Bent Hansen Sass: A numerical forecasting system for the prediction of slippery roads

No. 95-7

Per Høeg: Proceeding of URSI International Conference, Working Group AFG1 Copenhagen, June 1995. Atmospheric research and applications using observations based on the GPS/GLONASS System
Not published

No. 95-8

Julie D. Pietrzak: A comparison of advection schemes for ocean modelling

No. 96-1

Poul Frich (co-ordinator), H. Alexandersson, J. Ashcroft, B. Dahlström, G.R. Demarée, A. Drebs, A.F.V. van Engelen, E.J. Førland, I. Hanssen-Bauer, R. Heino, T. Jónsson, K. Jonasson, L. Keegan, P.Ø. Nordli, **T. Schmith, P. Steffensen**, H. Tuomenvirta, O.E. Tveito: North Atlantic Climatological Dataset (NACD Version 1) - Final report

No. 96-2

Georg Kjærgaard Andreassen: Daily response of high-latitude current systems to solar wind variations: application of robust multiple regression. Methods on Godhavn magnetometer data

No. 96-3

Jacob Woge Nielsen, Karsten Bolding Kristensen, Lonny Hansen: Extreme sea level highs: a statistical tide gauge data study

No. 96-4

Jens Hesselbjerg Christensen, Ole Bøssing Christensen, Philippe Lopez, Erik van Meijgaard, Michael Botzet: The HIRLAM4 Regional Atmospheric Climate Model

No. 96-5

Xiang-Yu Huang: Horizontal diffusion and filtering in a mesoscale numerical weather prediction model

No. 96-6

Henrik Svensmark and Eigil Friis-Christensen: Variation of cosmic ray flux and global cloud coverage - a missing link in solar-climate relationships

No. 96-7

Jens Havskov Sørensen and Christian Ødum Jensen: A computer system for the management of epidemiological data and prediction of risk and economic consequences during outbreaks of foot-and-mouth disease. CEC AIR Programme. Contract No. AIR3 - CT92-0652

No. 96-8

Jens Havskov Sørensen: Quasi-automatic of input for LINCOM and RIMPUFF, and output conversi-

on. CEC AIR Programme. Contract No. AIR3 - CT92-0652

No. 96-9

Rashpal S. Gill and Hans H. Valeur:

Evaluation of the radarsat imagery for the operational mapping of sea ice around Greenland

No. 96-10

Jens Hesselbjerg Christensen, Bennert Machenhauer, Richard G. Jones, Christoph Schär, Paolo Michele Ruti, Manuel Castro and Guido Visconti: Validation of present-day regional climate simulations over Europe: LAM simulations with observed boundary conditions

No. 96-11

Niels Larsen, Bjørn Knudsen, Paul Eriksen, Ib Steen Mikkelsen, Signe Bech Andersen and Torben Stockflet Jørgensen: European Stratospheric Monitoring Stations in the Arctic: An European contribution to the Network for Detection of Stratospheric Change (NDSC): CEC Environment Programme Contract EV5V-CT93-0333: DMI contribution to the final report

No. 96-12

Niels Larsen: Effects of heterogeneous chemistry on the composition of the stratosphere: CEC Environment Programme Contract EV5V-CT93-0349: DMI contribution to the final report

No. 97-1

E. Friis Christensen og C. Skøtt: Contributions from the International Science Team. The Ørsted Mission - a pre-launch compendium

No. 97-2

Alix Rasmussen, Sissi Kiilsholm, Jens Havskov Sørensen, Ib Steen Mikkelsen: Analysis of tropospheric ozone measurements in Greenland: Contract No. EV5V-CT93-0318 (DG 12 DTEE): DMI's contribution to CEC Final Report Arctic Tropospheric Ozone Chemistry ARCTOC

No. 97-3

Peter Thejll: A search for effects of external events on terrestrial atmospheric pressure: cosmic rays

No. 97-4

Peter Thejll: A search for effects of external events on terrestrial atmospheric pressure: sector boundary crossings

No. 97-5

Knud Lassen: Twentieth century retreat of sea-ice in the Greenland Sea

No. 98-1

Niels Woetman Nielsen, Bjarne Amstrup, Jess U. Jørgensen:

HIRLAM 2.5 parallel tests at DMI: sensitivity to type of schemes for turbulence, moist processes and advection

No. 98-2

Per Høeg, Georg Bergeton Larsen, Hans-Henrik Benzou, Stig Syndergaard, Mette Dahl Mortensen: The GPSOS project

Algorithm functional design and analysis of ionosphere, stratosphere and troposphere observations

No. 98-3

Mette Dahl Mortensen, Per Høeg:

Satellite atmosphere profiling retrieval in a nonlinear troposphere

Previously entitled: Limitations induced by Multipath

No. 98-4

Mette Dahl Mortensen, Per Høeg:

Resolution properties in atmospheric profiling with GPS

No. 98-5

R.S. Gill and M. K. Rosengren

Evaluation of the Radarsat imagery for the operational mapping of sea ice around Greenland in 1997

No. 98-6

R.S. Gill, H.H. Valeur, P. Nielsen and K.Q. Hansen: Using ERS SAR images in the operational mapping of sea ice in the Greenland waters: final report for ESA-ESRIN's: pilot projekt no. PP2.PP2.DK2 and 2nd announcement of opportunity for the exploitation of ERS data projekt No. AO2..DK 102

No. 98-7

Per Høeg et al.: GPS Atmosphere profiling methods and error assessments

No. 98-8

H. Svensmark, N. Woetmann Nielsen and A.M.

Sempreviva: Large scale soft and hard turbulent states of the atmosphere

No. 98-9

Philippe Lopez, Eigil Kaas and Annette Guldborg: The full particle-in-cell advection scheme in spherical geometry

No. 98-10

H. Svensmark: Influence of cosmic rays on earth's climate

No. 98-11

Peter Thejll and Henrik Svensmark: Notes on the method of normalized multivariate regression

No. 98-12

K. Lassen: Extent of sea ice in the Greenland Sea 1877-1997: an extension of DMI Scientific Report 97-5

No. 98-13

Niels Larsen, Alberto Adriani and Guido Di-Donfrancesco: Microphysical analysis of polar stratospheric clouds observed by lidar at McMurdo, Antarctica

No.98-14

Mette Dahl Mortensen: The back-propagation method for inversion of radio occultation data

No. 98-15

Xiang-Yu Huang: Variational analysis using spatial filters

No. 99-1

Henrik Feddersen: Project on prediction of climate variations on seasonal to interannual time-scales (PROVOST) EU contract ENVA4-CT95-0109: DMI contribution to the final report: Statistical analysis and post-processing of uncoupled PROVOST simulations

No. 99-2

Wilhelm May: A time-slice experiment with the ECHAM4 A-GCM at high resolution: the experimental design and the assessment of climate change as compared to a greenhouse gas experiment with ECHAM4/OPYC at low resolution

No. 99-3

Niels Larsen et al.: European stratospheric monitoring stations in the Arctic II: CEC Environment and Climate Programme Contract ENV4-CT95-0136. DMI Contributions to the project

No. 99-4

Alexander Baklanov: Parameterisation of the deposition processes and radioactive decay: a review and some preliminary results with the DERMA model

No. 99-5

Mette Dahl Mortensen: Non-linear high resolution inversion of radio occultation data

No. 99-6

Stig Syndergaard: Retrieval analysis and methodologies in atmospheric limb sounding using the GNSS radio occultation technique

No. 99-7

Jun She, Jacob Woge Nielsen: Operational wave forecasts over the Baltic and North Sea

No. 99-8

Henrik Feddersen: Monthly temperature forecasts for Denmark - statistical or dynamical?

No. 99-9

P. Thejll, K. Lassen: Solar forcing of the Northern hemisphere air temperature: new data

No. 99-10

Torben Stockflet Jørgensen, Aksel Walløe Hansen: Comment on "Variation of cosmic ray flux and global coverage - a missing link in solar-climate relationships" by Henrik Svensmark and Eigil Friis-Christensen

No. 99-11

Mette Dahl Meincke: Inversion methods for atmospheric profiling with GPS occultations

No. 99-12

Benzon, Hans-Henrik; Olsen, Laust: Simulations of current density measurements with a Faraday Current Meter and a magnetometer

No. 00-01

Høeg, P.; Leppelmeier, G: ACE: Atmosphere Climate Experiment: proposers of the mission

No. 00-02

Høeg, P.: FACE-IT: Field-Aligned Current Experiment in the Ionosphere and Thermosphere

No. 00-03

Allan Gross: Surface ozone and tropospheric chemistry with applications to regional air quality modeling. PhD thesis

No. 00-04

Henrik Vedel: Conversion of WGS84 geometric heights to NWP model HIRLAM geopotential heights

No. 00-05

Jérôme Chenevez: Advection experiments with DMI-Hirlam-Tracer

No. 00-06

Niels Larsen: Polar stratospheric clouds microphysical and optical models

No. 00-07

Alix Rasmussen, Jens Havskov Sørensen, Niels Woetmann Nielsen and Bjarne Amstrup: Uncertainty of meteorological parameters from DMI-HIRLAM, RODOS(WG2)TN(99)12, EU-Contract FI4P-CT95-0007

No. 00-08

A.L. Morozova: Solar activity and Earth's weather. Effect of the forced atmospheric transparency changes on the troposphere temperature profile studied with atmospheric models

No. 00-09

Niels Larsen, Bjørn M. Knudsen, Michael Gauss, Giovanni Pitari: Effects from high-speed civil traffic aircraft emissions on polar stratospheric clouds

No. 00-10

Søren Andersen: Evaluation of SSM/I sea ice algorithms for use in the SAF on ocean and sea ice, July 2000
(In Press)

No. 00-11

Claus Petersen, Niels Woetmann Nielsen: Diagnosis of visibility in DMI-HIRLAM

No. 00-12

Erik Buch: A monograph on the physical oceanography of the Greenland waters
(In Press)

No. 00-13

Michael Steffensen: Stability Indices as Indicators of Lightning and Thunder.

No. 00-14

Bjarne Amstrup, Kristian S. Mogensen and Xiang-Yu Huang: Use of GPS observations in an optimum interpolation based data assimilation system.

No. 00-15

Mads Hvid Nielsen: Dynamisk beskrivelse og hydrografisk klassifikation af den jyske kyststrøm.

No. 00-16

Kristian S. Mogensen, Jess U. Jørgensen, Bjarne Amstrup, Xiaohua Yang and Xiang-Yu Huang: Towards an operational implementation of HIRLAM 3D-VAR at DMI.

No. 00-17

Kai Sattler and Xiang-Yu Huang: Structure Function Characteristics for 2 meter Temperature and Relative Humidity in Different Horizontal Resolutions.

No. 00-18

Niels Larsen, Ib Sten Mikkelsen, Bjørn M. Knudsen, K. Mauersberger, J. Schreiner, C. Voigt, A. Kohlmann, J. Ovarlez, H. Ovarlez, J. Crespin, B. Gaubicher, A. Adriani, F. Cairo, F.

Cardillo, G. Di Donfrancesco, R. Morbidini, L. Pulvirenti, M. Viterbini, C. David, S. Bekki, G. Mégie, C. Flesia, A. Starkov, T. Deshler, C. Kröger, J. Rosen and N. Kjome: In-situ analysis of aerosols and gases in the polar stratosphere - A contribution to THESEO. Environment and Climate Research Programme, Contract No ENV4-CT97-0523, Final Report.

No. 00-19

Bjarne Amstrup: EUCOS observing system experiments with the DMI-HIRLAM Optimum Interpolation analysis and forecasting system.